The Effect of Astrocyte-derived Fatty Acid-binding Protein 7 on Blood-Brain Barrier Integrity in LPS-induced Inflammation

by

Deniz Altunsu

A Dissertation Submitted to the Graduate School of Health Sciences
in Partial Fulfillment of the Requirements for the Degree of

Doctor of Philosophy

in

Cellular and Molecular Medicine

KOÇ ÜNİVERSİTESİ

The Effect of Astrocyte-derived Fatty Acid-binding Protein 7 on Blood-Brain Barrier Integrity in LPS-induced Inflammation

Koç University

Graduate School of Health Sciences

This is to certify that I have examined this copy of a Ph.D. thesis by

Deniz Altunsu

and have found that it is complete and satisfactory in all respects and that any and all revisions required by the final examining committee have been made.

Committee Members:

Prof. Dr. Bülent Ahıshalı (Advisor)

Prof. Dr. Mehmet Kaya

Prof. Dr. Duygu Gezen Ak

Prof. Dr. Tuğba Bağcı Önder

Assoc. Prof. Prakash Pillai

Date: 27.07.2023

To my parents, Süreyya and Galip ALTUNSU, with endless thankfulness for their love and support…

ABSTRACT

The Effect of Astrocyte-derived Fatty Acid-Binding Protein 7 on Blood-Brain Barrier Integrity in LPS-induced Inflammation

Deniz Altunsu

Ph.D. in Cellular and Molecular Medicine

Sepsis is a life-threatening systemic inflammatory disease caused by infection, which causes disruption of blood-brain barrier (BBB) integrity. Fatty acid-binding protein 7 (FABP7), a transporter of fatty acids across the plasma membrane in astrocytes of the brain, modulates the caveolae formation in response to damage. However, the role of FABP7 in BBB disruption in the setting of septic inflammatory conditions caused by lipopolysaccharide (LPS) has not been clear yet. This study investigates the *in vitro* and *in vivo* effects of exogenous FABP7 administration on LPS-induced BBB disruption. bEnd.3 cells were treated with 0.5 µg/mL LPS for 24 hours followed by FABP7 (0.5 µg/mL) for 24 hours. Transendothelial electrical resistance (TEER) was measured to evaluate BBB integrity, whereas BBB permeability was assessed using sodium fluorescein (NaFl) tracer. Septic mice model was induced by intraperitoneally injecting LPS (3 mg/kg) and one hour later, the animals were treated with FABP7 (40 and 80 µg/kg). Body temperature was measured, and blood samples were collected from all experimental groups to determine the sepsis parameters. The anxiety levels of animals were measured by elevated plus maze test. The BBB permeability was evaluated by assessing the extravasation of albumin Alexa fluor 594 tracer injected after 23 hours of LPS and/or FABP7 treatments by IVIS imaging and confocal scanning fluorescence microscopy. The expression levels of tight junction (TJ) proteins claudin-5 and zonula occludens (ZO)-1, transcytosis-related proteins caveolin-1 and major facilitator superfamily domain containing 2a (mfsd2a), and inflammatory mediators NF-κB and

interleukin-1β were determined by immunofluorescence staining and western blotting. *In vitro* FABP7 administration to bEnd.3 cells following LPS challenge significantly increased the lowered TEER values ($p < 0.05$) and decreased the enhanced NaFl leakage ($p < 0.05$). In LPS-injected animals, 80 μg/kg FABP7 treatment decreased the elevated body temperature from 40ºC to 37-38ºC. Serum levels of procalcitonin (PCT), C-reactive protein (CRP), and reactive oxygen species (ROS) were significantly increased by LPS injection, whereas high dose FABP7 markedly decreased the levels of sepsis parameters ($p < 0.05$). In LPS-treated animals, a significant increase was observed in the severity of anxiety-like behavior which was significantly decreased by 80 μg/kg FABP7 ($p < 0.05$). LPS treatment increased the extravasation of albumin Alexa fluor 594 in the brain while high dose FABP7 decreased the BBB leakage of the tracer ($p < 0.05$). When the expressions of TJ proteins were evaluated following the LPS challenge, a substantial increase in the decreased claudin-5 expression was noted by FABP7 treatment *in vitro* and *in vivo* ($p < 0.0001$), while no statistically significant change was observed in the expression level of ZO-1 in bEnd.3 cells. *In vitro* and *in vivo* FABP7 administration following LPS significantly decreased the increased expression level of caveolin-1 ($p < 0.0001$), while a significant increase was found in the decreased expression level of mfsd2a ($p < 0.0001$). In terms of alterations in the inflammatory response, the increased levels of NF-κB *in vitro* and *in vivo* ($p < 0.01$) and interleukin-1β *in vitro* ($p < 0.001$) were markedly reduced by FABP7 treatment following LPS-induced BBB disruption. Our results suggest, for the first time, that exogenous FABP7 may account for a new pharmacological tool in the treatment of inflammation- and sepsis-related BBB disruption.

ÖZETÇE

Astrosit Kaynaklı Yağ Asidi Bağlayıcı Protein 7'nin LPS'ye Bağlı Enflamatuvar Koşullarda Kan-Beyin Bariyeri Bütünlüğü Üzerine Etkisi

Deniz Altunsu

Doktora, Hücresel ve Moleküler Tıp

Yoğun bakım hastalarında yaşamı tehdit eden ve önde gelen bir ölüm nedeni olan sepsis, kan-beyin bariyeri (KBB) bütünlüğünü bozar. Yağ asidi bağlayıcı protein 7 (FABP7), beyin astrosit hücreleri tarafından ekspres edilerek kaveola oluşumunu kontrol eder. Bununla birlikte, FABP7'nin lipopolisakkarid (LPS) ile gelişen enflamatuar koşullardaki KBB hasarı üzerindeki rolü henüz netleşmemiştir. Bu çalışma, eksojen FABP7 uygulamasının LPS'nin neden olduğu KBB yıkımı üzerindeki in vitro ve in vivo etkilerini araştırmaktadır. bEnd.3 hücrelerine 24 saat 0.5 μg/mL LPS ve ardından 24 saat FABP7 (0.5 μg/ml) uygulandı. KBB bütünlüğünü değerlendirmek için transendotelyal elektrik direnci (TEER) ölçülürken, KBB geçirgenliği sodyum floresein (NaFl) izleyicisi kullanılarak değerlendirildi. *In vivo* septik fare modeli intraperitonel LPS (3 mg/kg) enjeksiyonu ile elde edildi. LPS enjeksiyonundan 1 saat sonra, uyarılan hayvanlara 40 ve 80 μg/kg FABP7 enjeksiyonu intraperitonel olarak yapıldı. Deney grubundaki hayvanların vücut sıcaklıkları ve anksiyete seviyeleri ölçüldü. *In vivo* ve *ex vivo* KBB geçirgenliğini tayin edebilmek için enjeksiyonların 23. saatinde kuyruk damarından albümin Alexa fluor 594 belirteci verildi. Deney sonunda tüm hayvanlardan kan örneği alınarak prokalsitonin, C-reaktif protein ve serbest radikal seviyeleri ölçüldü. Sıkı bağlantı (TJ) proteinleri klaudin-5 ve zonula okkludens (ZO)-1, transsitozla ilişkili proteinler kaveolin-1 ve "major facilitator superfamily domain containing 2a" (mfsd2a) ve enflamatuvar medyatörler NF-κB ve interlökin-1β'nın ekspresyon düzeyler immünofloresan boyama ve western blotlama ile belirlendi. LPS uygulamasını takiben

FABP7 tedavisi, artan NaFl geçişini azaltırken ($p< 0.001$), azalan TEER değerlerini önemli ölçüde artırdı ($p< 0.05$). LPS koşullarında artan vücut sıcaklığı yüksek doz FABP7 tedavisini takiben düşerken, yine aynı koşullarda artan anksiyete seviyesi yüksek doz FABP7 ile önemli ölçüde azalmıştır ($p< 0.05$). Bununla birlikte LPS koşullarında artış gösteren PCT, C-RP ve ROS seviyeleri yüksek doz FABP7 enjeksiyonuyla beraber azalırken, yine aynı koşullarda meydana gelen KBB hasarı FABP7 tedavisiyle azalış göstermiştir ($p< 0.05$). FABP7 tedavisi, *in vitro* ve *in vivo* koşullarda azalmış olan claudin-5 ekspresyonunda da önemli bir artışa yol açarken ($p< 0.0001$), bEnd.3 hücrelerindeki ZO-1'in ekspresyon düzeyinde istatistiksel olarak anlamlı bir değişiklik gözlenmedi. Ayrıca, LPS'yi takiben FABP7 uygulaması artmış kaveolin-1'in ekspresyon düzeyini önemli ölçüde azaltırken ($p< 0.0001$), azalmış mfsd2a ekspresyon düzeyinde anlamlı bir artışa yol açmıştır ($p< 0.0001$). Enflamatuar yanıttaki değişiklikler değerlendirildiğinde, LPS'ye bağlı olarak *in vitro* ve *in vivo* NF-κB ($p< 0.01$) ve *in vitro*'daki interlökin-1β ($p< 0.001$) düzeyleri FABP7 tedavisi ile belirgin şekilde azaldı. Bulgularımız, ekzojen FABP7'nin, enflamasyon ve sepsise bağlı BBB yıkımının tedavisinde yeni bir farmakolojik yaklaşım olarak kullanılabileceğini önermektedir.

ACKNOWLEDGMENTS

First and foremost, I would like to express my heartfelt gratitude to my thesis advisor, Prof. Dr. Bülent Ahıshalı, for his unwavering kindness and support throughout my Ph.D. journey. His exceptional knowledge, meticulousness, encouragement, and unwavering belief in me and my research have been of immense assistance to my thesis and other research endeavors.

I would like to special thanks to Prof. Dr. Mehmet Kaya who graciously shared his valuable perspective and scientific expertise with me during my Ph.D. life. His guidance and insights have greatly contributed to the development of myself and my research history.

I would like to extend special thanks to Dr. Arzu Temizyürek for always being there when I needed her support, diligently reviewing my progress, and guiding me throughout my Ph.D. studies. I am truly honored to have had the opportunity to work with Dr. Temizyürek

I would like to give my deepest thanks to MK Lab members, Ecem Ayvaz and İrem Akbulak for their endless support and contributions to my thesis.

I would like to thank give my thankfulness to my love Esat Kurt for all support, strength, and love during my academic journey. I consider myself incredibly fortunate to be his life partner.

Finally, I would like to biggest thank to my mother, Süreyya Altunsu, and my father, Galip Altunsu, for endless support, love, and courage throughout my academic life. I wouldn’t be without their unconditional love, support, and unwavering faith in me. They have provided me with hope and strength. Their love is truly remarkable, and I am forever grateful for it...

TABLE OF CONTENTS

ABSTRACT ii
ÖZETÇE iv
ACKNOWLEDGMENTS vi
TABLE OF CONTENTS vii
LIST OF TABLES x
LIST OF FIGURES xi
ABBREVIATIONS xiii
CHAPTER 1 1
INTRODUCTION 1
CHAPTER 2 4
LITERATURE REVIEW 4
2.1 Blood-Brain Barrier and Neurovascular Unit 4
2.2 Historical Perspective of the Blood-Brain Barrier 5
2.3 Brain Barriers in the Central Nervous System 6
2.3.1 Blood-Brain Barrier 7
2.4 Molecular and Cellular Structure of Blood-Brain Barrier 8
2.4.1 Glycocalyx 8
2.4.2 Endothelial cells 9
2.4.3 Basal Lamina 10
2.4.4 Astrocytes 10
2.4.5 Pericytes 11
2.4.6 Microglia 12
2.4.7 Neurons 12
2.5 Molecular Compositions of the Tight Junctions 13
2.5.1 Occludins 14
2.5.2 Claudins 15
2.5.3 Junctional Adhesion Molecules 16
2.5.4 Membrane-associated Cytoplasmic Proteins in the Blood-Brain Barrier 17
2.5.6 Adherens Junctions 17
2.6 Transport Pathways Across the Blood-Brain Barrier 18
2.6.1 Paracellular Pathway 18
2.6.2 Transcellular Pathway 19

2.6.2.1 Carrier-Mediated Transport 19
2.6.2.2 Carbohydrate Transporters 19
2.6.2.3 Amino acids Transporters 20
2.6.2.4 Fatty Acids Transporters 20
2.6.2.5 Receptor-Mediated Transports 21
2.6.2.6 Caveolar Transcytosis 22
2.6.2.7 Efflux Transporters at the Blood-Brain Barrier 23
2.7 Inflammation in the Brain 24
2.7.1 Sepsis-induced Inflammation in Blood-Brain Barrier 27
2.8 Physiology of Fatty Acid Binding Proteins in Central Nervous System 29
2.8.1 Fatty Acid Binding Proteins 29
2.8.2 Fatty Acid Binding Proteins 31
2.9 Aims of the Study 33
CHAPTER 3**:** 35
MATERIALS 35
3.2 Chemicals 35
3.4 Laboratory Equipments 37
CHAPTER 4: 39
METHODS 39
4.1. In vitro Experimental Procedure 39
4.1.1. Endothelial Cell Culture 39
4.1.3. Cell Treatments 40
4.1.4. Sulforhodamine B Assay 40
4.1.5. Transendothelial Electrical Resistance 41
4.1.6. Sodium Fluorescein Permeability Assay 41
4.1.7. Western Blotting 42
4.1.8 Immunofluorescence Staining 43
4.2. In vivo Experimental Procedures 44
4.2.1. LPS and FABP7 Administrations 45
4.2.2. Monitoring Body Temperature 45
4.2.3. Behavioral Test 46
4.2.4. Evaluation of Inflammatory Biomarkers 46
4.2.5. Immunofluorescence Staining 46
4.2.6. Evaluation of Blood-Brain Barrier Permeability 47
4.2.7. Western Blot Analysis 48
4.3. Statistical Analysis 49
CHAPTER 5: 50

RESULTS 50
5.1 Effects of LPS Treatment on in vitro Blood-Brain Barrier Model 50
5.1.1 Effects of LPS on bEnd.3 Cell Viability 50
5.1.2 Effects of LPS on Transendothelial Electrical Resistance 51
5.1.3 Effects of LPS on Permeability 52
5.2 The Effects of FABP7 on in vitro Blood-Brain Barrier Model in Physiological Conditions 53
5.2.1 Effects of FABP7 on bEnd.3 Cell Viability 53
5.2.2 Effects of FABP7 on Transendothelial Electrical Resistance 54
5.2.3 Effects of FABP7 on Permeability 55
5.3 The Effects of FABP7 on in vitro Blood-Brain Barrier Model following exposure to LPS 56
5.3.1 Effects of FABP7 on Transendothelial Electrical Resistance 56
5.3.2 Effects of FABP7 on Permeability 57
5.4 Effects of FABP7 on the Immunoreactivity of BBB Proteins and Inflammatory Mediators in LPS-treated bEnd.3 Cells 58
5.4.1 Effects of FABP7 on Tight Junction Proteins 58
5.4.2 Effects of FABP7 on Transcytosis Regulating Proteins 60
5.4.3 Effects of FABP7 on Inflammatory Mediators 62
5.5 Effects of FABP7 on the Expression of BBB Proteins and Inflammatory Mediators in LPS-treated bEnd.3 Cells 64
5.6 Effects of FABP7 in C57Bl/6 mice under LPS-induced Inflammatory Condition .. 65
5.6.1 Effects of FABP7 on Body Temperature 65
5.6.2 Effects of FABP7 on Inflammatory Biomarkers 66
5.6.3 Effects of FABP7 on Anxiety-like Behavior 69
5.6.4 Effects of FABP7 on Blood-Brain Barrier Permeability 70
5.6.5 Effects of FABP7 on Blood Brain Barrier Permeability 72
5.6.6 Effects of FABP7 on the Claudin-5 Immunoreactivity in Cerebral Cortex and Hippocampus 75
5.6.7 Effects of FABP7 on the Expression Levels of BBB Proteins and NF-κB in the Brain 77
CHAPTER 6: 81
DISCUSSION 81
CHAPTER 7: 89
CONCLUSION 89
BIBLIOGRAPHY 90

LIST OF TABLES

Table 3. 1 List of cell line used in experiments. 35
Table 3. 2 List of chemicals used in experiments. 35
Table 3. 3 List of antibodies used in experiments. 37
Table 3. 4 List of laboratory equipment used in experiments. 37

LIST OF FIGURES

Figure 2.1 Biological barriers in the central nervous system (Kadry et al., 2020)..... 6
Figure 2.2 The main components of blood-brain barrier (Galea, 2021). 8
Figure 2.3 The multifunctional roles of pericytes at the NVU (Sweeney et al., 2016). 11
Figure 2.4 Schematic representation of Adherens and Tight junction complexes between brain type endothelial cells (Kaya & Ahishali, 2021). 14
Figure 2.5 Transport pathways across the blood-brain barrier(Cockerill et al., 2018) 18
Figure 2.6 Positive and negative features of neuroinflammation in the central nervous sytem (DiSabato et al., 2016). 26
Figure 2.7 Alteration in brain barriers under septic conditions (Danielski et al., 2018). 28
Figure 2.8 Uptake of PUFAs in the brain (W. Zhang et al., 2018). 31
Figure 4.2 The coronal brain section from P56 (https://mouse.-brain-map.org). 48
Figure 5.1 The effects of LPS on cell viability of bEnd.3 cells. The data were presented as mean±SD.****p< 0.001. 51
Figure 5.2 Effects of LPS on transendothelial electrical resistance in bEnd.3 cells. The data were presented as mean±SD. **p< 0.01 and ***p< 0.001. 52
Figure 5.3 Effects of LPS on BBB permeability. The data were presented as mean±SD. **p< 0.01, ***p< 0.001 and ****p< 0.0001. 53
Figure 5.5 Effect of FABP7 on transendothelial electrical resistance in bEnd.3 cells. The data were presented as mean±SD. *p< 0.05. 55
Figure 5.6 Effects of FABP7 on endothelial leakage in bEnd.3 cells. The data were presented as mean±SD..... 56
Figure 5.7 Effects of FABP7 on TEER in LPS-treated bEnd.3 cells. The data were presented as mean±SD. *p< 0.05 and **p< 0.01. 57
Figure 5.8 Effects of FABP7 on BBB permeability in LPS-treated bEnd.3 cells. The data were presented as mean±SD. ***p< 0.001 and ****p< 0.0001. 58
Figure 5.9 Immunofluorescence staining for claudin-5 in bEnd.3 cells exposed to LPS treated or untreated with FABP7 and quantification of immunofluorescence intensity with image analysis. In the micrographs, red color represents immunoreactivity for claudin-5 while the nuclei are stained with Hoechst (blue). The data in the graph were presented as mean±SD. ****p< 0.0001. 59
Figure 5.10 Immunofluorescence staining for ZO-1 in bEnd.3 cells exposed to LPS treated or untreated with FABP7 and quantification of immunofluorescence intensity with image analysis. In the micrographs, green color represents immunoreactivity for ZO-1 while the nuclei are stained with Hoechst (blue). The data in the graph were presented as mean±SD. ****p< 0.0001. 60
Figure 5.11 Immunofluorescence staining for caveolin-1 in bEnd.3 cells exposed to LPS treated or untreated with FABP7 and quantification of immunofluorescence intensity with image analysis. In the micrographs, red color represents immunoreactivity for caveolin-1 while the nuclei are stained with Hoechst (blue). The data in the graph were presented as mean±SD. ****p< 0.0001. 61

Figure 5.12 Immunofluorescence staining for mfsd2a in bEnd.3 cells exposed to LPS treated or untreated with FABP7 and quantification of immunofluorescence intensity with image analysis. In the micrographs, red color represents immunoreactivity for mfsd2a while the nuclei are stained with Hoechst (blue). The data in the graph were presented as mean±SD. ****p< 0.0001. 62
Figure 5.13 Immunofluorescence staining for NF-κB in bEnd.3 cells exposed to LPS treated or untreated with FABP7 and quantification of immunofluorescence intensity with image analysis. In the micrographs, red color represents immunoreactivity for NF-κB while the nuclei are stained with Hoechst (blue). The data in the graph were presented as mean±SD. ****p< 0.0001. 63
Figure 5.14 Immunofluorescence staining for IL-1β in bEnd.3 cells exposed to LPS treated or untreated with FABP7 and quantification of immunofluorescence intensity with image analysis. In the micrographs, red color represents immunoreactivity for IL-1β while the nuclei are stained with Hoechst (blue). The data in the graph were presented as mean±SD. ****p< 0.0001..... 64
Figure 5.16 Effects of LPS and/or FABP7 on body temperature in mice. 66
Figure 5.19 Effects of FABP7 on serum levels of ROS in experimental groups. The data were presented as mean±SD. **p< 0.01 and ***p< 0.001. 69
Figure 5.20 Effects of FABP7 on anxiety-like behavior in experimental groups. The data were presented as mean±SD. *p< 0.05 and **p< 0.01. 70
Figure 5.21 The in vivo effects of FABP7 on BBB leakage following LPS treatment. The data were presented as mean±SD. *p< 0.05 and **p< 0.01..... 71
Figure 5.22 The ex vivo effects of FABP7 on BBB leakage following LPS treatment. The data were presented as mean±SD. ***p< 0.001 and ****p< 0.0001..... 72
Figure 5.23 The effects of FABP7 on the increased BBB permeability by LPS in cerebral cortex. In the micrographs, red color represents the fluorescence of albumin Alexa fluor 594 tracer, and the nuclei are stained with Hoechst (blue). The data were presented as mean±SD. *p< 0.05, **p< 0.01 and ****p< 0.0001..... 73
Figure 5.24 The effects of FABP7 on the increased BBB permeability by LPS in hippocampus. In the micrographs, red color represents the fluorescence of albumin Alexa fluor 594 tracer, and the nuclei are stained with Hoechst (blue). The data were presented as mean±SD. **p< 0.01 and ****p< 0.0001..... 74
Figure 5.25 The effects of FABP7 on the increased BBB permeability by LPS in midbrain. In the micrographs, red color represents the fluorescence of albumin Alexa fluor 594 tracers, and the nuclei are stained with Hoechst (blue). The data were presented as mean±SD. *p< 0.05 and ****p< 0.0001..... 74
Figure 5.26 Effects of FABP7 on the immunofluorescence intensity of claudin-5 in the cerebral cortex following LPS treatment. In the micrographs, blue and red colors represent immunoreactivity for claudin-5 and lectin, respectively, while the nuclei are stained with Hoechst (gray). The data were presented as mean±SD. *p< 0.05, **p< 0.01 and ****p< 0.0001. 76
Figure 5.27 Effects of FABP7 on the immunofluorescence intensity of claudin-5 in the hippocampus following LPS treatment. In the micrographs, blue and red colors represent immunoreactivity for claudin-5 and lectin, respectively, while the nuclei are stained with Hoechst (gray). The data were presented as mean±SD. *p< 0.05, **p< 0.01, ***p< 0.001 and ****p< 0.0001..... 77
Figure 5.28 Effects of FABP7 on the expression levels of claudin-5, caveolin-1, mfsd2a and NF-κB in cerebral cortex of mice following LPS treatment. The data were presented as means±SD. *p< 0.05, **p< 0.01, ***p< 0.001 and ****p< 0.0001. 78

ABBREVIATIONS

AD	Alzheimer's Disease
Aβ	Amyloid Beta
BBB	Blood-Brain Barrier
BCRP	Breast Cancer Resistance Protein
CNS	Central Nervous System
CSF	Cerebrospinal Fluid
dH_2O	Distilled Water
DHA	Docosahexaenoic Acid
DMEM	Dulbecco's Modified Eagle Medium
FBS	Fetal Bovine Serum
HBSS	Hanks' Balanced Salt Solution
HEPES	Hydroxyethyl-Piperazineethane-Sulfonic Acid Buffer
HII	Hypoxic Ischemic-Induced Inflammation
HRP	Horseradish Peroxidase
IF	Immunofluorescent
IFN	Interferon
IL	Interleukin
IRF1	Interferon Regulatory Factor 1
IκBα	Inhibitor of Nuclear Factor-Kappa B

L-Glu	L-Glutamine
LPS	Lipopolysaccharide
Mfsd2a	Major Facilitator Super Family Domain Containing 2a
MMP	Matrix Metalloproteinase
MyD88	Myeloid Differentiation Factor 88
NaFl	Sodium Fluorescein
NF-κB	Nuclear Factor-kappa B
NGS	Normal Goat Serum
NO	Nitric Oxide
NRF2	Nuclear factor erythroid 2-related factor 2
OD	Optical Density
P-gp	P-glycoprotein
P/S	Penicillin-Streptomycin
PBS	Phosphate Buffered Saline
PBST	Triton X-100/PBS Solution
PD	Parkinson's Disease
RFU	Relative Fluorescence Units
ROS	Reactive Oxygen Species
SAE	Sepsis-Associated Encephalopathy
SD	Standard Deviation
SRB	Sulforhodamine B
SAH	Subarachnoid Hemorrhage
TC	Tissue Culture
TEER	Transendothelial Electrical Resistance

TGF-β	Transforming Growth Factor Beta
TJ	Tight Junction
TLR	Toll-Like Receptor
TNF-α	Tumor Necrosis Factor-Alpha
TNFR	Tumor Necrosis Factor-Alpha Receptor
TRAF6	Tumor Necrosis Factor Receptor Associated Factor
ZO	Zonula Occludens

CHAPTER 1

INTRODUCTION

Sepsis is one of the most common and serious pathologic conditions caused by dysregulated host response to infection, leading to multiple organ dysfunction. The disorder affects more than five hundred thousand people in the United States annually, with a hospitalization incidence of 62%, and shows high morbidity and mortality rates (Nwafor et al., 2019). The general symptoms of sepsis vary from person to person with the most prominent ones being headache, fewer, cognitive dysfunction, memory decline, delirium, and sepsis-associated encephalopathy (SAE) (Gofton & Bryan Young, 2012).

The stages of sepsis can be defined as the initial, severe, and septic shock. The infection derived from bacteria, viruses, or fungi induce the initial stage of sepsis, which results in systemic inflammatory response syndrome (SIRS). Severe sepsis commonly results in organ dysregulation, hypoperfusion, or hypotension, whereas septic shock is a severe sepsis complication that leads to multiple organ failures.

Sepsis-associated encephalopathy causes acute neurological dysfunction followed by neuroinflammation and mitochondrial dysfunction in the central nervous system (CNS). The disorder of SAE increases the number of leukocytes and the level of free radicals in the neural tissues which results in clinical coma and seizures. The diagnosis is made by clinical examination, detection of biomarkers in serum, and EEG changes, but is limited because of the multifaced syndrome (Orhun et al., 2020).

The blood-brain barrier (BBB) is defined as a semipermeable biological interface that separates the brain parenchyma from peripheric tissues and provides optimal neuronal microenvironment in the brain. The main component of BBB is the brain capillary endothelial cells that express specialized tight junction (TJ) proteins, receptors, and carrier proteins which restrict the passage of blood-borne substances and immune cells into the brain via paracellular and transcellular pathways. Septic conditions

contribute to the activation of endothelial cells, breakdown of TJs, and increased BBB permeability, resulting in the development of neuroinflammation, and disruption of BBB integrity (Barichello et al., 2021). The activated endothelial cells release the inflammation-related mediators such as tumor necrosis factor-alpha (TNF-α), interleukin (IL)-1β, and matrix metalloproteinases (MMPs) 2/9 (Cabral-Pacheco et al., 2020).

The disruptive effects of sepsis on BBB have been demonstrated by various experimental models, encompassing both *in vitro* and *in vivo* studies, but the underlying mechanisms have not yet been clarified. In order to mimic septic conditions, immunogenic components have been used in preclinical studies where lipopolysaccharide (LPS) is the routinely utilized endotoxin in *in vitro* and *in vivo* setups. A recent study showed that the severity of LPS-induced septic inflammatory conditions may change in a dose- and time-dependent manner and disrupt the BBB integrity with diverse patterns (Banks et al., 2015).

When LPS binds to Toll-Like Receptor-4 (TLR-4), the initiator cytoplasmic proteins, including Myeloid Differentiation Primary Response Gene 88 (MyD88) and TIR Domain-Containing Adaptor Protein (TIRAP) are activated (Du & Wang, 2020a; Sakai et al., 2017). It is reported that the activated cytoplasmic proteins lead to the translocation of nuclear factor kappa-light-chain-enhancer of activated B cells (NF-κB) from the cytoplasm to the nucleus (Sakai et al., 2017; Trask, 2004). The translocated NF-κB caused by LPS activates the inflammation-related genes, thereby increasing the levels of inflammatory mediators and reactive oxygen species.

Recent studies showed that LPS disrupts the integrity of BBB by decreasing transendothelial electrical resistance (TEER), degrading TJs, disrupting the endothelial glycocalyx, and increasing astrocytic activities (Boitsova et al., 2018; Peng et al., 2021).

The fatty acid binding protein 7 (FABP7), a small cytoplasmic protein, is predominantly expressed by astrocytes and precursors of oligodendrocytes during the embryonic development of the brain. It also modulates astrocytic function by controlling intracellular fatty acid homeostasis by delivering fatty acids. Moreover, FABP7 controls the function of lipid rafts in the plasma membrane of astrocytes by regulating caveolin-1 protein. Accumulated data have shown that the expression of FABP7 is increased in activated astrocytes under pathologic conditions (Islam et al., 2019a; Rui et al., 2019a). A recent study demonstrated that the activation and migration of astrocytes are directly

related to increased expression of FABP7 in pathological conditions (Killoy et al., 2020). It is reported that docosahexaenoic acid (DHA), a member of omega-3 fatty acid families, supports brain development so the circulating fatty acids reach the brain parenchyma via FABP7 (Choi et al., 2021; Matsumata et al., 2012).

In light of the above-mentioned literature data, our current study aims to clarify the role of FABP7 on BBB disruption in the setting of septic inflammatory conditions caused by LPS, by evaluating BBB permeability, expression of BBB related proteins, inflammatory mediators, and behavioral changes.

CHAPTER 2

LITERATURE REVIEW

2.1 Blood-Brain Barrier and Neurovascular Unit

It is well known that the brain is the most complex organ which needs extremely well-balanced environment for proper brain function. The CNS requires a specific protection which is provided by certain barrier systems, including BBB, blood-cerebrospinal fluid barrier (CSF), and arachnoid barrier (Mahringer et al., 2014; Saunders et al., 2008). The barrier systems control the passage of ions, nutrients, and immune cells into the brain, thus they maintain neuronal homeostasis in the CNS. The mentioned barrier systems have also significant challenge to develop drugs and antibodies for treatment of neurodegenerative disorders/diseases. It is reported that recombinant peptides, anti-sense agents, almost 98% of small substances, and all macromolecules cannot reach the brain because of the architecture of the barrier system (Pardridge, 2005b).

The blood-brain barrier consisted of capillary endothelial cells is supported by basal lamina, pericytes, astrocytes, microglia, and neurons, and this complex structure is called as neurovascular unit (NVU). This unique barrier plays a vital role in maintaining normal neuronal environment by preventing the passage of blood-borne toxic substances and immune cells into the brain (Tajes et al., 2014). The barrier-type endothelial cells are tightly sealed to other endothelial cells via TJ proteins to control the paracellular pathway (Wang et al., 2021).

2.2 Historical Perspective of the Blood-Brain Barrier

An early indication of a barrier in the brain was recorded by German immunologist Paul Ehrlich in 1885 (Davson, 1989; Villabona-Rueda et al., 2019). When he injected a water-soluble dye into the circulation of the rabbit, all peripheric organs were stained, but this dye cannot reach the brain parenchyma and spinal cord. Firstly, his observations were related with the low-affinity binding of dyes for the unstained regions regardless of a barrier between the blood and brain tissue. Next, he conducted different experimental setups with the same dye. When the dye was injected into the subarachnoid space, German observed the stained brain/spinal cord and unstained peripheral tissues. In the light of these studies, German came up with the idea of a barrier between the blood and brain (Galea et al., 2007).

In 1898-1900, the idea of a barrier in the CNS was discovered by Kraus and Lewandowsky who used two different nontoxic pharmacological substances, cholic acids and sodium ferrocyanide. After the injection of these substances into the circulation, they observed unstained brain tissues. According to their observations, since certain dyes had a high affinity to bind the plasma proteins, these dyes cannot pass from blood to the brain.

In 1909-1913, Goldmann performed two different experimental setups followed by the injection of trypan blue into the brain ventricular system and circulation of dogs and rabbits. When he introduced dye to the circulation, he observed the stained whole body of the animal and choroid plexuses, except for the brain and spinal cord. In contrast to injection into the circulation, when Goldmann injected dye into the brain ventricular system, he observed stained brain and spinal cord. According to Goldmann, these results were not related to the binding affinity of dyes and related to the transport of dye into CNS via spinal fluid.

In 1930, Friedrich Karl Walter mentioned the differences between the BBB and blood-CSF barrier, and other barriers must be involved in the CNS because the flow of CSF via the blood-CSF barrier alone was not enough to support gas exchange (Bothwell et al., 2019; Pachter et al., 2003).

In 1960, the current composition of the BBB was defined by Karnovsky who used electron microscopy to show the accumulation of horseradish peroxidase (HRP) in the lumen of blood microvessels but not within the vascular endothelium.

2.3 Brain Barriers in the Central Nervous System

The proper neural function where in the CNS is provided by different barrier systems including, the BBB, the blood-CSF barrier, the arachnoid barrier, blood–retinal and spinal cord barriers. The primary functions of these barriers are to protect the neurons from blood-borne toxic substances, maintain neuronal homeostasis and provide a favorable environment for CNS. These barriers are constituted by different cell types of CNS. A previous study mentioned that the BBB constituted by the brain microvessel endothelial cells, the blood-CSF barrier formed by the epithelial cells of the choroid plexus, and the arachnoid barrier consisted of the avascular epithelium under the dura control the free passages of molecules and protect the CNS against undesirable microorganisms by managing the immune system in the brain (Wolburg, Noell, Mack, et al., 2009).

Brain-type endothelial cells express specialized tight junction (TJ) proteins to prevent the paracellular movement of substances across the brain parenchyma and preserve the electrolyte levels in the brain from fluctuations in the blood (Kimelberg, 2004). It is reported that TJ proteins tightly control the passage of circulatory immune cells across the brain (Kimelberg, 2004).

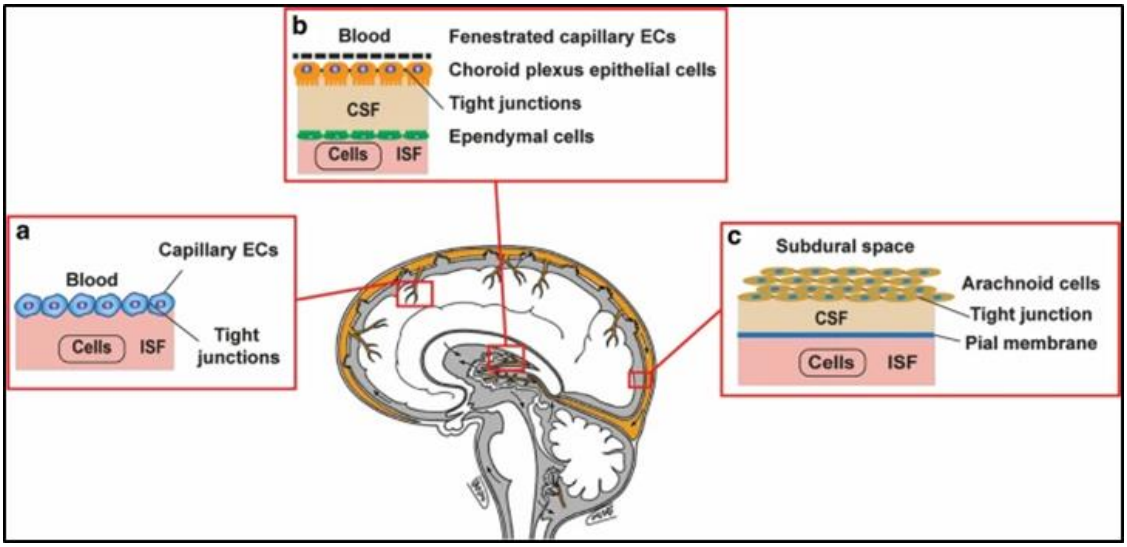

Figure 2.1 Biological barriers in the central nervous system (Kadry et al., 2020).

Certain areas in the brain lack barrier properties, and these areas are called as the circumventricular organs (CVOs) in the third and fourth ventricles do not contain barrier-type blood microvessels instead, they have fenestrated-type blood microvessels but are present in pial arteries, arterioles as well as veins. (Bentivoglio et al., 2018; Oldfield & McKinley, 2015). A previous study highlighted that the fenestrated capillaries with loosely connected astrocytic endfeet allow the penetration of blood-borne substances into the CVO tissue (Sisó et al., 2010). On the other hand, CVOs help to maintain brain homeostasis with contact points among the blood, CSF, and brain parenchyma (Ueno, 2007). The CVOs are classified into secretory and sensory types. The neurohypophysis (NH), median eminence (ME), and pineal gland (PG) are involved in secretory CVOs which are responsible for the transport of neurochemicals, hormones, peptides, and chemoreception into the peripheral vascular system (Jeong et al., 2021). The sensory types of CVOs are the subfornical organ (SFO), organum vasculosum of the lamina terminalis (OVLT), and area postrema (AP) (Horsburgh & Massoud, 2013). The SFO manages the salt-water intake in the sodium channels (Hiyama et al., 2004). The OVLT is a chemosensory area and identifies peptides and other substances. The AP also controls the vomiting reflexes and feeding.

2.3.1 Blood-Brain Barrier

The BBB is defined as a dynamic interface between the tissues of the CNS and the bloodstream (Knox et al., 2022). It is well-known that the BBB constituted by brain microvessel endothelial cells is called as a selective barrier. A recent review mentioned that this complex structure protects the neuronal tissues thereby maintaining homeostasis in the CNS (Kaya & Ahishali, 2021). The penetration of molecules including pathogens and blood-borne substances from the circulation into the brain is prevented by BBB (Strazielle & Ghersi-Egea, 2015), thus it protects the brain parenchyma. Moreover, BBB provides an optimal environment for ion and protein homeostasis via neuronal signaling and connectivity (Zidarič et al., 2022).

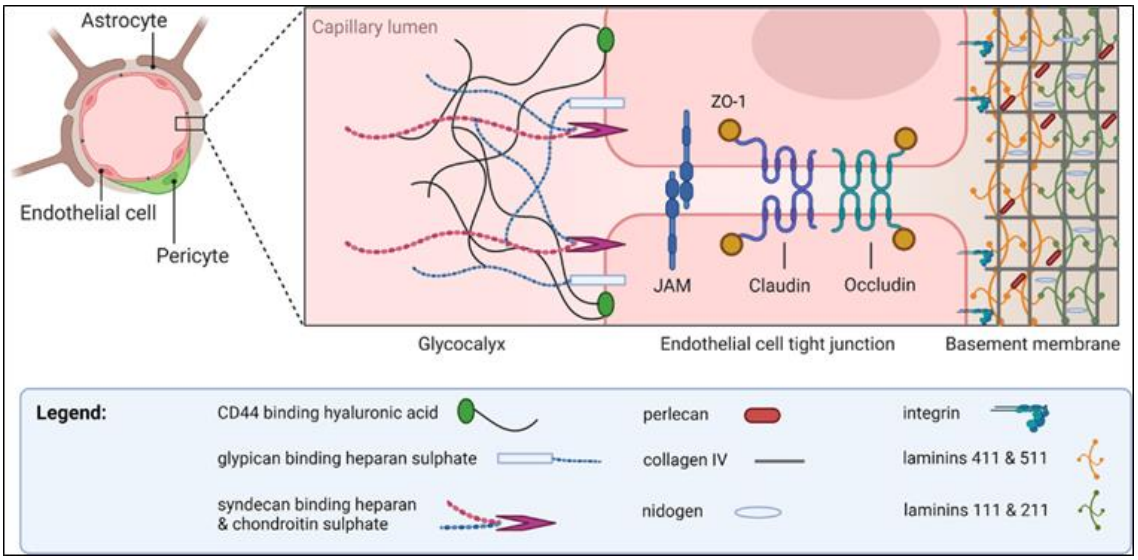

Figure 2.2 The main components of the blood-brain barrier (Galea, 2021).

The endothelial cells of cerebral blood microvessels have distinct features compared with other endothelial cells in peripheral tissues. The capillary endothelial cells in the brain are sealed by specialized TJ proteins and lack of fenestration between the neighboring cells to prevent the freely paracellular passage of substances across the brain. The brain endothelial cells also express the specific types of transporter and receptor to adjust the influx/efflux of nutrients, essential amino acids, and unwanted substances, thereby limiting transcytosis.

The composition of NVU is described by the interactions between the endothelial cells, basal lamina, pericytes, astrocytes, microglia, and neurons. Previous studies showed that each component of NVU provides a dynamic interaction with other cells in CNS, thereby managing the synaptic activity, controlling the BBB permeability, and regulating the CNS development (Ballabh et al., 2004; Iadecola, 2004; Langen et al., 2019; Staddon & Rubin, 1996; Zonta et al., 2003). Therefore, the NVU is also responsible for preserving normal brain function by regulating BBB integrity (X. Yu et al., 2020).

2.4 Molecular and Cellular Structure of Blood-Brain Barrier

2.4.1 Glycocalyx

The glycocalyx constituted by glycosaminoglycans, glycoproteins, and proteoglycans protects the luminal side of blood microvessels, which is attached to the surface of endothelial cells through the protein CD44 (Möckl, 2020). The capillary brain endothelial cells produce the orosomucoid which gives a negative charge to the glycocalyx. Therefore, plasma proteins with a negative charge cannot reach the BBB (Sörensson et al., 1999). A recent study showed that the overall coverage of a capillary luminal surface was found to be highest in the brain (40%), followed by the heart (15%), and then the lungs (4%) (Galea, 2021) and therefore, the glycocalyx found in the brain provides a more formidable barrier compared to that of the rest of the body. Accumulated data have demonstrated that the activated MMPs by LPS degraded the cerebral endothelial glycocalyx by reducing in thickness and coverage of basal lamina in rodents (Ando et al., 2018; J. H. Yoon et al., 2017).

2.4.2 Endothelial cells

The specialized brain capillary endothelial cells express TJ proteins, show low levels of caveolar transcytosis, and have specific transporters for polar substances via solute carriers. Additionally, they have efflux transporters to remove the toxic molecules from brain parenchyma into the circulation via ATP-binding cassette and p-glycoproteins (Huttunen et al., 2022; Lippmann et al., 2012; Zlokovic, 2009). There is also no fenestration between the brain-type endothelial cells thanks to TJs, such as claudins, occludin, and junctional adhesion molecules (Lochhead et al., 2020). These molecular complexes block the paracellular diffusion of molecules by creating a continuous line between the endothelial cells of blood microvessels. The zonula occludens (ZO-1, ZO-2, and ZO-3) expressed by brain type endothelial cells create a bridge between the TJ proteins and actin cytoskeleton. Moreover, cerebrovascular endothelial cells express low levels of E- and P-selectins, adhesion molecules mediating the first step in leukocyte extravasation, and the integrin ligands ICAM-1, PECAM-1, and VCAM-1.

2.4.3 Basal Lamina

The thickness of the basement membrane is approximately 20–200 nm, which is present within the basal surface of the vascular endothelial cells. The structural components of the basal lamina are sulfate, laminins, collagen-IV, fibrillins, vitronectin, fibronectin, elastin, and nidogens (Destefano et al., 2018). The basal lamina is classified into the endothelial and parenchymal basal lamina which are separated by pericytes (Luissint et al., 2012). The essential role of basal lamina is to preserve the BBB integrity by involving signal transduction, structural support, and cell communications between the cells of NVU (L. Xu et al., 2019).

2.4.4 Astrocytes

One of the main components of NVU is astrocytes which are the most abundant cell type of glial cells. They are vital to maintain brain homeostasis because 99% of brain capillaries are covered by astrocyte end-feet, thereby providing cell-cell communications between the cells in NVU. Moreover, astrocytes play essential roles in the regulation of blood flow and transportation of nutrients from the blood to the brain through direct contact with blood vessels. They also support pH regulation in the extracellular side of the brain (Gee & Keller, 2005; Kubotera et al., 2019). In the meantime, astrocytes control the BBB integrity via neurotransmitter clearing, recirculation, and modulation of immune responses (Gee & Keller, 2005). The communication of astrocytes and endothelial cells is crucial to secrete several inducible factors for the morphology and phenotype of BBB during angiogenesis. It is reported that the regulation of brain endothelial cells is managed by vascular endothelial growth factor (VEGF), angiopoietin-1, and glial cell line-derived neurotrophic factor (GDNF) by astrocytes, leading to maintain BBB homeostasis (Cabezas et al., 2014; Heithoff et al., 2021; S. Zhang et al., 2021).

Throughout the early stage of embryogenesis, embryonic blood microvessels need VEGF for vascular genesis. A previous study showed that GDNF promotes the survival and differentiation of dopaminergic neurons, thereby protecting neurons in the brain (Kokaia, 2009). Angiopoietin-I interacts with tyrosine kinase (Fiedler et al., 2003), which shows protective effects on BBB integrity via reducing plasma leakage, vascular inflammation, and endothelial cell mortality (Brindle et al., 2006).

2.4.5 Pericytes

Pericytes were discovered by Rouget in 1874 (Dore-Duffy, 2008). Pericytes are branched cells and show the contractile properties that envelop microvessel endothelial cells in the brain. Pericytes maintain the brain homeostasis at BBB throughout providing communication between the endothelial cells and the rest of the cells of NVU. Pericytes are separated from endothelial cells, and astrocytes endfeet by the basal lamina. Pericytes are mainly present in the capillary wall and are directly connected with endothelial cells by sharing basal lamina. Integrin receptors are responsible for the attachment of pericytes and endothelial cells to the extracellular matrix of the basal lamina (Edwards & Bix, 2019). So, these two cells construct direct peg-socket contacts like membrane structures to support microvascular stability and vessel constancy (Perrot et al., 2020). Pericytes regulate the structure and diameter of brain capillaries, thereby managing cerebral blood flow (Hariharan et al., 2022). A recent study showed that the permeability of the BBB is directly related to the coverage and the number of pericytes; a reduction in pericyte coverage is correlated with a higher permeability of BBB (Z. Sun et al., 2021). In addition, pericytes regulate the tightness and permeability of BBB by managing TJs (Hori et al., 2004). The differentiation and proliferation of endothelial cells are managed by pericytes during angiogenesis therefore, they contributed to the new formation of vessels (Hattori, 2022).

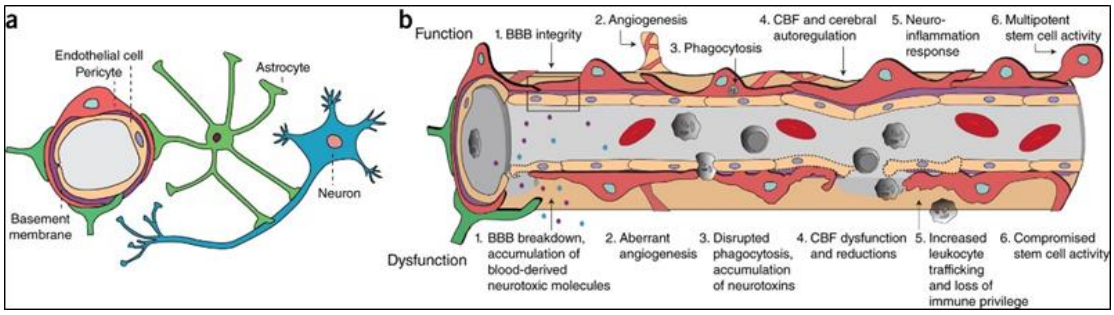

Figure 2.3 The multifunctional roles of pericytes. (a) The cells of NVU and (b). the role of pericytes under physiological and pathological conditions (Sweeney et al., 2016).

2.4.6 Microglia

Microglia were defined as different types of glial cells in CNS by del Rio-Hortega in 1932 (Boullerne & Feinstein, 2020). Since these cell types are involved in the first line of immune responses for the preservation of brain tissue against pathological conditions including sepsis, infection related diseases, or neurological disorders, they can be called immune cells of the brain. There are two types of microglia; these are M1 and M2 states and they show positive and negative activities under pathologic conditions. While M1 microglia stimulates inflammation and neurotoxicity, M2 microglia show protective effects by releasing anti-inflammatory cytokines and neurotrophic factors (S. Guo et al., 2022; O'Loughlin et al., 2018). Microglia switch to their activated state under inflammatory conditions. So, reactivated microglia induce neuroinflammation by increasing the levels of cytokines, chemokines, and ROS (Subhramanyam et al., 2019). Both activated microglia and induction of neuroinflammation are directly related to the impairment of BBB. A recent study suggested that activated microglia caused by LPS increased the production of chemokines in the co-culture of microglia and astrocytes (Kirkley et al., 2017). While LPS dramatically decreased TEER and increased tracer permeability in in vitro BBB model (Shimizu et al., 2018).

2.4.7 Neurons

Since the neurons have a complex homeostatic microenvironment, they can be considered peacemakers of NVU. Since neurons are sensitive cells in the CNS, any alterations in their supply of nutrients and oxygen affect neuronal cells, thereby converting these signals into electrical or chemical signals for other neurons and astrocytes (Macvicar & Newman, 2015). In addition, neurons affect the vascular tone and the blood supply for the microenvironment (Kaplan et al., 2020). It is well known that astrocytes control the neuronal levels of glutamate and GABAergic neurons by converting these signals into vasomotor commands. Pathological conditions, including ischemia, hemorrhage, and traumatic brain injury, cause the disruption of the BBB integrity by fluctuating cerebral blood flow and perfusion pressure. Accordingly, there has been proof that BBB permeability can be modulated by neuronal microvascular communication. Nerve cells have a great neuronal networks supplied by microvessels

thus, this communication between neurons and capillary blood vessels is crucial for the BBB integrity (Moolayil, 2019). Another study showed that the interaction of brain type endothelial cells with astrocytes is regulated by the neurons of noradrenergic, acetylcholinergic, and GABAergic (T. Ronaldson & P. Davis, 2012).

2.5 Molecular Compositions of the Tight Junctions

The first concept of TJs was discovered by Farquhar and Palade in 1960 (Cummins, 2012). Tight junction proteins between the endothelial cells provide structural integrity for these cells by managing apical interactions between adjacent cells. They provide a highly selective and restrictive barrier to control the paracellular pathway. Under physiological conditions, the molecules with small lipophilic, <400 Da or up to eight hydrogen bonds, and dissolved gases can pass into the brain parenchyma from the circulation. Both the high electrical resistance of BBB (more than 1500 Ω cm^2) and TJs prevent the free passage of substances thus, controlling the paracellular pathway (Greene & Campbell, 2016).

There are two main types of junctional molecules at BBB. These are tight and adherent junctions. Tight junctions and integral membrane proteins of BBB are claudins, occludin, junctional adhesion molecules (JAMs), and different cytoplasmic proteins including ZO-1, ZO-2, ZO-3, and cingulin. The connections between trans-membrane proteins and actin are provided by zonula occludens-1, -2, -3 which manage endothelial cells' structural and functional integrity (Kadry et al., 2020b). Adherent junctions are formed by the cadherin-catenin complexes with their integrated proteins. Cytoplasmic and integral membrane proteins are directly associated with the permeability of brain microvessel endothelial cells. The other components of TJ proteins are endothelial selective adhesion molecules (ESAM) and JAM from the immunoglobulin superfamily. The primary role of all junctional components is to control the paracellular permeability between brain type endothelial cells (Costea et al., 2019; Steed et al., 2010). The structural dislocation or disruption of TJ proteins disrupts the BBB integrity, which contributes to the development of cancers, stroke, diabetic retinopathy, and inflammatory diseases in the brain (Förster, 2008; Wardlaw et al., 2009).

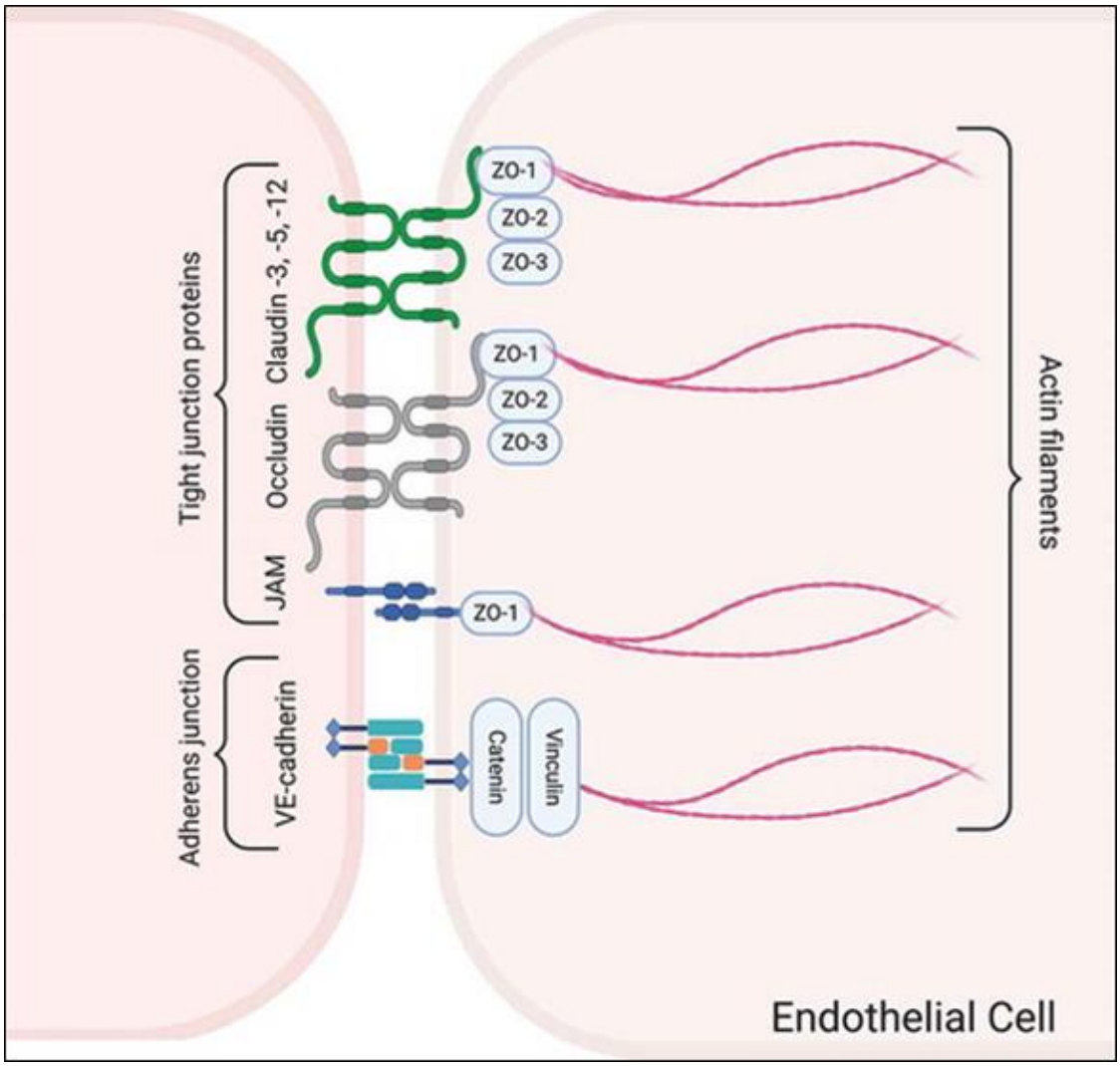

Figure 2.4 Schematic representation of Adherens and Tight junction complexes between brain type endothelial cells (Kaya & Ahishali, 2021).

2.5.1 Occludins

Occludin, 65 kDa phosphoprotein, was first defined in chickens and mammals (Ando-Akatsuka et al., 1996; Furuse et al., 1993). The authors demonstrated that occludin protein is expressed in the brain of rodents and adult humans, while its expression has not been detected in fetal and human newborn brains (Kadry et al., 2020b). Occludin consists of two extracellular loops and four transmembrane helix structures besides of long carboxyl (COOH)- and a short amino (NH2)-groups in the cytoplasm (Furuse, 2010). The occludin proteins found in a cytoplasmic domain are directly linked to the guanylate kinase domain (GUK) domains of ZO proteins (Bauer et al., 2010), therefore it plays structural and signaling roles at BBB (McCaffrey et al., 2009)

It is well-known that occludin is vital for proper function of TJ proteins. While overexpression of occludin protein improved the TEER (McCarthy et al., 1996), the inhibition of this protein did not alter intact BBB properties in mice (Saitou et al., 2000). Since the occludin regulates the leakage in brain endothelial cell, it is essential for BBB integrity (Keaney & Campbell, 2015). Another study showed that the downregulation of occludin protein by VEGF or phospholipase D2 (PLD2) is closely related to an increase in endothelial permeability (Murakami et al., 2009; Zeiller et al., 2009). Therefore, the primary function of occludin is to control the paracellular pathway via providing the TJ stability.

2.5.2 Claudins

Claudins, 20-27 kDa phosphoproteins, especially claudin-1 and -5 are the essential component of TJs in terms of forming the BBB. The cytoplasmic proteins, ZO-1, ZO-2, and ZO-3 are connected with claudin proteins via the carboxy terminus (Furuse et al., 1999). Claudin proteins are defined as pore-forming claudins and sealing claudins depending on tissue types. The pore-forming claudins increase permeability, whereas the sealing claudins control paracellular permeability. The study showed that the inflammatory conditions significantly increased the expression level of pore-forming claudin-2, which resulted in increased BBB permeability (Barrett, 2020). While other pore-forming claudins are also claudin-7, -10, -15, and -16, the sealing claudins, claudin-1, -3, -5, -11, and -19, control the paracellular permeability in tissues (Uc et al., 2020).

The most important TJ protein is claudin-5 expressed in brain type endothelial cells, which is directly related to the paracellular pathway of BBB (Vanlandewijck et al., 2018). It has been reported that *in vivo* knockout model of claudin-5 allowed the penetration of substances with 400-800 Da into the brain from blood circulation and increased the permeability of BBB (Nitta et al., 2003). Accordingly, the size-selective modulation of BBB permeability is managed by claudin-5 (Nitta et al., 2003).

Accumulated data have shown that inflammation and diabetic conditions decreased the expression level of claudin-5, which resulted in increased BBB permeability (Arima et al., 2020; Camire et al., 2015). The expression level of claudin-5 is decreased under pathologic conditions, which results in the penetration of leukocytes,

neurotransmitter, and/or free radicals into the brain, thus the BBB integrity is lost. While increased expression of claudin-5 in the endothelium is directly related to the tightness of BBB, the high expression level of claudin-5 disrupts the barrier in the alveolar epithelia (Overgaard et al., 2011).

It is shown that the activation of MMPs increases the BBB permeability through the breakdown of claudin-5 (Rempe et al., 2016a). Since there are reversely relationship between MMPs and TJ proteins, some MMP inhibitors are used to avoid the rapid disruption of claudin-5, thereby restoring BBB integrity (Y. Yang & Rosenberg, 2011). Otherwise, accumulated data suggested that inhibition of claudin-5 could be a promising technique for delivering drugs with small molecular weight to treat some CNS disorders/diseases (Hashimoto et al., 2021; Tachibana et al., 2020).

2.5.3 Junctional Adhesion Molecules

Junctional adhesion molecules, 40 kDa proteins, were described in 1998. They belong to the immunoglobulin superfamily (Tachibana et al., 2020). The cells of the leukocytes, endothelial and epithelial predominantly express the JAMs (Kummer & Ebnet, 2018). These adhesion molecules are created by one transmembrane domain and two immunoglobulin-like loops, and they are attached to each other via disulfide bonds in their extracellular component (Kadry et al., 2020b). It has been demonstrated that JAM-1 and JAM-3 are expressed in BBB, but JAM-2 are not (Aurrand-Lions et al., 2001). The junctional adhesion molecules are responsible for the adhesivity between the cells, and transmigration of monocytes across BBB (Bazzoni et al., 2000).

JAM-1, the first identified junction molecule, is present in TJs of endothelial cells. So, JAM-1 manages the BBB permeability (W. Y. Liu et al., 2012). JAM-2, a part of TJ proteins, is presided by serine phosphorylation. The fundamental role of JAM-2 is to maintain BBB integrity by providing cell adhesion. A recent study showed that JAM-3 is expressed by brain capillary endothelial cells, and dysfunction of JAM-3 leads to hemorrhage (De Rose et al., 2021).

2.5.4 Membrane-associated Cytoplasmic Proteins in the Blood-Brain Barrier

Cytoplasmic proteins are defined as ZO-1, ZO-2, ZO-3, and cingulin. These proteins regulate the integrity of TJ proteins by creating a cytoplasmic bridge between TJs and cell cytoskeleton (W. Y. Liu et al., 2012). The ZOs are known as membrane-associated guanylate kinase-like proteins (MAGUKs), and there is a similar sequence between ZO-1 (220 kDa), ZO-2 (160 kDa), and ZO-3 (130 kDa) (Oliva et al., 2012). These proteins located in the plasma membrane serve as protein-binding molecules and they are constituted by complex structure of PDZ, sh3, and GUK domains (Te Velthuis et al., 2007). In order to bind the ZO-1 to the COOH side of claudins and occludin, the domains of PDZ and GUK are used (Itoh et al., 1999; Mitic et al., 2000). The cytoskeleton protein of actin is attached to the COOH-side of ZO-1 and ZO-2, thereby providing structural support with transmembrane proteins (Haskins et al., 1998; Kadry et al., 2020b).

2.5.6 Adherens Junctions

Adherens junctions (AJs) can be defined as cell–cell adhesion complexes and they have essential roles in contributing the embryogenesis and tissue homeostasis (Gumbiner, 2005; Halbleib & Nelson, 2006; Harris & Tepass, 2010). This complex structure is formed by cadherin adhesion molecules, which participate in the actin cytoskeleton by means of catenin to construct the adhesive contacts between cells (W. Li et al., 2018). The scaffold proteins of ZO-1, ZO-2, and ZO-3 attach the occludin proteins to intracellular actin molecules via cingulin at the BBB (Wolburg, Noell, Wolburg-Buchholz, et al., 2009; Wolburg & Lippoldt, 2002)

A recent study indicated that the brain microvessels express the proteins of cadherin and vinculin in rats (Singh & Vellapandian, 2022). It has been reported that the assembly of TJ proteins is affected by the interactions of ZO-1 and catenins in the BBB (Matter & Balda, 2003), because the negative alterations in the adhesivity of AJs increased the permeability of BBB (Staddon & Rubin, 1996). The authors showed that both intracellular and extracellular calcium ion concentrations are regulated by the assembly of TJ and AJs, which is resulted in enhanced TEER (Abbott et al., 2006; Balda et al., 1991).

2.6 Transport Pathways Across the Blood-Brain Barrier

Cerebral microvessels endothelial cells have distinct properties from endothelial cells in peripheric tissues as they express specialized TJ proteins and contain a few cytoplasmic vesicles. These TJs restrict the paracellular route. There are two main transport systems across BBB. They are paracellular and transcellular pathways for ions, nutrients, immune cells, and some macromolecules. These two-barrier systems control the movement of substances across the brain.

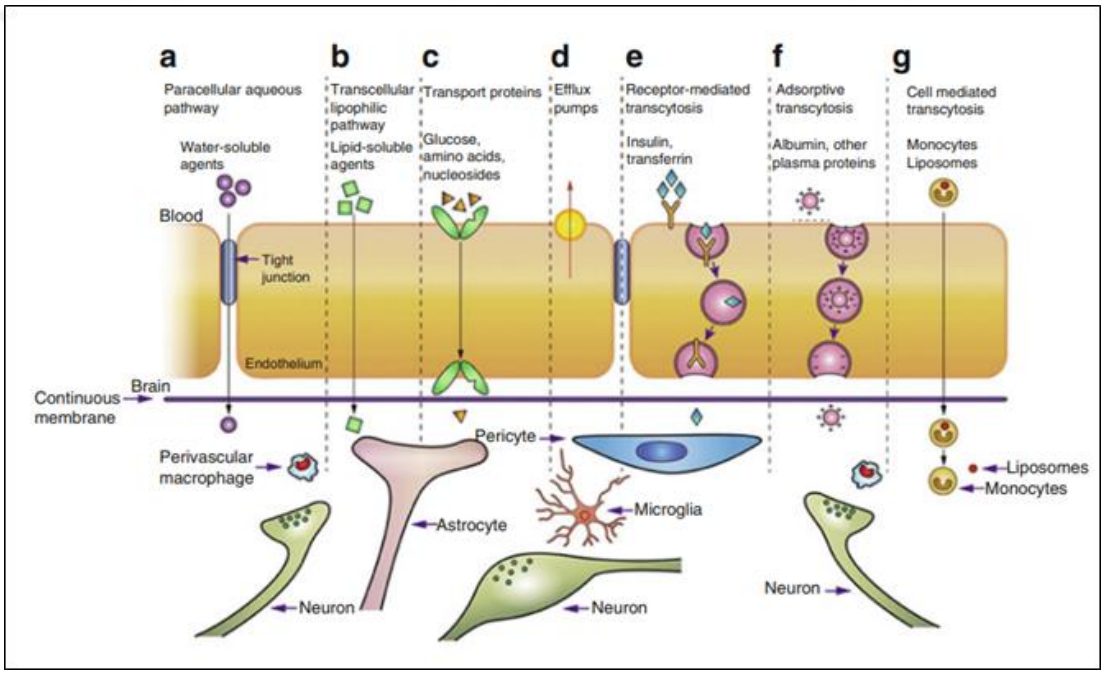

Figure 2.5 Transport pathways across the blood-brain barrier (Cockerill et al., 2018) .

2.6.1 Paracellular Pathway

The paracellular pathway can be defined as passive diffusion. The hydrophilic substances use paracellular route to pass into the brain, while the lipophilic substances with small molecular weight (<400 Da) passively enter the brain via tight junction proteins (Pardridge, 1995). In addition, paracellular diffusion is an energy-independent process and is directly related to the concentration of unbound substances gradient (Cocucci et al., 2017; Tarran et al., 2001). However, small-lipophilic molecules like

diazepam or opioids can pass into BBB using transcellular passive diffusion (Puris et al., 2022). As chemical features of molecules affect the BBB permeability, their improvement can be used for CNS drug development (Pajouhesh & Lenz, 2005; Waring, 2009). Nevertheless, the paracellular pathway serves a limited role in the development of brain-targeted medications for the treatment of certain brain-related disorders (Cockerill et al., 2018).

2.6.2 Transcellular Pathway

Although BBB freely allows the penetration of O_2, CO_2, and small lipophilic molecules, the hydrophilic molecules of glucose, ions, and amino acids cannot enter the brain without substrate specific receptors (Aragón-González et al., 2022). So, electrical-charged and hydrophilic molecules use different transport systems on brain endothelial cells, and these are defined as carrier-mediated transport (CMT), receptor-mediated transport, and efflux/influx transporters at BBB (Komarova & Malik, 2009).

2.6.2.1 Carrier-Mediated Transport

Some macromolecules, including glucose, galactose, amino acids, vitamins, fatty acids, nucleotides as wells as hormones, enter the brain parenchyma via the CMT system (Khan et al., 2018). The ATP-dependent system carries these substances from the blood to the brain. The proteins involved in this pathway are expressed by the solute carrier transporter genes, which are located at both the luminal and abluminal parts of the capillary endothelial cells (Morris et al., 2017).

2.6.2.2 Carbohydrate Transporters

Glucose molecules cannot pass into the brain parenchyma without a glucose transporter (GLUT-1) (Koepsell, 2020). GLUT-1, an uniporter transporter, has a single binding part to access glucose molecules. If glucose concentration is lower in the brain, glucose in circulation is transferred from blood to the brain via GLUT-1. The GLUT-1 transporter expressed by SLC2A is present within the luminal and abluminal sides of

cerebral endothelial cells (Maher et al., 1991; Örnek Ergüzeloğlu et al., 2020; Zheng et al., 2010). In addition, sodium-glucose transporter-1 (SGLT-1) is also expressed by the SLC5A1 gene in capillary endothelial cells (Gyimesi et al., 2020).

2.6.2.3 Amino acids Transporters

The main amino acid transporters expressed on barrier-type endothelial cells are large neutral amino acid transporters 1 and 2 (LAT1/2) which are used for the passage of the necessary amino acids (AA) into the brain parenchyma (Zhang et al., 2020). Large neutral AAs such as tyrosine and tryptophan use bidirectionally LAT1/2 transporters (Taslimifar et al., 2018; Z. Y. Zhang et al., 2018), while cationic AAs, including arginine and lysine, use cationic transporter 1 and 3 (CAT1/3) to enter the brain (Y. Huang et al., 2007; Jungnickel et al., 2018). The study showed that the number of essential AAs is elevated in the circulation than that of in the brain, which supports blood-to-brain transport (Zaragozá, 2020). Other essential transporters are SNAT1/2/3/5 or sodium-coupled neutral AA transporters, which are responsible for the clearance of glutamine from the brain to circulation in case the level of glutamine is higher in the brain (Cubelos et al., 2005). First of all, glutamine is hydrolyzed into glutamate via glutaminase in brain endothelial cells and then efflux into circulation (O'Kane et al., 1999). So, sodium-dependent transporters for excitatory AA (EAAT1/2/3) on the abluminal endothelial membrane carry away both glutamate and aspartate from the brain to circulation (Fontana et al., 2022; Hawkins et al., 2006).

2.6.2.4 Fatty Acids Transporters

Proper neural function in the postnatal stage and brain development is provided by essential fatty acids, but fatty acid molecules cannot move to enter the brain because of the features of BBB. Thus, they need specific transporters including fatty acid transport protein 1/2 and mfsd2a expressed by brain type endothelial cells to uptake the fatty acids into the brain parenchyma (Mitchell et al., 2011; Nguyen et al., 2014a). One of the essential fatty acids is DHA which is necessary for brain development during the

embryonic stage. Accumulated data have demonstrated that the DHA is transported from the circulation into the brain via mfsd2a (B. Huang & Li, 2021; Nguyen et al., 2014a).

A previous study showed that the expression level of mfsd2a is higher than that in lung cells (Ben-Zvi et al., 2014a). In terms of protecting and maintaining BBB integrity, the mfsd2a is crucial. Because the genetically deleting mfsd2a causes low levels of DHA in the brain, leading to severe anxiety, cognitive deficits, and microcephaly (Ben-Zvi et al., 2014a). Another important point is that mfsd2a is involved in the transcellular pathway by controlling caveolar formation (Andreone et al., 2017a) thus, it can be served as an inhibitor of transcytosis (J. Z. Wang et al., 2016). A high number of vesicles in the barrier-type endothelial cells is a crucial indicator of increased transcytosis. A previous study has demonstrated that suppression of mfsd2a protein increased BBB leakage in the brain of mice and decreased mfsd2a expression caused increased transcytosis (Ben-Zvi et al., 2014a). A recent study has indicated that the overexpression of mfsd2a increased the penetration of DHA into the brain endothelial cells which protects BBB integrity by decreasing caveolae formation (C. Zhao et al., 2020).

2.6.2.5 Receptor-Mediated Transports

Another vesicular transcellular pathway is a receptor-mediated transcytosis which is used to deliver nutrients and circulating proteins, including fibrinogen, immunoglobulins, transferrin, and insulin across the brain parenchyma (Pardridge, 2005a). In contrast to the rate of nutrient transport across the BBB, the circulating peptides are slowly transported into the brain. When the macromolecules bind to their specific ligand receptors on the apical side of the capillary brain endothelial cell, endocytic events are initiated. Carrier proteins, receptors, and their ligand cluster together in intracellular vesicles or caveola for membrane invagination (Matthaeus & Taraska, 2021). Some nutrients including iron, transferrin, glucose, low-density lipoprotein receptor-related protein-1 (LPR1), and leptin, can enter the brain parenchyma via transcytosis or receptor-mediated transport (Georgieva et al., 2014a). These ligands are also used for CNS drug delivery through Trojan horse technology which provides high efficiency for transporting target molecules into the brain (Georgieva et al., 2014b). Another transcellular pathway is adsorptive-mediated transcytosis which is used for the transportation of positively charged large molecules into the brain (Hervé et al., 2008).

Transcytosis is initiated via the interaction of these molecules with specific binding sites on the cell surface of barrier type brain endothelial cells.

The capillary endothelial cells in the brain express low-density lipoproteins located on the luminal side to deliver cholesterol across the BBB. The low-density lipoproteins are characterized into size, lipid composition, and apolipoproteins (Feingold, 2021). Previous studies have shown that the LRP1 removed the Aβ plaques from the brain to the circulation (Kim & Priefer, 2020; Storck et al., 2018). In contrast to LRP1, the receptors for advanced glycation end products (RAGE) are located on the luminal side of endothelial cells and induces the accumulation of Aβ via increasing ROS levels and activating MAP kinase signaling pathway in AD (Donahue et al., 2006; Shi et al., 2009). In AD, an increase in the level of RAGE allows the circulating Aβ to enter the brain, which is induced neuroinflammation and caused severe BBB breakdown (Ding et al., 2020).

2.6.2.6 Caveolar Transcytosis

Caveola is a flask-shaped membrane-bound vesicle (Zhou et al., 2022). It is defined as a special type of lipid raft, which is 50-100 nanometers (S. Lei et al., 2023; Roy & Patra, 2023). It is mainly examined in the cytoplasm of brain microvessel endothelial cells. This structure consists of proteins and lipids, including cholesterol and sphingolipids (Svec., 2008). Sphingolipids produce ceramides which are responsible for neural differentiation (Kagan et al., 2022). Cholesterol provides structural support for caveola and the production of new caveolar vesicles. The primary function of caveola is to regulate ion channel activity, calcium signaling, cell migration, endocytosis, pinocytosis, and vesicular trafficking (Andreone et al., 2017b).

Caveolin, a 22-24 kDa integral membrane protein, is responsible for the formation and maintenance of caveola (Gautier-Stein et al., 2023; Peruzzu et al., 2022). There are three types of caveolin: caveolin-1, -2, and -3 (Thomas & Smart, 2008). The barrier type of capillary endothelial cells predominantly express caveolin-1 and -2, whereas caveolin-3 by astrocytes (Zhong et al., 2019). In contrast to caveolin-1, the caveolar formation is not regulated by caveolin-2 protein (Breuza et al., 2002; Cohen et al., 2004). It is well known that caveolin-1 is directly related to the permeability of BBB under pathological

conditions. The study showed that caveolin-1 implicates the mechanism of the paracellular pathway by regulating MMPs (Q. Huang et al., 2018a). The study reported that the expression level of caveolin-1 is markedly enhanced in the brain endothelial cells in case of pathological conditions and aging, but the inhibition of caveolin-1 expression mitigates pathological injury (Y. L. Zhao et al., 2014).

2.6.2.7 Efflux Transporters at the Blood-Brain Barrier

A stable microenvironment in the BBB is provided by preserving the brain tissues against blood-borne harmful molecules. The active efflux transport system prevents the penetration of toxins, xenobiotics, and undesired substances into the brain. Multiple efflux transporters involved in this transport system are expressed in the apical and basolateral membranes of barrier-type microvessel endothelial cells (Strazielle & Ghersi-Egea, 2015). Some of them are defined as solute carrier family and ATP binding cassette transporters (ABC) which are mainly expressed on the luminal side of brain endothelial cells. In order to efflux the unwanted substances from the brain into the circulation, these transporters need ATP energy. ATP-derived efflux pumps eliminate the xenobiotics and endogenous metabolites from the brain tissue, thereby controlling the permeability of unwanted molecules and therapeutic agents. In a previous study, ABC transporters showed a protective effect in the brain by preventing the accumulation of Aβ (Abuznait & Kaddoumi, 2012) therefore, especially in AD, affected ABC transporters lead to increase concentration of Aβ peptide in the brain.

Moreover, essential efflux transporters including p-gp, breast cancer-resistant protein (BCRP), and multidrug resistance-associated proteins such as MRP1/3/4/6 are expressed by brain capillary endothelial cells (Hashimoto et al., 2022). The ATP-derived p-gp and BCRP expressed on the luminal side of BBB remove the toxic molecules from brain endothelial cells to circulation (Kadry et al., 2020b), thereby preventing the accumulation of drugs in the brain.

The multidrug resistance proteins, 190 kDa molecular weight, are expressed in the luminal and abluminal side of brain capillary endothelial cells. In contrast to p-gp, MRPs mediate the transport of organic anions and glucuronide or glutathione-conjugated compounds (Begley, 2004). They are also used in bidirectional transport between

endothelium and circulation. Since they prefer the water-soluble conjugates as a substrate to transport, it seems they are less cytotoxic. Briefly, MRPs contribute to BBB integrity and maintenance of neuronal homeostasis by decreasing drug accumulation in the brain.

2.7 Inflammation in the Brain

Inflammation is described as a physiological response of the immune system that can be induced by infections-derived pathogens, some physical factors like trauma or heat, exogenous chemical molecules, as well as tissue damaging. These factors cause acute or chronic inflammation in different parts of the body. Inflammation is essential for the physiological process in terms of the immune system's response to toxic substances, damaged cells, and pathogens (Chen et al., 2018).

As the brain directly interacts with the immune and endocrine systems, it is the most active organ as immunologically. So, the homeostasis of the brain is directly affected by inflammatory reactions and responses (Farooqui et al., 2007). Some neurological disorders and/or diseases caused by infections, autoimmune disorders, injury of peripheral organs, and mental or metabolic stress prompt the severity of inflammation in the CNS (Klein et al., 2019; Y. Sun et al., 2022). Although the proper microenvironment and function of the BBB are maintained by certain mechanisms, inflammation-induced factors result in BBB disruption. Neuroinflammation considered as a defense mechanism in CNS provides a proper microenvironment by removing injured brain tissue from healthy parts, eliminating damaged cells, and restoring the extracellular matrix (ECM) (Correale & Villa, 2004). The main features of neuroinflammation are increasing levels of inflammatory cytokines, IL-1, IL-6, and TNF-α, chemokines, NO, and ROS, and they are secreted by innate immune cells of CNS (DiSabato et al., 2016). Neuroinflammation is moderated by microglia, the primary immune cells in the brain (Sun et al., 2022). While the resting side of microglia support tissue integrity in CNS under physiological conditions, activated microglia participate in neuronal damage in pathological conditions. Reactive microglia increase the number of inflammatory cytokines, ROS, and proteinases, contrary they contribute to the restoration process in the damaged tissue owing to the release of neurotrophic factors and anti-inflammatory mediators (Gomes-Leal, 2012; Wolf et al., 2017).

The secretion of pro-inflammatory cytokines from activated microglia causes synaptic dysfunction, inhibits neurogenesis, and neuronal death (Lyman et al., 2014). While IL-1β decreases the synaptic function by increasing the production of prostaglandin E2, TNF-α induces neuronal damage via the activation of TNF receptor-1 (TNFR1) (Micheau & Tschopp, 2003; Mishra et al., 2012). Activated microglia are classified into their profiles, including morphology and cell surface marker expression (Prinz et al., 2019). Traditionally, microglia are classified in M1 and M2 states. The state of M1 is characterized by a phagocytic phenotype associated with the regulation of NF-κB which causes the release of proinflammatory cytokines. The M1 state is mainly activated by injured neurons, Th1 lymphocytes, and pathogens, and M1 type microglia also produce pro-inflammatory agents and some cell surface markers, including iNOS, CD16 as well as CD32 (Orihuela et al., 2016). In contrast to the M1 state, the induced M2 state by apoptotic cells and Th2 lymphocytes remove the unwanted debris by increasing the phagocytic activity via the production of IL-10 and TGF-β, thereby suppressing inflammation and recovering damaged tissue (Simon et al., 2017; Mosser & Edwards, 2008). If M1 state becomes continuously active, it can be destructive for microglia and neighboring cells. Because the prolonged generation of pro-inflammatory agents triggers the inflammation state and increases the number of reactive astrocytes, free radicals as well as nitric oxide, neuroinflammation leads to an increase in Aβ, phosphorylated tau, and alpha (α)-synuclein in the brain and causes neurodegeneration and results in cell death in the neurons (Streit et al., 2004; Torres-Garcia et al., 2022).

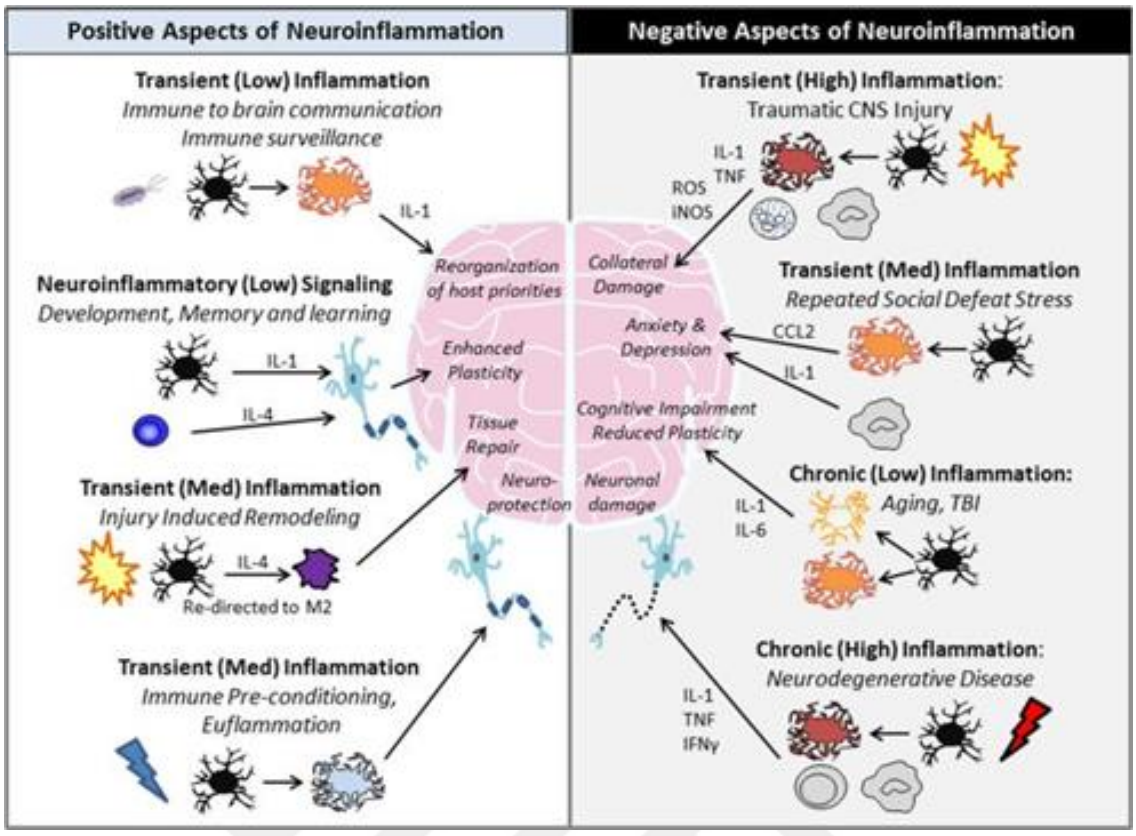

Figure 2.6 Positive and negative features of neuroinflammation in the central nervous sytem (DiSabato et al., 2016).

The AD is one of the most common and serious neurodegenerative diseases. The main reasons of AD are uncontrolled accumulation of Aβ plaques and tau tangles in the brain parenchyma, which results in dementia, cognitive dysfunction, and memory decline (Leng & Edison, 2021). Even though Aβ proteins are removed by microglia in a physiological state, the progression of AD triggers neuronal damage; consequently, activated microglia induce additional neurotoxicity by increasing pro-inflammatory mediators.

There are two types of neuroinflammation in CNS: acute and chronic. Any kind of inflammation can lead to neurological disorder and/or damage and neuronal death which results in the disruption of BBB integrity. In case of acute neuroinflammation caused by stroke, hypoxia, or neurotrauma, activated microglia immediately response to inflammation by means of their phagocytic activity and inflammatory mediators. In order to protect the CNS against future damage, the immune cells in the brain give response to acute signals from injured cells, thus they start the neuroinflammation processes. During chronic neuroinflammation, T-cell infiltration across the brain is increased thereby

disrupting the BBB integrity which results in neuronal damage (Glass et al., 2010; Q. Wang et al., 2015).

2.7.1 Sepsis-induced Inflammation in Blood-Brain Barrier

Sepsis is a primary pathological syndrome and a global health problem in the world. It has been reported that more than 19.4 million people have been affected, and 5.3 million died because of sepsis (Q. Gao & Hernandes, 2021). So, sepsis is a life-threatening pathological condition caused by bacterial infection, viruses, fungi, or parasites. The diagnosis and treatment of patients with sepsis are highly difficult because it has complex pathophysiology which depends on the age, source, and severity of the pathogen and other factors like chronic disorders (Evans, 2018; Leligdowicz & Matthay, 2019). Sepsis causes cognitive dysfunction, such as memory decline, anxiety as well as depression, which results in disruption of BBB and brain injury (Barichello et al., 2021). The septic conditions decrease the tightness of TJs and increase the influx of immune cells, free radicals, and proteins from blood to the brain which results in the BBB impairment (Handa et al., 2008; Van Der Poll et al., 2017). All these circulatory cells and substances contribute to the activation of neuroinflammation processes in the brain.

Sepsis-associated encephalopathy is a multifactorial condition and is described as diffuse cerebral dysfunction. In contrast to CNS infection, it is directly related to a systemic inflammatory response to infection (Sonneville et al., 2013). In SAE, both acute and chronic changes may occur in CNS. For instance, delirium is one of the most common acute changes observed in SAE (Danielski et al., 2018). Accumulated data showed that the chronic alterations in SAE are memory decline, behavioral changes, losing learning capacity, and neuronal death (Iwashyna et al., 2010; Semmler et al., 2007).

The sepsis or systemic inflammatory condition caused by stimulation of the intrinsic defense system via the “pattern recognition receptors (PRRs) like TLRs and nucleotide-binding and oligomerization domain (NOD)-like receptors” (Kawai & Akira, 2010; Räpple & Schilling, 2020). These receptors activate the intracellular signaling pathways by recognizing the PAMPs and DAMPs, leading to an increase in the levels of inflammation-associated genes (D. Li & Wu, 2021). While inactivated NF-κB is present within the cytoplasm under physiological conditions, activated NF-κB is translocated

across the nucleus via TLR4 and TNF-α receptor (TNFR) 1 signaling pathways under septic conditions (T. Zhang et al., 2021). So, the activated NF-κB increases the levels of IL 1-6-8 and TNF-α, thereby increasing the severity of inflammation (Nedeva et al., 2019).

In sepsis, proinflammatory cytokines can pass into the BBB via receptor-mediated endocytosis and some area that lack BBB (Manabe & Heneka, 2022). Accumulated data demonstrated that the receptors expressed on the cerebral endothelial cells allow the IL-1β, IL-6, and TNF-α to enter the brain parenchyma, which results in the activation of the endothelium (Ericsson et al., 1995; Nadeau & Rivest, 1999, Gutierrez et al., 1993; X. Liu et al., 2019; Skelly et al., 2013). One of the main endotoxins found in the cell wall of gram-negative bacteria is LPS (Page et al., 2022). Since LPS activates the TLR-4 signaling pathway, it has been commonly used as an inflammation model in experimental setups (Banks & Robinson, 2010; Batista et al., 2019; Heine & Zamyatina, 2022). The LPS activates the MyD88 and TRIF via binding of LPS to TLR4 (Bovijn et al., 2013).

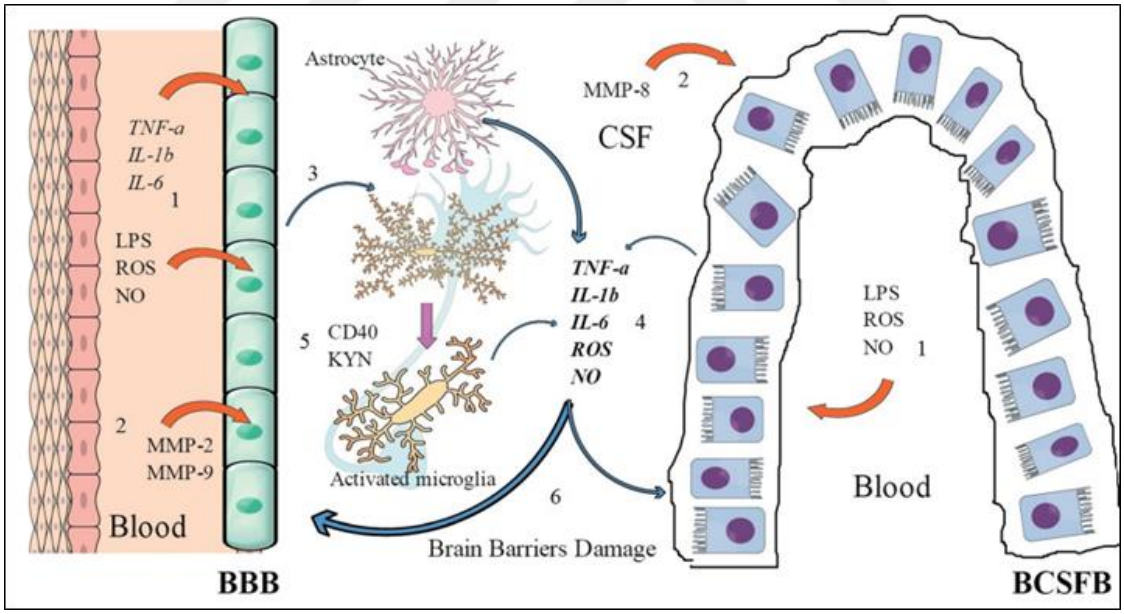

Figure 2.7 Alteration in brain barriers under septic conditions (Danielski et al., 2018).

LPS is the main inducer of neuroinflammation and negatively effects the BBB integrity by increasing the number of free radicals in the CNS. Under septic conditions, the activation of MMP2/9 is elevated by proinflammatory agents in the cerebral cortex and hippocampus, which is resulted in increased permeability of BBB (Dal-Pizzol et al.,

2013). Another inducer factor is that TNF-α increases the leakage of BBB and neuronal apoptosis by regulating MMP9 in the brain (Rempe et al., 2016b; Turner & Sharp, 2016). Additionally, LPS-induced sepsis upregulates the expression level of caveolin-1 in the brain endothelial cells (M. G. Lei & Morrison, 2000) and increased caveolin-1 shows a high level of transcytosis which increases the infiltration of peripheral immune cells across the BBB (Q. Huang et al., 2018b). Caveolin-1 mediates T-cell passaging between circulation and CNS via ICAM-1 located on the endothelial luminal membrane, which controls the transcellular migration (Lyck & Engelhardt, 2012).

About half of the patients acquire a hospital infection that leads to sepsis. According to World Health Organization, 20% of patients pass away because of sepsis in the world. Even so, there are insufficient treatments for sepsis. In order to suppress the infection or prevent multiple organ failures, traditional treatments have been used for patients with sepsis, still. The combined therapies may be helpful for septic patients, but their effects are not stable for each patient. Accumulated data showed that inhibition of the iNOS enzyme reduced apoptotic cell death in neurons and cognitive dysfunction in experimental setups (Kadoi & Goto, 2004; Weberpals et al., 2009). In addition, calcium channel blockers, magnesium, steroids, and antioxidant treatments showed protective effects on inflammatory conditions in rodents (Artym & Zimecki, 2023; Bilici et al., 2002; Khalilzadeh et al., 2018).

2.8 Physiology of Fatty Acid Binding Proteins in Central Nervous System

2.8.1 Fatty Acid Binding Proteins

Fatty acids (FA) have been described to involve in the signaling process in CNS (Falomir-Lockhart et al., 2019). Since half of the brain consists of lipids, including cholesterol, sphingomyelin, gangliosides, and phospholipids, lipid metabolism is essential for proper CNS function, maintaining brain homeostasis, and supporting neural processes (Garcia Corrales et al., 2021). The distribution of FA is not equal for all regions in the brain. For example, polyunsaturated glycolipids and cholesterol are more abundant in neurons other than cellular structures of NVU (Yoon et al., 2022). In contrast to circulating cholesterol, its content in the brain is essential for signal transduction, oxidative stress metabolism, synaptic transmission, regulation of lipid rafts, cell

development, and production of membrane proteins (Lee et al., 2021a). Different lipid-associated proteins manage the lipid signaling pathway, so they show distinct regulatory functions depending on tissue type. For instance, the brain tissue has two most significant polyunsaturated fatty acids (PUFA); DHA and arachidonic acid (AA). The productions of DHA and AA are quite limited especially in the brain when compared to peripheral tissues. The cerebral neurons are responsible for only FA elongation, but they cannot manage the desaturation process to generate total DHA and AA while brain endothelial cells can manage both elongation and desaturation of FA to produce DHA and AA for brain development (DHA and AA: Neuroprotective Nutrient, n.d.). The microvascular endothelial cells mainly produce AA, while astrocytes markedly produce DHA, respectively. A recent study showed that the conversion of DHA and AA from PUFA is abundant in astrocytes (Kaduce et al., 2008) and the entry of DHA and AA into the brain is provided by β-oxidization (Mayes et al., 2006). Thus, neurons are able to pick up DHA and AA to participate in their plasma membrane. In physiological conditions, DHA and AA directly manage brain development, cell growth, neurotransmission, and neuroinflammation. On the other hand, in pathological conditions, they control the process of inflammation, immunity, and tissue regeneration (Grant & Guest, 2016).

Although there are two possible pathways to import FAs into the brain, the transport mechanism(s) of FAs into the brain is still unclear. These are passive diffusion for lipophilic molecules and receptor-mediated transport for other FAs (Tracey et al., 2018). In free diffusion, lipophilicity and molecular size of FAs is so important to transport into the brain. In addition, FAs bind to the luminal side of endothelial cells after dislocating from albumin to enter the brain (Mitchell et al., 2011). In contrast to lipophilicity and molecular size, carrier-mediated transporters carry FAs into the brain from the blood. They are intracellular fatty acid binding proteins 1–9 (FABP), fatty acid transportation proteins (FATP), and caveolin-1 (Doege & Stah, 2006; Kazantzis & Stahl, 2012). In addition to these transporters, mfsd2a is responsible for the uptake of DHA into the brain (Wong et al., 2016).

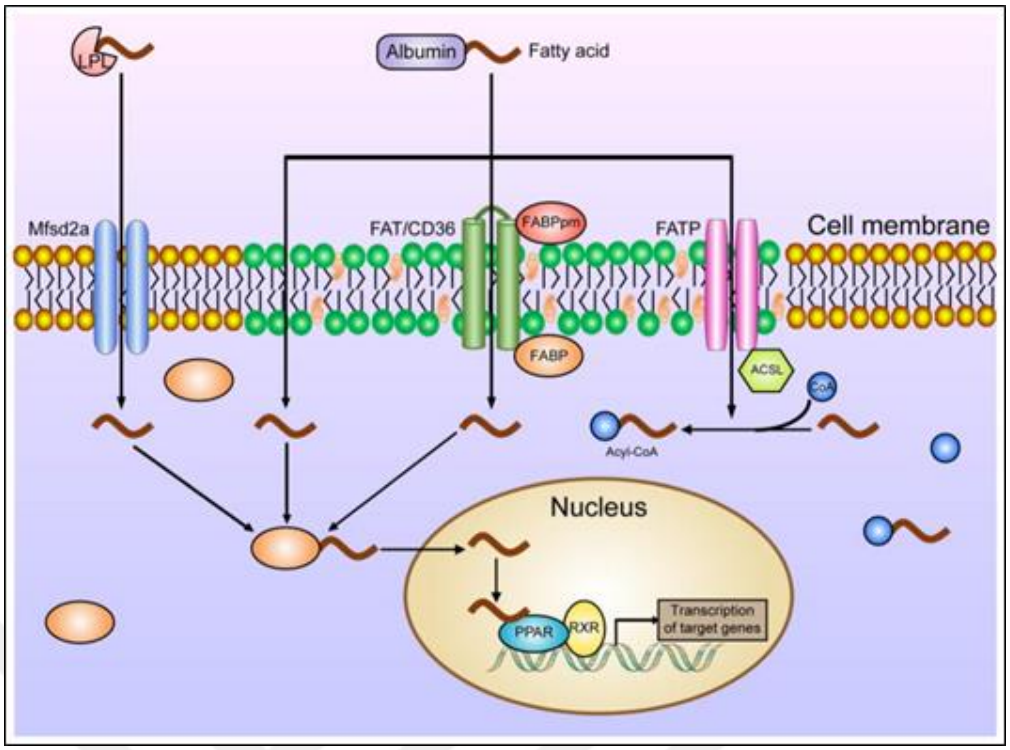

Figure 2.8 Uptake of PUFAs in the brain (W. Zhang et al., 2018).

2.8.2 Fatty Acid Binding Proteins

There are two main types of FABP and defined as subcellular localization. They are plasma membrane-associated fatty acids (FABPpm) and cytoplasmic FABPs. FABPpm is a 40 kDa molecular weight and is expressed in the outer surface of the cell membrane. It is responsible for transporting esterified acids (Roepstorff et al., 2004). In contrast to FABPpm, cytoplasmic FA (cFA) or lipid-binding proteins are 15 kDa molecular weight. There are nine different cFA which are named as tissue localization. Three of them have been identified in the CNS of rodents. These are heart type (H-FABP; FABP3), epidermal-type (E-FABP; FABP5), and brain type (B-FABP; FABP7).

The FABP3 is predominantly expressed by heart tissue, and its expression has not been discovered in the embryonic brain of human (Falomir-Lockhart et al., 2019). However, FABP3 expression progressively increases only in the prenatal brain of rodents (Owada, 2008). In adult age, it is demonstrated that there is a stable expression of FABP3 in the cerebral cortex, hippocampus, and interneurons of the retina (Dieriks et al., 2018). FABP3 is critical for membrane viscosity, neuronal synaptogenesis, and intracellular lipids transport. FABP3 impacts the dopamine signaling pathways in AD via ARA-

mediated transport (Dulewicz et al., 2021). The data showed that increased Aβ concentration is directly related to the increased expression level of FABP3 in CSF of patients with AD (Dulewicz et al., 2021). In pathologic circumstances, elevated FABP3 contributes to neurodegeneration (Shioda et al., 2014). Nevertheless, it is reported that the remarkably increased FABP3 expression was found to be in Down syndrome (Zhuang et al., 2021). Accordingly, the abnormal expression level of FABP3 causes PUFA accumulation which results in the disruption of membrane integrity and the progression of neurodegenerative disorders (Clarke et al., 2004).

FABP5 is expressed in the brain tissue during development and the adult stage. In contrast to other FABPs, their role in CNS is not clear yet. FABP5 is described as a lipid chaperone that helps transfer lipid molecules across the target region (Carbonetti et al., 2019). As for functions of FABP5, it is involved in signal transduction, lipid droplet storage, energy metabolism, cell proliferation, and the immune system (B. Xu et al., 2022). In physiologic conditions, FABP5 controls the intracellular distribution of FABPs from the cytoplasm to organelles. Under pathological conditions, the expression level of FABP5 is increased which influences the development of AD, breast cancer, prostate cancer, and psoriasis (Balcom et al., 2017; B. Xu et al., 2022). So, FABP5 contributes to the memory and learning process by degradation of endocannabinoid anandamide and the PPARβ/δ activation (Tan et al., 2016).

The brain-type fatty acid binding protein or FABP7, is a low-molecular-weight protein (15-17 kDa). This protein can be described as cellular chaperons for hydrophobic compounds (Rui, Ni et al. 2019). Although FABP7 is expressed in brain tissue throughout life, it shows high expression in the radial glial cells during the development stage. After the embryonic stage, there has still been a higher expression of FABP7 in gray and white matter regions of the brain. But aging process progressively decreases the expression level of FABP7.

FABP7 is mainly expressed by astrocytes and precursors of oligodendrocytes in the brain during embryonic development and postnatal life (Sharifi, Morihiro et al. 2011). However, its expression has not been detected in neurons, microglia, or mature oligodendrocytes (Islam, Kagawa et al. 2019). In addition, FABP7 is involved in different signaling pathways including metabolism, signal transduction, and gene-regulating activities by controlling the uptake and intracellular distribution of fatty acids to target

tissue (Kipp, Clarner et al. 2011). When FABP7 binds to n-3 PUFA, it increases the binding affinity of DHA to enter the brain parenchyma. The DHA improves the functional development and growth of the brain via differentiation and proliferation of neural stem cells throughout embryogenesis. A previous study showed that FABP7 plays an essential role in the proliferation of neural stem progenitor cells in the embryonic stage during neurogenesis (Matsumata et al., 2012). It also enhances the memory and learning capacity of the brain (Needham et al., 2022).

FABP7 plays an important role in controlling caveolae formation by regulating caveolin-1 in astrocytes under pathological conditions. In addition, FABP7, defined as a trophic factor, shows different phenotypes in the injured brain and MS disease (Kamizato et al., 2019; Killoy et al., 2020; Rui et al., 2019a). In response to damage in the brain, FABP7 also provides vascular regeneration in the damaged brain by differentiation of astrocytes (Rui et al., 2019a). Although only one study reported the protective and recovery effects of FABP7 in damaged brain caused by external stimuli (Rui et al., 2019a), the role of FABP7 in the regulation and maintenance of BBB under physiological and pathological settings remains unclear.

2.9 Aims of the Study

In this study, our purpose was to investigate the potential effects of exogenous FABP7 administration on LPS-induced BBB disruption in *in vitro* and in vivo conditions. In addition, the alterations in the expression of BBB-related proteins and inflammatory response in LPS-induced conditions were also explored. Consequently, we intended to elucidate the possible roles of FABP7 in the mechanistic pathways involving paracellular and transcellular in this experimental setting.

There has not been yet clear evidence of whether FABP7 has a protective role on BBB integrity under LPS conditions. In order to expose such an unknown question about FABP7, we established both an in vitro model of BBB and a septic mice model with LPS. To show the effects of FABP7 on BBB damage caused by LPS, different doses of FABP7 were used in in vitro bEnd.3 cells and in vivo septic mice. In order to show the possible effects of FABP7 on body temperature, depression, serum CRP, PCT, and ROS levels in

LPS-injected mice. In addition, we studied the expression levels of BBB proteins and inflammatory response in vitro and in vivo conditions in the same experimental setup.

Therefore, our objective was to explore the role of FABP7 on BBB integrity in septic conditions, which represents a significant challenge that needs to be addressed.

CHAPTER 3:

MATERIALS

All chemicals, antibodies, and laboratory equipment are listed in tables 3.1, 3.2, 3.3, and 3.4.

3.1 Cell Lines

Table 3. 1 List of cell line used in experiments.

Cell Line	Cell Type	Tissue	Organism	Company	Catalog number
bEnd.3	Endothelial cell	Brain; Cerebral cortex	Mus musculus, mouse	ATCC	CRL-2299

3.2 Chemicals

Table 3. 2 List of chemicals used in experiments.

Chemical	Company	Catalog number
0.25% Trypsin-EDTA	Wisent Bioproducts	325-043-EL
10X Tris/Glycine Buffer	Bio-Rad	1610771
10X Tris/Glycine/SDS Buffer	Bio-Rad	1610772
2-Mercaptoethanol	Bio-Rad	1610710
4X Laemmli Sample Buffer	Bio-Rad	1610747
Acetic Acid	Merck	6199969
Albumin Alexa Fluor 594	Invitrogen	A13101
Bovine Serum Albumin	Thermo Fisher Scientific	A9418-500G

Citrate Buffer 10X	Sigma Aldrich	C9999-100ML
cOmplete ULTRA tablets	Roche	05892970001
DMEM: F12	Lonza	6195494
DMSO	Sigma	6195067
Ethanol	Merck	6199918
Fetal Bovine Serum	Biowest	S181H-500
Fluorescein Sodium Salt	Sigma Aldrich	F6377
Glycerol	Sigma Aldrich	49782
HBSS	Biowest	6150847
HEPES	Gibco	6195442
Hoechst 33342	Thermo Fisher Scientific	62249
Hydrochloric acid 37%	Merck	6110029
L-Glutamine	Biowest	6194078
LPS	Enzo Life Sciences	ALX-581-012-L002
Methanol	Sigma	6195123
Normal Goat Serum	Sigma Aldrich	P9416
Paraformaldehyde	Sigma Aldrich	158127
PBS	Biowest	L0615-500
Penicillin-Streptomycin	Biowest	L0018-100
Pierce BCA Protein Assay Kit	Thermo Fisher Scientific	23225
Pierce ECL Substrate	Thermo Fisher Scientific	32106
Poly-L-Lysine		
Hydrochloride	Sigma	6195011
Polyvinyldene Difluoride (PVDF) Mebrane	Bio-Rad	1620177
Recombinant FABP7	Proteintech	Ag1123
RIPA Lysis Buffer	Eco-Tech	RIPA-100
Sodium Hydroxide	Sigma	6195191
SRB	Sigma	230162
Trichloroacetic acid	Sigma Aldrich	T6399
Triton X-100	Fisher Bioreagent	BP151-100
Trypan Blue	Thermo Fisher Scientific	6195080

3.3 Antibodies

Table 3. 3 List of antibodies used in experiments.

Antibody	Host	Company	Catalog Number
Anti-mouse Alexa Fluor 488	Goat	Invitrogen	A-11029
Anti-rabbit Alexa Fluor 488	Goat	Invitrogen	A-11008
Anti-rabbit Alexa Fluor 647	Goat	Jackson Immunoresearch	6195040
Caveolin-1	Rabbit	Abcam	ab192869
Claudin-5	Mouse	Invitrogen	35-2500
IL-1β	Rabbit	Invitrogen	P420B
Mouse HRP	Mouse	Abcam	ab97021
Mfsd2a	Rabbit	Invitrogen	PA5-21049
NF-κB	Rabbit	Abcam	ab16502
Rabbit HRP	Rabbit	Abcam	ab97051
ZO-1	Rabbit	Abcam	ab216880

3.4 Laboratory Equipments

Table 3. 4 List of laboratory equipment used in experiments.

Name	Company
24-well Plate	Sarstedt
24-well TC Inserts, 0.4 □m	Sarstedt
6-well Plate	Sarstedt
96-well Black Flat Bottom Plate	Corning
96-well Plate	Sarstedt
Attune NxT Flow Cytometer	Thermo Fisher Scientific
Blood Cell Analyzer	Prokan pe-6800 vet

Centrifuge	Thermo Fisher Scientific
Class II, Type C1 Biosafety Cabinet	Labconco
CO2 Incubator	Eppendorf
Coverslips	VWR
Cryogenic Storage System	Thermo Fisher Scientific
DMI/SP8 Laser Scanning Confocal	Leica
Microscope	Leica
Filtropur V50, Vacuum Filtration Unit	Sarstedt
Hemocytometer	Weber Scientific
Light Microscope	Leica
Micropipettes	Thermo Fisher Scientific
Millicell ERS-2 Voltohmmeter	Merck Millipore
Polysine Slides	Thermo Fisher Scientific
S220 SevenCompact pH/Ion Meter	Mettler Toledo
Synergy H1 Microplate Reader	Bio Tek Instrument
T75 Flask	Sarstedt
Ultra-Low Temperature Freezer	Thermo Fisher Scientific
Waterbath	Memmert
Western Blot Imaging Device	Li-Cor

CHAPTER 4:

METHODS

4.1. In vitro Experimental Procedure

Experimental Groups

1- Control

2- LPS

3- FABP7

4- LPS + FABP7

Sub-Groups

1- SRB Assay

2- TEER and NaFl Permeability Assay

3- Immunofluorescence Staining

4- Western Blot

4.1.1. Endothelial Cell Culture

Mouse brain type endothelial cell line (bEnd.3) was purchased from American Type Culture Collection. These cells were cultured in Dulbecco's Modified Eagle Medium F12 (DMEM-F12) supplemented with 10% heat-inactivated fetal bovine serum, 1% penicillin-streptomycin and 1% L-glutamine in T75 flasks. Cells were incubated in a

humidified incubator with 5% CO_2 at 37ºC, and the media was replaced with fresh medium twice a week. The trypsinized cells were centrifuged at X300 g for 5 minutes and subcultured in a fresh medium. The experimental procedures were performed when cells reached at least 90% of confluency. bEnd.3 cells were used before passage number 30 to prevent the risk of losing their barrier properties.

4.1.2. Establishment of in vitro Blood-Brain Barrier Model

In order to construct the *in vitro* BBB model, bEnd.3 cells were seeded onto the luminal side of non-coated transwell inserts with 0.4-μm diameter-sized pores in 24-well plates and incubated for 96 hours.

4.1.3. Cell Treatments

LPS was dissolved in physiological saline solution and kept at 4ºC. bEnd.3 cells were treated with 0.05, 0.1, 0.5, 1, 10, and 100 μg/ml concentrations of LPS for 24 hours. The recombinant FABP7 was dissolved in 50% glycerol solution and administered to LPS-treated and -untreated cells at 0.05, 0.1, 0.5, 1, and 10 μg/ml doses for 24 hours.

4.1.4. Sulforhodamine B Assay

Sulforhodamine B (SRB) assay was performed to measure cell viability. For this purpose, bEnd.3 cells ($5x10^3$ cells/well) were seeded in 96-well plates and treated with different doses of LPS and FABP7 for 24 hours. Without removing the culture medium, 25 μl (i.e., ¼ volume of culture medium) trichloroacetic acid solution (fixative solution) was added to each well and incubated at 4°C for 1 hour. Afterward, the solution in each well was removed, and the wells were washed with 200 μl dH_2O 3-5 times. The washing was performed smoothly to avoid the disturbances in cell monolayer. Next, 50 μl SRB dye dissolved in 10 mM Tris base solution was added to each well and incubated at room temperature for 30 minutes in dark room conditions. The unbound dye was removed by washing with 1% acetic acid (150 μl per well) and the plate was placed on an orbital

shaker at 150 rpm for 10-15 minutes to homogenize the dye. The optical density (OD) was measured at a wavelength of 564 nm using a Synergy H1 microplate reader. The viability percentage of experimental groups was calculated according to the following formula: (ODexperimental sample/ODcontrol) × 100.

4.1.5. Transendothelial Electrical Resistance

To evaluate the resistance of the endothelial barrier, TEER was measured using a voltohmmeter (Millicell ERS-2). For this purpose, b.End3 cells were treated with different doses of LPS and/or FABP7 for 24 hours. Additionally, three transwells without cells were filled with DMEM-F12 for blanks. The voltohmmeter was set to the ohm (Ω) scale and calibrated until the display showed a reading of 1000 Ω.

Resistance values were obtained by inserting the probe perpendicularly into the transwells, ensuring that the apical electrode was away from the insert membrane and the basolateral electrode touched the bottom of the transwell. Electrical resistance was measured for each transwell and calculated using the following formula: TEER (Ω) = (Ωsample–Ωblank).

4.1.6. Sodium Fluorescein Permeability Assay

Sodium fluorescein was used to evaluate the permeability of barrier type endothelial cells. For this purpose, b.End3 cells cultured on the luminal side of transwell inserts were treated with different doses of LPS and/or FABP7 for 24 hours. 0.1 mg/ml concentration of NaFl solution was prepared in dH_2O with 25 mM hydroxyethyl-piperazineethane-sulfonic acid buffer and 10% Hanks' Balanced Salt Solution. Three different experimental setups were conducted for LPS and/or FABP7 treatments.

DMEM-F12 in apical and basolateral compartments of transwells was removed and replaced with dH_2O+HEPES+HBSS. In the meantime, different doses of LPS and FABP7 prepared in NaFl solution were administered into the apical compartment of transwells and incubated for 24 hours. For FABP7 administrations following LPS, bEnd.3 cells in apical compartments of transwells were treated with 0.5 µg/ml LPS for 24 hours and DMEM-F12 in both compartments was replaced with dH_2O+HEPES+HBSS. Next,

0.5 µg/ml FABP7 was prepared in NaFl solution and administered into the apical compartment for 24 hours. In order to detect the tracer intensity in each lower compartment for each experimental group, the samples were collected to put in triplicates in a black 96-well plate. The fluorescence intensity of NaFl was measured at excitation and emission wavelengths of 494 and 512 nm, respectively, using a microplate reader.

4.1.7. Western Blotting

The alterations in the expression levels of claudin-5, caveolin-1, mfsd2a, and NF-κB were evaluated by western blot. For this purpose, bEnd3 cells ($2x10^6$ cells/culture dish) were seeded on 100 mm culture dishes and incubated for 24 hours. Next, the cultured cells were treated with 0.5 µg/ml LPS for 24 hours followed by 0.5 µg/ml FABP7 for 24 hours. Then, the cells were washed with cold PBS and lysed with RIPA buffer for 30 minutes on ice. The cell lysates were centrifuged at X14,000 g for 20 minutes at 4°C and the protein content in cell lysates was measured with a BCA kit. Forty µg of proteins were separated by SDS-polyacrylamide gel electrophoresis (SDS-PAGE) and electrophoretically transferred to polyvinylidene difluoride (PVDF) transfer membranes. The membranes were then incubated with blocking solution [5% non-fat milk in tris-buffered saline containing 0.1% Tween 20 (TBST)] at room temperature for 1 hour and incubated with the following primary antibodies in blocking solution overnight at 4ºC.

- mouse anti-claudin-5 (1:1000)
- rabbit anti-caveolin-1 (1:1000)
- rabbit anti-mfsd2a (1:1000)
- rabbit anti-NF-κB (1:1000)
- rabbit anti-actin (1:10000)

Next, the membranes were washed with TBST and incubated with appropriate secondary antibodies (goat-anti mouse HRP and goat-anti rabbit HRP; 1:5000) at room temperature for 1 hour. After washing with TBST, protein bands on membranes were treated with enhanced chemiluminescence solution. The Image J macro/plugin was then employed to quantify the chemiluminescence intensity of bands. This macro

automatically estimated the background level of actin and the targeted protein based on mean intensity.

4.1.8 Immunofluorescence Staining

Immunofluorescence staining was performed to assess the alterations in claudin-5, ZO-1, caveolin-1, mfsd2a, NF-κB, and IL-1β immunoreactivity. For this purpose, bEnd.3 cells were seeded (2 x 10^5 cells/well) on 6-well plates containing autoclaved coverslips for 24 hours. Next, the cells were treated with LPS (0.5 µg/mL) for 24 hours followed by 0.5 µg/mL FABP7 for 24 hours. Then, the cells were washed with PBS and fixed with 4% paraformaldehyde (PFA) dissolved in PBS (pH=7.4) at room temperature for 20 minutes. After washing with PBS, the permeabilization of cells was performed with 0.1% Triton X-100 in PBS (PBST) at room temperature for 15 minutes. The washed cells with PBS were blocked with the following blocking buffers for 1 hour at room temperature.

- 5% normal goat serum (NGS) in 0.5% PBST for claudin-5 and mfsd2a,
- 5% NGS in 0.3% PBST for ZO-1,
- 10% NGS in 0.1% PBST for caveolin-1 and NF-κB,
- 2% bovine serum albumin in 0.1% PBST for IL-1β.

Subsequently, the cells were incubated with mouse anti-claudin-5 (1:100), rabbit anti-ZO-1 (1:100), rabbit anti-caveolin-1 (1:500), rabbit anti-mfsd2a (1:50), rabbit anti-NF-κB (1:1000) and rabbit anti-IL-1β (1:200) primary antibodies overnight at 4ºC. Then, coverslips were washed with PBS, and stained with the appropriate secondary antibodies (Alexa Fluor 647-conjugated goat anti-mouse IgG for claudin-5, caveolin-1, mfsd2a, NF-κB, and IL-1β; Alexa fluor 488-conjugated goat anti-rabbit IgG for ZO-1) diluted at 1:1000 at room temperature for 1 hour. The cells on the coverslips were then rinsed with PBS and mounted onto microscopy slides with a mounting solution prepared using PBS and glycerol in the ratio of 1:1 containing 10 mg/ml Hoechst 33342.

The slides were evaluated with a laser scanning confocal microscope (Leica DMI/SP8) and 20 images were taken from each experimental group under 40X objectives to analyze the images with Image J software (ImageJ 1.52a, Wayne Rasband, National

Institute of Health, USA). The immunofluorescence intensities of ZO-1, mfsd2a, claudin-5, NF-κB, caveolin-1, and IL-1β were assessed according to the software formula.

4.2. In vivo Experimental Procedures

The experimental design of this study is shown in Figure 4.1. The experimental procedures were approved by the Local Ethics Committee for Animal Experimentation of Koç University (2021.HADYEK.028). Young adult C57BL/6 male/female mice weighing 20-25 grams, were obtained from Koç University, KUTTAM. The animals were housed in individually ventilated cages under constant temperature (22ºC) and humidity conditions with a 12:12 hours light dark cycle. The total number of animals used in this study was 144.

Mice were randomly divided into the following six main experimental groups.

1. Control
2. LPS
3. 40 μg/kg FABP7
4. 80 μg/kg FABP7
5. LPS + 40 μg/kg FABP7
6. LPS + 80 μg/kg FABP7

Separate subsets of experimental groups (n=6) were used for the following experimental procedures.

1. BBB permeability measurement
2. Immunofluorescence staining
3. Western blotting

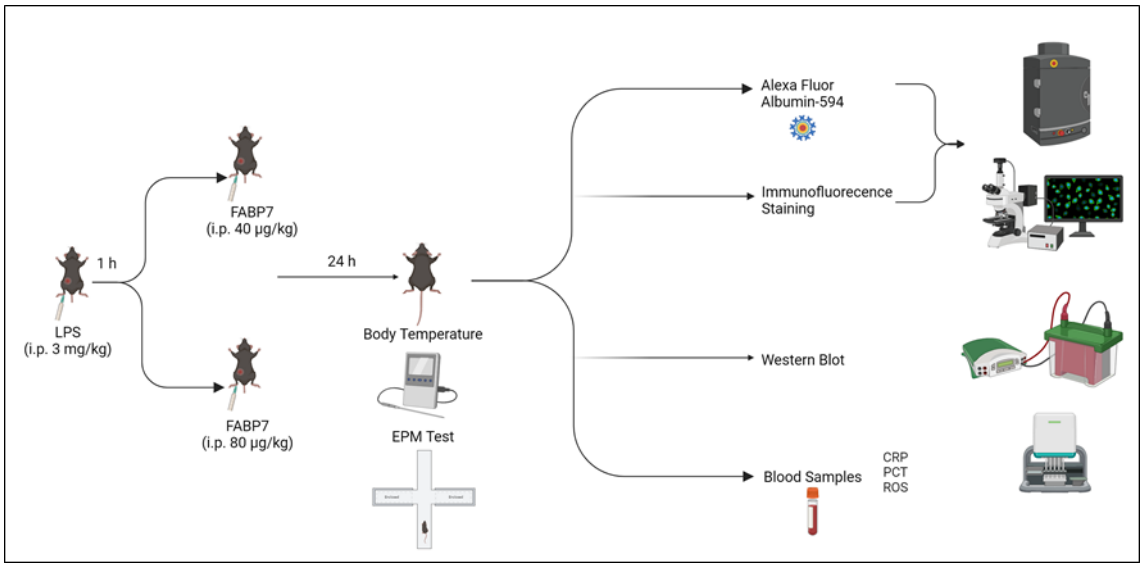

Figure 4.1 *In vivo* experimental design of this study.

4.2.1. LPS and FABP7 Administrations

In order to induce septic conditions in mice, LPS was dissolved in physiological saline solution and intraperitoneally (i.p.) injected into animals at the dose of 3 mg/kg. The control animals received administration of 0.9% sterile saline. To investigate the effects of FABP7 in this experimental setting, recombinant FABP7 was dissolved in 50% glycerol solution and injected into animals at two doses; 40 and 80 µg/kg, one hour after LPS administration.

4.2.2. Monitoring Body Temperature

In order to measure the body temperature, a probe was inserted into the rectum (1.5 cm depth) of the animals and kept for 30 seconds to obtain a stabilized reading. A body temperature above the normal range (36.5-38°C) was considered indicative of LPS-induced fever. The body temperature of mice was measured at 1, 6, and 24 hours of treatments of LPS and/or FABP7.

4.2.3. Behavioral Test

In order to assess the anxiety-like behaviour of the animals in experimental groups, the elevated plus maze (EPM) test was performed. For this purpose, a platform comprising an elongated "+"-shaped labyrinth with two open-white arms, two closed-black arms, and a center area was used. The open and closed arms, each measuring 50 cm long and 10 cm wide, were positioned opposite to each other on the platform. Three days before the experiment, mice underwent a training program to familiarize with the setup. At 24 hours after LPS and/or FABP7 administration, the mice were placed in the middle of the platform, and their tendency to stay in either the open or closed arms under white light conditions were recorded with a video camera for 5 minutes for each mouse. The time spent in the arms was assessed, and a greater time spent in the open arms or a higher propensity towards the open space was considered as indicative of low anxiety-like behavior or a normal phenotypic behavior in mice. Conversely, if the time spent in the closed arms was greater than the time spent in the open arms, this was interpreted as high anxiety-like behavior.

4.2.4. Evaluation of Inflammatory Biomarkers

In order to evaluate sepsis-associated inflammatory biomarkers, serum levels of C-reactive protein (CRP), procalcitonin (PCT), and ROS were measured. For this purpose, at the end of the experiments, the animals were exposed to high dose of ketamine (300 mg/kg) and xylazine (30 mg/kg) to open the chest. Approximately 500 µl of blood samples was collected from the left ventricle and the levels of CRP and ROS in serum were measured using commercially available kits according to the manufacturers' instructions (mouse CRP ELISA kit; E021Mo and ROS assay kit; SH0403). Serum PCT levels were determined using fully automated blood cell analyzer (Prokan pe-6800 vet).

4.2.5. Immunofluorescence Staining

To demonstrate the alterations in the immunoreactivity of claudin-5 in the cerebral cortex and hippocampus following LPS and/or FABP7 administrations, immunofluorescence staining was performed. For this purpose, the thoracic cavity of

animals was opened under high dose ketamine (300 mg/kg, i.p.) and xylazine (30 mg/kg, i.p.) anesthesia. Next, transcranial bolus administration of 25 ml saline solution was performed from the left ventricle for 30 seconds. Then, the animals were perfusion fixed with 100 ml 4% PFA (pH:7.4) for 15 minutes. After decapitation, the brains were removed and kept in the same fixative solution for 3 hours and immersed in 30% sucrose solution for approximately 24 to 72 hours. The brains were stored at -80°C after freezing in dry ice. Fifteen μm thick brain sections were cut using a cryostat, mounted onto positively charged slides, and stored at -80°C. For antigen retrieval, the sections were heated in citrate buffer (pH:6.0) with microwave oven at 600 watts for 15 minutes. Next, the sections were blocked with 10% normal goat serum in PBST for 1 hour at room temperature and incubated with mouse anti-claudin-5 primary antibody (1:100) overnight at 4°C. After washing with PBS, the sections were incubated with Alexa fluor 488-conjugated goat anti-mouse IgG secondary antibody (1:1000) for 1 hour. The sections were then rinsed with PBS and mounted with mounting solution prepared using PBS and glycerol in the ratio of 1:1 containing 10 mg/ml Hoechst 33342.

The sections were evaluated with a laser scanning confocal microscope (Leica DMI/SP8) and 20 images were taken from the cerebral cortex and hippocampus of each animal under 40X objective. The images were then analyzed using Image J software (ImageJ 1.52a, Wayne Rasband, National Institute of Health, USA), and the relative intensity of claudin-5 immunostaining was assessed according to the software formula. For comparison of experimental groups, a one-way analysis of variance (ANOVA) followed by Tukey's test was used.

4.2.6. Evaluation of Blood-Brain Barrier Permeability

The permeability of BBB was determined by assessment of albumin Alexa fluor 594 extravasation using IVIS imaging and confocal laser scanning microscopy. Twenty-three hours after LPS and/or FABP7 administration, the animals were injected with 100 μl albumin Alexa fluor 594 (1%) in saline via the tail vein. One hour after the injection of the tracer, the animals were imaged with an excitation wavelength of 440 nm and emission wavelength of 620 nm in the Optical In Vivo Imaging System (IVIS) under mild isoflurane anesthesia. After IVIS imaging, the thoracic cavity of the animals was opened under over dose ketamine/xylazine, and transcardial bolus administration of 25 ml saline

solution was performed through the left ventricle for 30 seconds. The animals were perfusion fixed with 100 ml 4% PFA (pH:7.4) for 15 minutes. After decapitation, the brains were removed, kept in the same fixative for 3 hours, immersed in 30% sucrose solution for approximately 24-72 hours, and stored at -80°C. Fifteen μm coronal sections were taken from the level of P56 of the mouse brain shown in Figure 4.2 using a cryostat. The sections were mounted with mounting solution prepared using PBS and glycerol in the ratio of 1:1 containing 10 mg/ml Hoechst 33342. Next, the sections were evaluated with a laser scanning confocal microscope (Leica DMI/SP8), and 30 images were taken from coronal sections of the P56 level of each animal under 40X objective. The images were then analyzed using Image J software (ImageJ 1.52a, Wayne Rasband, National Institute of Health, USA), and the relative intensity of albumin Alexa fluor 594 was assessed according to the software formula. For comparison of experimental groups, one-way ANOVA followed by Tukey's test was used.

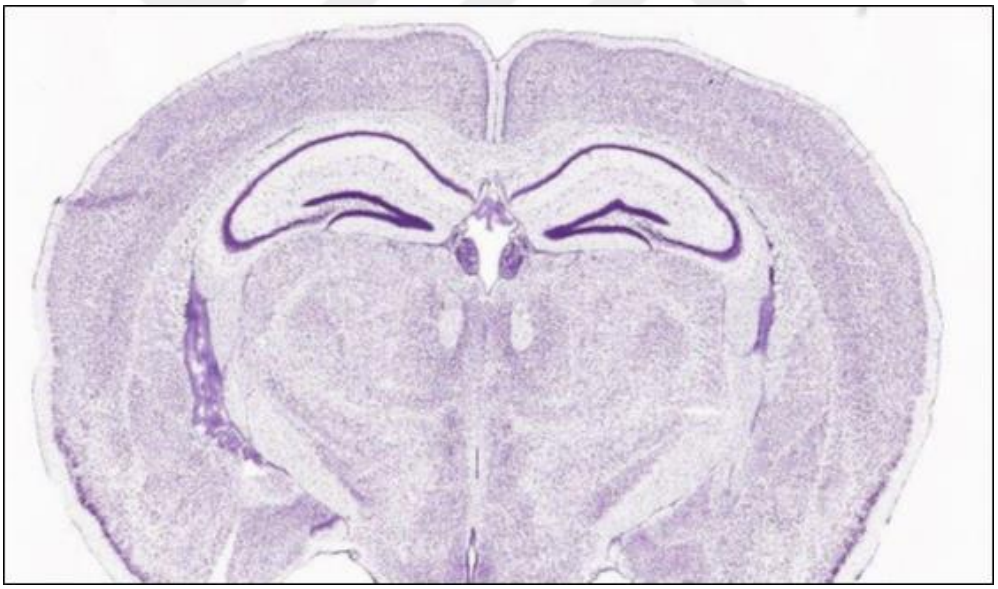

Figure 4.2 The coronal brain section from P56 (https://mouse.-brain-map.org).

4.2.7. Western Blot Analysis

In order to evaluate the alterations in the expression levels of claudin-5, caveolin-1, mfsd2a, and NF-κB western blotting was performed. For this purpose, at the end of the experiment, the cerebral cortex and hippocampus of the brain were dissected and

homogenized/lysed in ice-cold RIPA buffer with phosphatase inhibitor cocktails. Lysates were centrifuged at X14,000 g for 20 minutes at 4°C to detect the protein content of tissue lysates with a BCA assay kit. Forty μg of proteins were separated by 10% SDS-PAGE and electrophoretically transferred to PVDF transfer membranes. The membranes were then incubated with blocking solution (5% non-fat milk in TBS-T) at room temperature for 1 hour and incubated with the following primary antibodies in blocking solution overnight at 4ºC.

- mouse anti-claudin-5 (1:1000)
- rabbit anti-caveolin-1 (1:1000)
- rabbit anti-mfsd2a (1:1000)
- rabbit anti-NF-κB (1:1000)
- rabbit anti-actin (1:10000)

Next, the membranes were washed with TBST and incubated with appropriate secondary antibodies (goat-anti mouse HRP and goat-anti rabbit HRP; 1:5000) at room temperature for 1 hour. After washing with TBST, protein bands on membranes were treated with enhanced chemiluminescence solution. The Image J macro/plugin was then employed to quantify the chemiluminescence intensity of bands. This macro automatically estimated the background level of actin and the targeted protein based on mean intensity.

4.3. Statistical Analysis

The data were presented as mean ± standard deviation (SD). GraphPad software (GraphPad Prism, CA, USA) was used to analyze the data from the experimental groups. In order to show the individual group differences in the SRB assay, TEER, and NaFl assay, one-way ANOVA followed by Tukey's test was used. The Kruskal-Wallis test was applied to analyze the differences in body temperature before and after LPS and/or FABP7 injections. To analyze the behavioral data, two-way ANOVA followed by Tukey's test was used. In all experimental groups, differences between the means were considered significant if $p < 0.05$.

CHAPTER 5:

RESULTS

5.1 Effects of LPS Treatment on in vitro Blood-Brain Barrier Model

5.1.1 Effects of LPS on bEnd.3 Cell Viability

Figure 5.1 shows the impact of LPS on cell viability as evaluated by SRB assay. bEnd.3 cells were treated with different concentrations of LPS (0.05, 0.1, 0.5, 1, 10, and 100 μg/ml) for 24 hours. The results showed that 0.05, 0.1, and 0.5 μg/ml doses of LPS decreased the viability of bEnd.3 cells compared to nontreated controls, however, the difference did not reach statistically significant levels. When bEnd.3 cells were treated with higher doses of LPS (1, 10, and 100 μg/ml), a significant decrease in cell viability was observed with respect to nontreated cells ($p < 0.001$). In light of the above-mentioned data, 0.05, 0.1, and 0.5 μg/ml were considered as safe concentrations for 24 hours of LPS treatment.

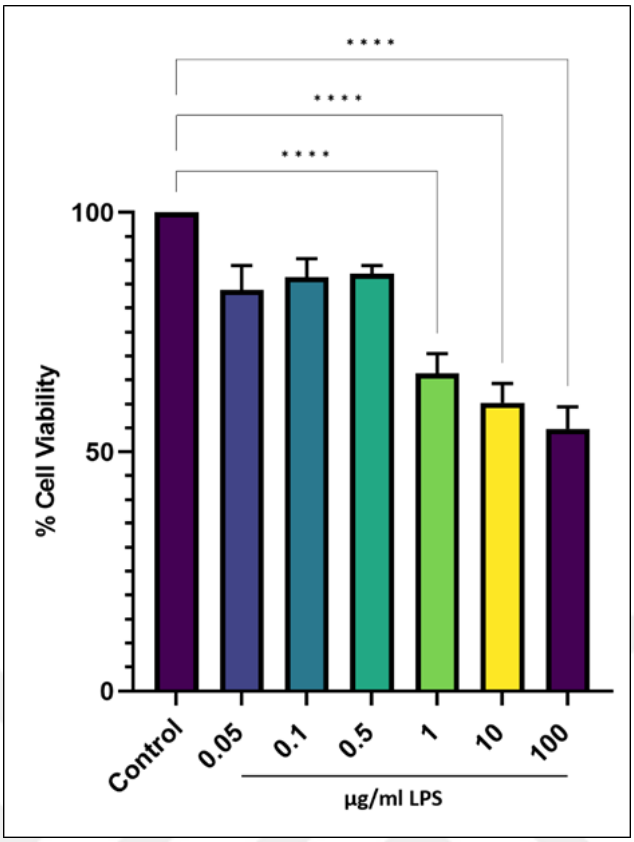

Figure 5.1 The effects of LPS on cell viability of bEnd.3 cells. The data were presented as mean±SD.****p< 0.001.

5.1.2 Effects of LPS on Transendothelial Electrical Resistance

Figure 5.2 shows the effects of LPS on the transendothelial electrical resistance of bEnd.3 cells cultured on luminal side of transwell inserts to examine the integrity of the BBB *in vitro*. When bEnd.3 cells were treated with 0.05 and 0.1 µg/ml doses of LPS, no marked changes were found in TEER values. In contrast, higher doses of LPS at 0.5, 1, 10, and 100 µg/ml significantly decreased TEER values in bEnd.3 cells compared to untreated controls ($p < 0.01$ and $p < 0.001$).

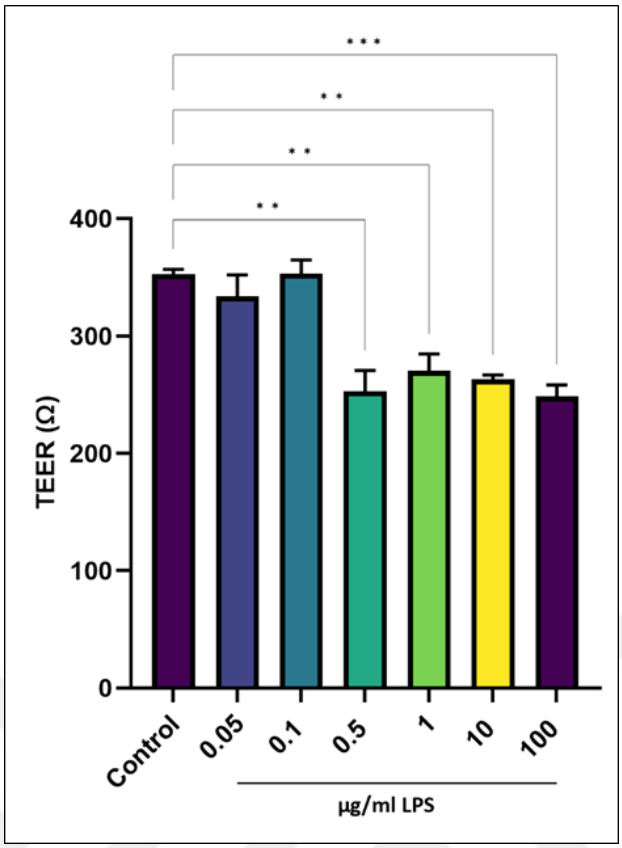

Figure 5.29 Effects of LPS on transendothelial electrical resistance in bEnd.3 cells. The data were presented as mean±SD. **p< 0.01 and ***p< 0.001.

5.1.3 Effects of LPS on Permeability

Figure 5.3 shows the effect of LPS on the penetration of the NaFl tracer across the monolayer of bEnd.3 cells cultured on the luminal side of transwell inserts to evaluate the permeability of BBB *in vitro*. The fluorescence intensity of NaFl in the abluminal compartment of transwells was significantly increased by 0.5, 1, 10, and 100 µg/ml doses of LPS ($p < 0.01$, $p < 0.001$ and $p < 0.0001$), while the lower doses did not alter BBB integrity. When the above-mentioned data from SRB and NaFl assays, and TEER measurements were considered as a whole, 0.5 µg/ml LPS treatment for 24 hours was decided to be used in the subsequent *in vitro* experiments, since this dose of LPS was found to cause a significant disruption in BBB integrity without evoking a marked cytotoxicity in bEnd.3 cells.

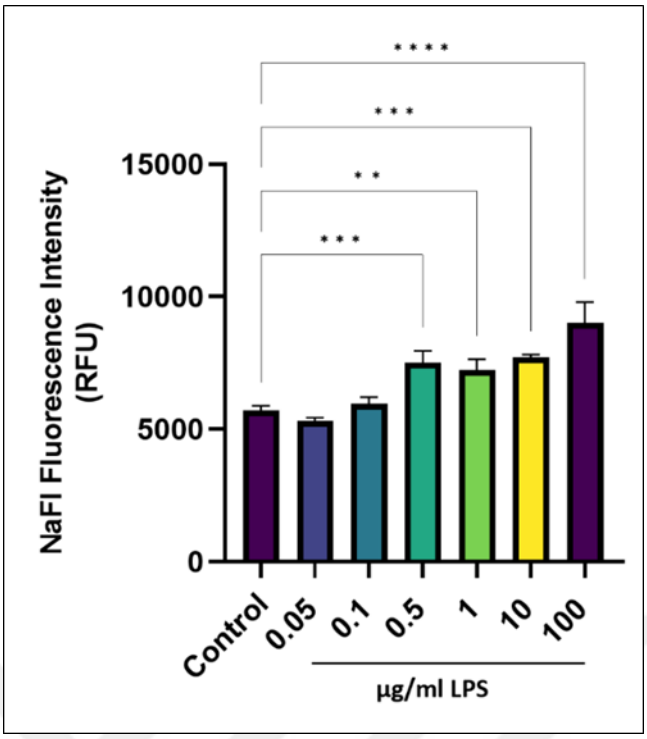

Figure 5.3 Effects of LPS on BBB permeability. The data were presented as mean±SD. **p< 0.01, ***p< 0.001 and ****p< 0.0001.

5.2 The Effects of FABP7 on in vitro Blood-Brain Barrier Model in Physiological Conditions

5.2.1 Effects of FABP7 on bEnd.3 Cell Viability

In order to show the *in vitro* effects of FABP7 on cell viability in bEnd.3 cells under physiological conditions, bEnd.3 cells were treated with 0.05, 0.1, 0.5, 1, and 10 µg/ml FABP7 for 24 hours. The data from the SRB assay showed that these concentrations did not cause any marked effects on endothelial cell viability (Figure 5.4).

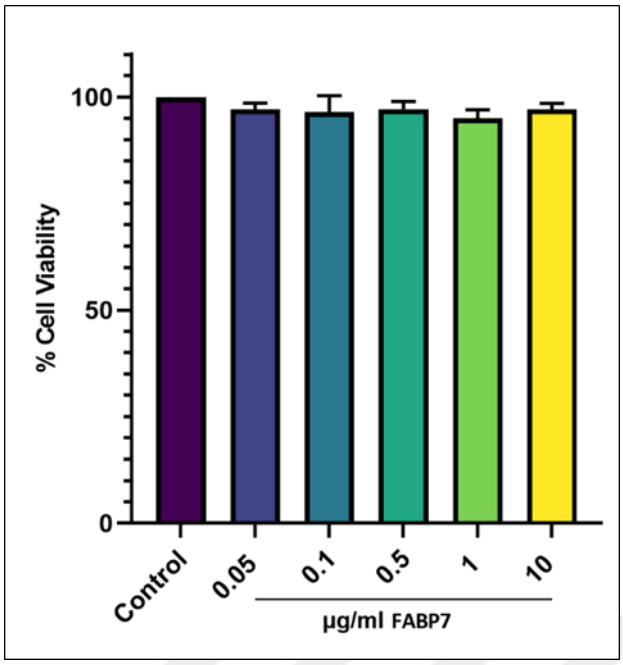

Figure 5.4 Effects of FABP7 on endothelial cell viability under physiological conditions. The data were presented as mean±SD.

5.2.2 Effects of FABP7 on Transendothelial Electrical Resistance

In order to show the *in vitro* effect of FABP7 administration on BBB integrity under normal conditions, barrier resistance was measured in bEnd.3 cells following 0.05, 0.1, 0.5, 1, and 10 µg/ml FABP7 treatments for 24 hours. It was determined that the endothelial barrier resistance increased in bEnd.3 cells upon 0.5 and 10 µg/ml FABP7 treatment for 24 hours compared to the rest of the experimental groups (Figure 5.5; $p < 0.05$), while no marked alterations were observed with 0.05, 0.1, and 1 µg/ml doses of FABP7.

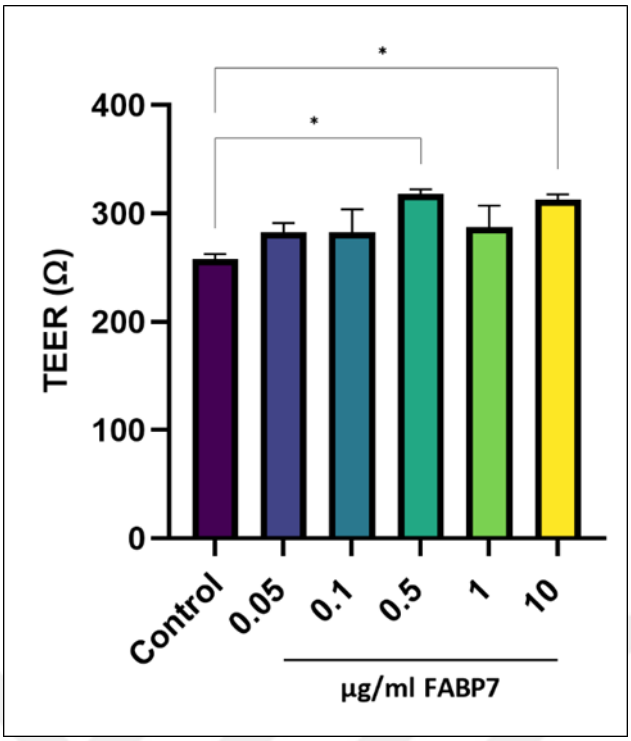

Figure 5.5 Effect of FABP7 on transendothelial electrical resistance in bEnd.3 cells. The data were presented as mean±SD. *p< 0.05.

5.2.3 Effects of FABP7 on Permeability

In order to show the in vitro effect of FABP7 administration on BBB permeability, bEnd.3 cells were treated with 0.05, 0.1, 0.5, 1, and 10 µg/ml doses of FABP7 for 24 hours. No significant alterations were observed in the fluorescence intensity of NaFl in the abluminal compartment of transwells following treatment with FABP7 at all doses (Figure: 5.6).

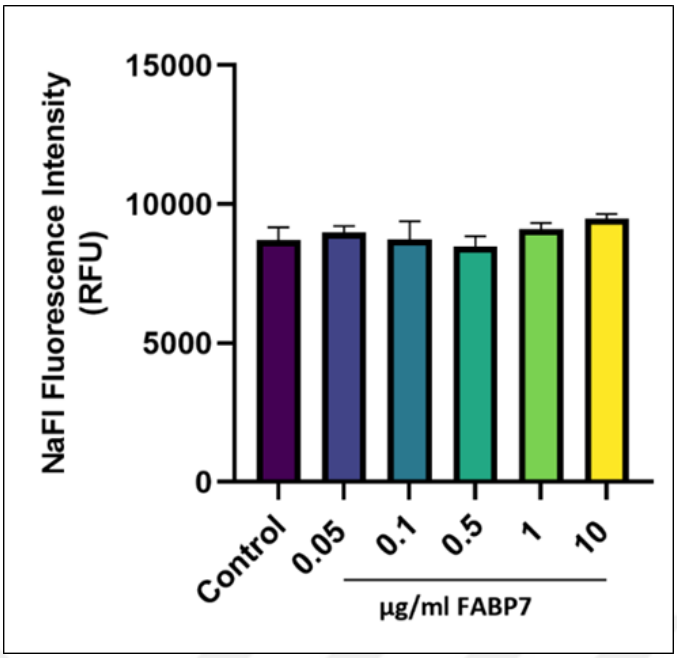

Figure 5.6 Effects of FABP7 on endothelial leakage in bEnd.3 cells. The data were presented as mean±SD.

5.3 The Effects of FABP7 on in vitro Blood-Brain Barrier Model following exposure to LPS

5.3.1 Effects of FABP7 on Transendothelial Electrical Resistance

In order to assess the in vitro effect of different doses of FABP7 on the integrity of BBB exposed to LPS, TEER values were measured after administration of 0.05, 0.1, 0.5, 1, and 10 µg/ml doses of FABP7 to bEnd.3 cells following treatment with LPS. As shown in Figure 5.7, LPS treatment caused a significant decrease in TEER values compared to the untreated control cells ($p < 0.01$). On the other hand, 0.5 µg/ml FABP7 treatment for 24 hours to these cells significantly increased the decreased TEER values ($p < 0.05$).

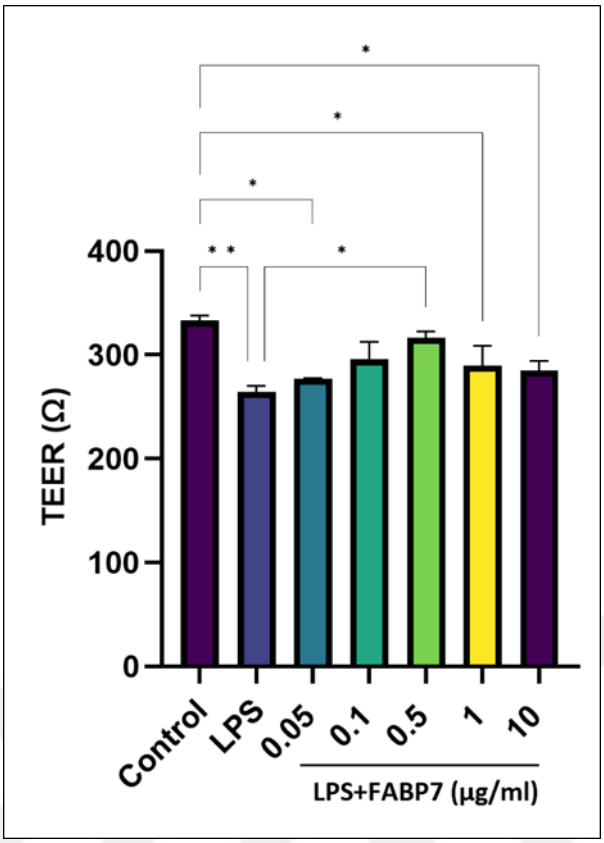

Figure 10.7 Effects of FABP7 on TEER in LPS-treated bEnd.3 cells. The data were presented as mean±SD. *p< 0.05 and **p< 0.01.

5.3.2 Effects of FABP7 on Permeability

Figure 5.8 shows the effect of FABP7 on the BBB leakage caused by exposure to LPS. Our results showed that LPS treatment caused a significant increase in the fluorescence intensity of NaFl in the abluminal compartment of transwells compared to the untreated controls ($p < 0.001$). The treatment of these cells with all doses of FABP7 significantly decreased the transport of NaFl across the bEnd.3 monolayer on the transwell inserts ($p < 0.001$ and $p < 0.0001$). In addition, no marked differences were found between the tested doses of FABP7 after LPS treatment.

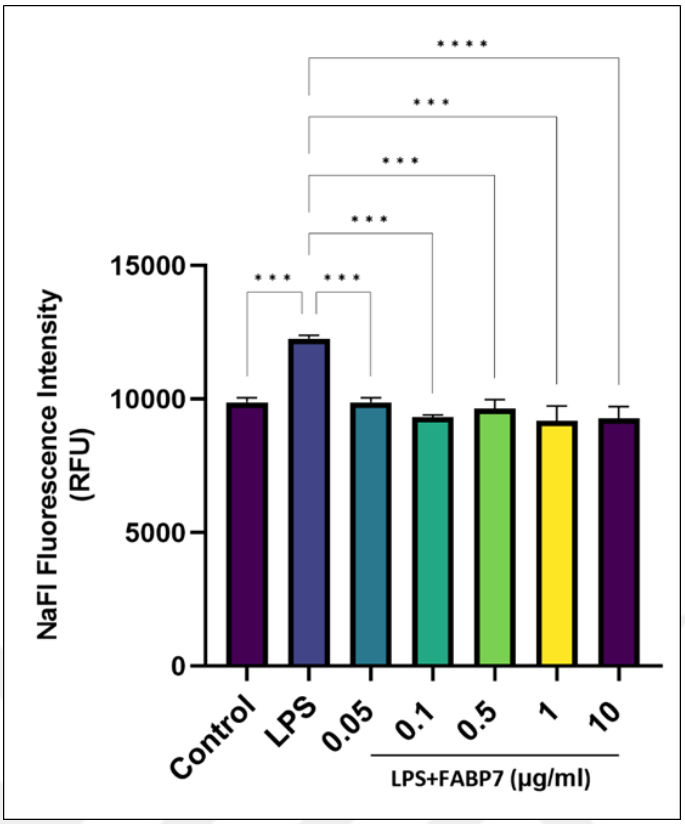

Figure 5.811 Effects of FABP7 on BBB permeability in LPS-treated bEnd.3 cells. The data were presented as mean±SD. ***p< 0.001 and ****p< 0.0001.

5.4 Effects of FABP7 on the Immunoreactivity of BBB Proteins and Inflammatory Mediators in LPS-treated bEnd.3 Cells

In order to show the in vitro effects of FABP7 on the immunoreactivity of barrier-related proteins (claudin-5, ZO-1, caveolin-1, and mfsd2a) and proinflammatory agents (IL-1β, NF-κB) in BBB exposed to LPS, FABP7 was administered to bEnd.3 cells at the dose of 0.5 µg/ml for 24 hours following LPS treatment (0.5 µg/ml, 24 hours). Next, the immunofluorescence staining was performed and the immunoreactivity was quantified by image analysis.

5.4.1 Effects of FABP7 on Tight Junction Proteins

bEnd.3 cells treated with LPS showed markedly weak immunostaining for claudin-5, while FABP7 administration to these cells led to stronger staining of claudin-5 comparable to that of controls (Figure 5.9). In parallel, quantification of claudin-5

immunoreactivity by image analysis showed that LPS treatment significantly decreased the immunofluorescence intensity of claudin-5 in bEnd.3 cells (Figure 5.9; $p < 0.0001$). In addition, a significant increase of the decreased claudin-5 immunoreactivity was noted by FABP7 administration to these cells ($p < 0.0001$).

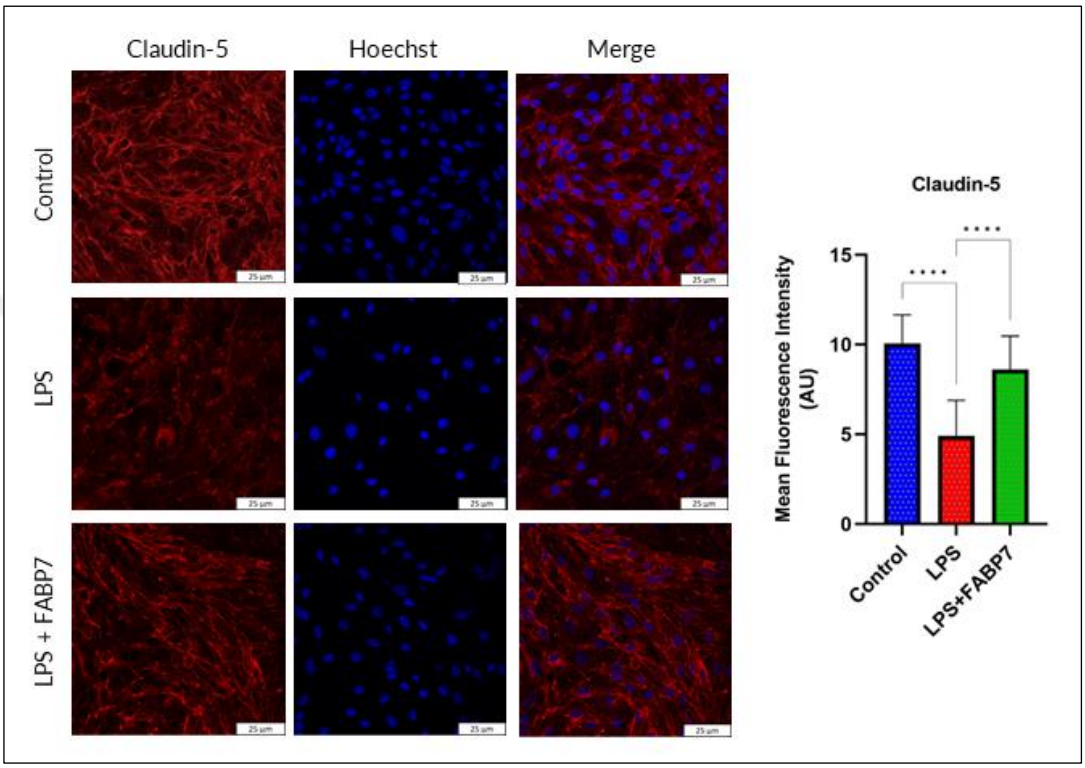

Figure 5.9 Immunofluorescence staining for claudin-5 in bEnd.3 cells exposed to LPS treated or untreated with FABP7 and quantification of immunofluorescence intensity with image analysis. In the micrographs, red color represents immunoreactivity for claudin-5 while the nuclei are stained with Hoechst (blue). The data in the graph were presented as mean±SD. ****$p < 0.0001$.

When the bEnd.3 cells were treated with LPS, considerably weak immunostaining for ZO-1 was observed compared to controls (Figure 5.10). FABP7 administration to these cells led to slightly stronger ZO-1 immunostaining. Accordingly, quantification of immunoreactivity by image analysis showed that LPS treatment to bEnd.3 cells significantly decreased the immunofluorescence intensity for ZO-1 (Figure 5.10; $p < 0.0001$). In addition, although an increase was noted in the ZO-1 immunoreactivity by FABP7 administration to these cells, the difference failed to reach statistical significance and furthermore, immunofluorescence intensity was found to be significantly lower than that of control.

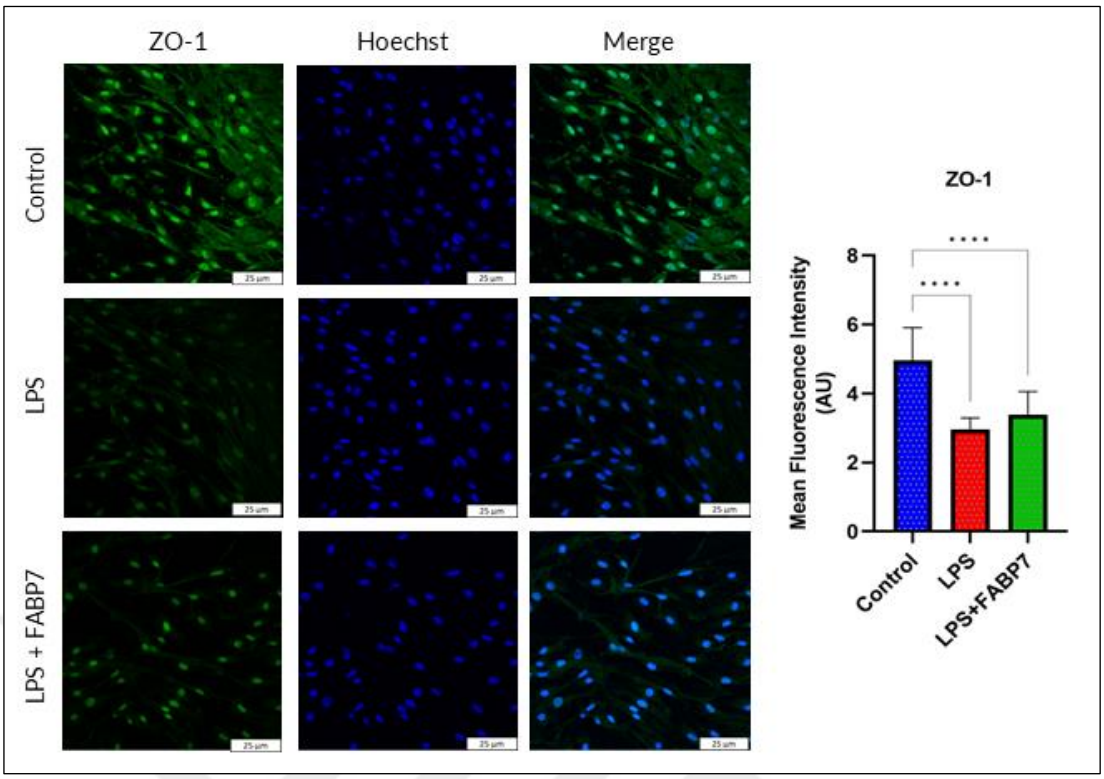

Figure 5.10 Immunofluorescence staining for ZO-1 in bEnd.3 cells exposed to LPS treated or untreated with FABP7 and quantification of immunofluorescence intensity with image analysis. In the micrographs, green color represents immunoreactivity for ZO-1 while the nuclei are stained with Hoechst (blue). The data in the graph were presented as mean±SD. ****p< 0.0001.

5.4.2 Effects of FABP7 on Transcytosis Regulating Proteins

LPS-treated bEnd.3 cells showed a strong immunostaining for caveolin-1 compared to the untreated control cells (Figure 5.11), whereas FABP7 administration to these cells yielded a markedly weaker immunostaining comparable to that of control cells. Quantification of immunostaining with image analysis showed that LPS treatment to bEnd.3 cells significantly increased caveolin-1 immunofluorescence intensity, while a significant decrease in caveolin-1 immunoreactivity was noted following FABP7 administration to these cells (Figure 5.11; p< 0.0001).

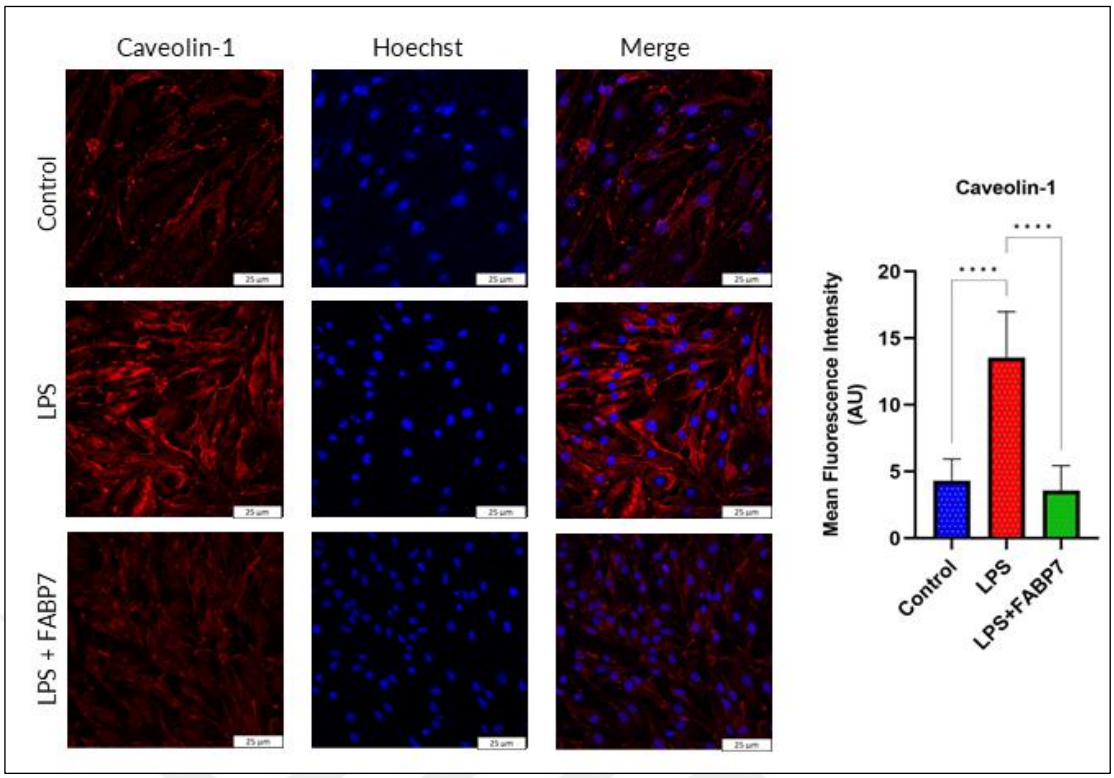

Figure 5.11 Immunofluorescence staining for caveolin-1 in bEnd.3 cells exposed to LPS treated or untreated with FABP7 and quantification of immunofluorescence intensity with image analysis. In the micrographs, red color represents immunoreactivity for caveolin-1 while the nuclei are stained with Hoechst (blue). The data in the graph were presented as mean±SD. ****p< 0.0001.

bEnd.3 cells treated with LPS showed markedly weak immunostaining for mfsd2a, while FABP7 administration to these cells led to a stronger staining comparable to that of controls (Figure 5.12). In parallel, quantification of mfsd2a immunoreactivity by image analysis showed that LPS treatment significantly decreased the immunofluorescence intensity of mfsd2a in bEnd.3 cells (Figure 5.12; p< 0.0001). In addition, a significant increase of the decreased mfsd2a immunoreactivity was noted by FABP7 administration to these cells (p< 0.0001).

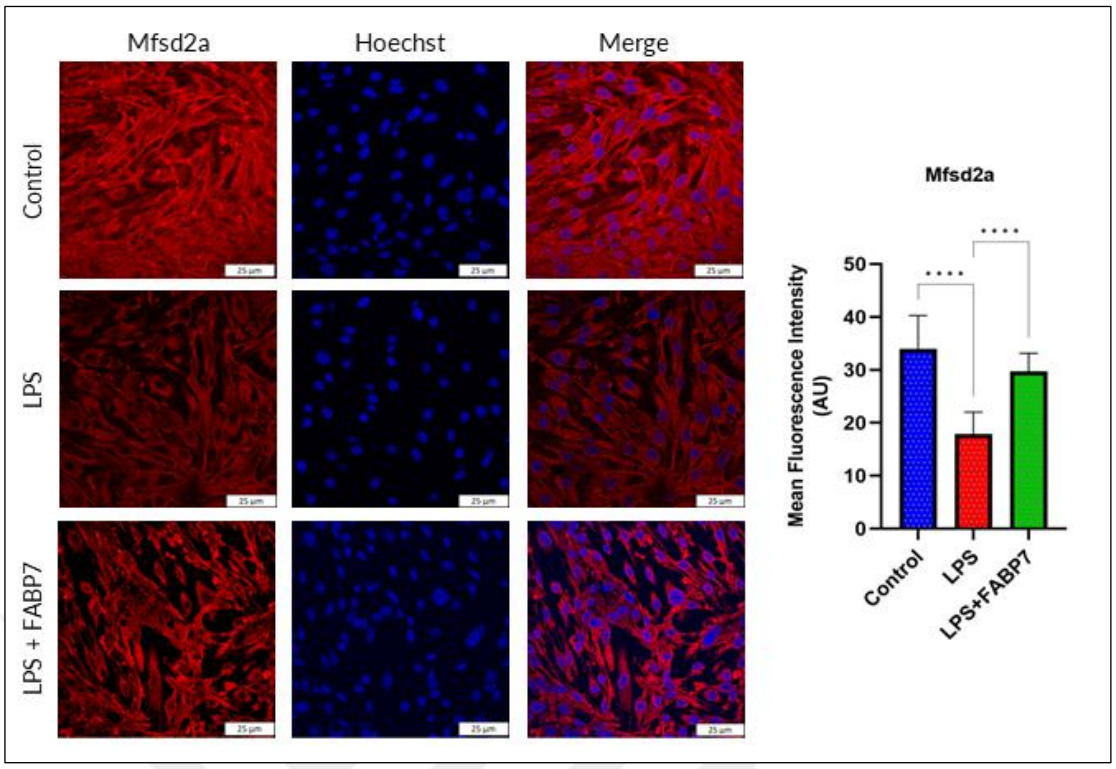

Figure 5.12 Immunofluorescence staining for mfsd2a in bEnd.3 cells exposed to LPS treated or untreated with FABP7 and quantification of immunofluorescence intensity with image analysis. In the micrographs, red color represents immunoreactivity for mfsd2a while the nuclei are stained with Hoechst (blue). The data in the graph were presented as mean±SD. ****p< 0.0001.

5.4.3 Effects of FABP7 on Inflammatory Mediators

LPS-treated bEnd.3 cells showed a strong immunostaining for NF-κB compared to the untreated control cells (Figure 5.13), whereas FABP7 administration to these cells yielded a markedly weaker immunostaining comparable to that of control cells. Quantification of immunostaining with image analysis showed that LPS treatment to bEnd.3 cells significantly increased NF-κB immunofluorescence intensity, while a significant decrease in NF-κB immunoreactivity was noted following FABP7 administration to these cells (Figure 5.13; p< 0.0001).

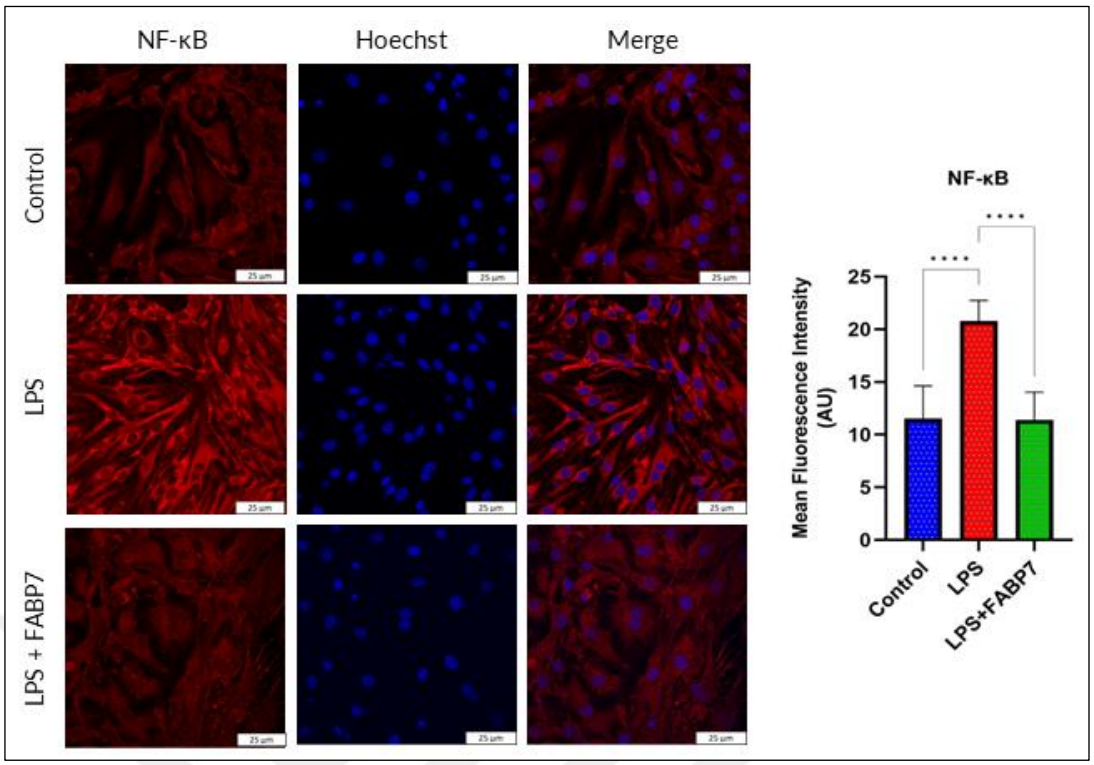

Figure 5.13 Immunofluorescence staining for NF-κB in bEnd.3 cells exposed to LPS treated or untreated with FABP7 and quantification of immunofluorescence intensity with image analysis. In the micrographs, red color represents immunoreactivity for NF-κB while the nuclei are stained with Hoechst (blue). The data in the graph were presented as mean±SD. ****p< 0.0001.

bEnd.3 cells treated with LPS showed markedly strong immunostaining for IL-1β, while FABP7 administration to these cells decreased the immunostaining of IL-1β comparable to that of controls (Figure 5.14). Accordingly, quantification of IL-1β immunoreactivity by image analysis showed that LPS treatment significantly increased the immunofluorescence intensity of IL-1β in bEnd.3 cells (Figure 5.14; p< 0.0001). In addition, a significant decrease of the increased IL-1β immunoreactivity was noted by FABP7 administration to these cells (p< 0.0001).

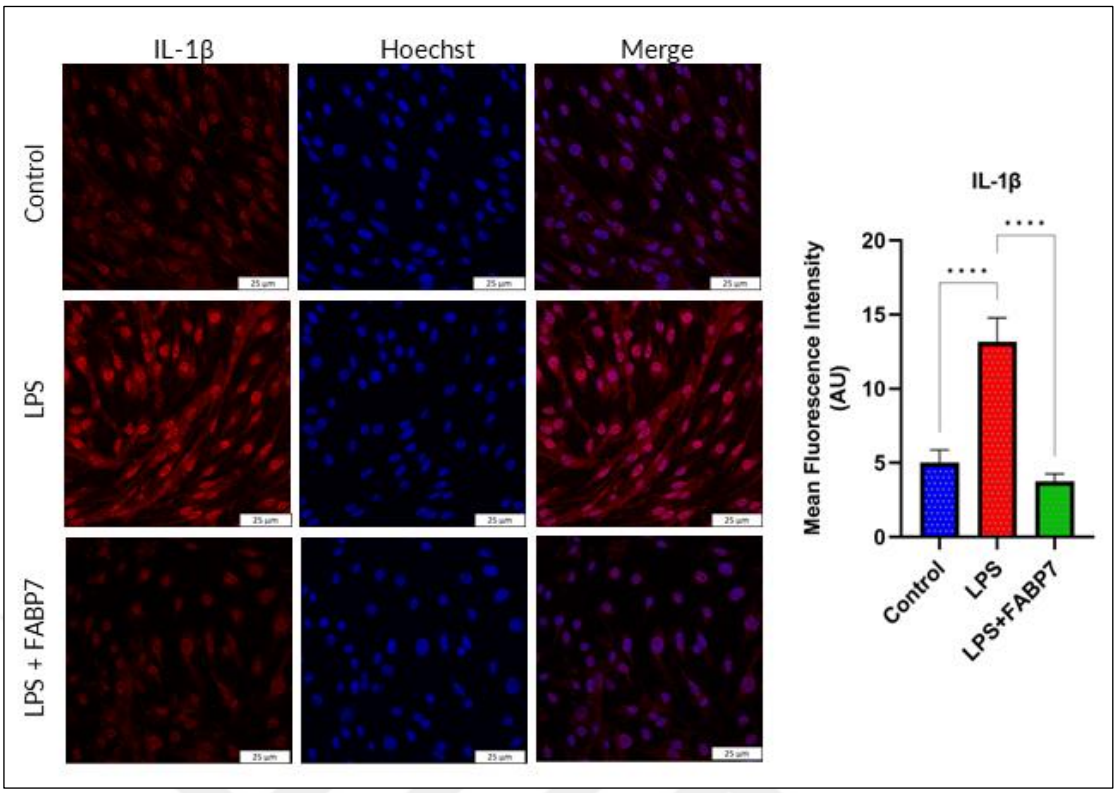

Figure 5.14 Immunofluorescence staining for IL-1β in bEnd.3 cells exposed to LPS treated or untreated with FABP7 and quantification of immunofluorescence intensity with image analysis. In the micrographs, red color represents immunoreactivity for IL-1β while the nuclei are stained with Hoechst (blue). The data in the graph were presented as mean±SD. ****$p < 0.0001$.

5.5 Effects of FABP7 on the Expression of BBB Proteins and Inflammatory Mediators in LPS-treated bEnd.3 Cells

The treatment of LPS to bEnd.3 cells significantly decreased claudin-5 expression compared to the untreated control group as detected by western blotting (Figure 5.15; $p < 0.01$), while FABP7 administration to these cells significantly increased the decreased claudin-5 expression ($p < 0.05$). Caveolin-1 expression was found to be significantly increased in bEnd.3 cells by LPS, however, FABP7 administration to these cells significantly reduced the increased expression of caveolin-1 (Figure 5.15; $p < 0.0001$). The treatment of LPS to bEnd.3 cells significantly lowered the expression of mfsd2a (Figure 5.15; $p < 0.01$). In these cells, the decrease in mfsd2a expression was observed to be reversed significantly by FABP7 administration ($p < 0.05$). NF-κB expression was found to be significantly increased in bEnd.3 cells by LPS, however, FABP7 administration to these cells significantly reduced the increased expression of NF-κB (Figure 5.15; $p < 0.0001$).

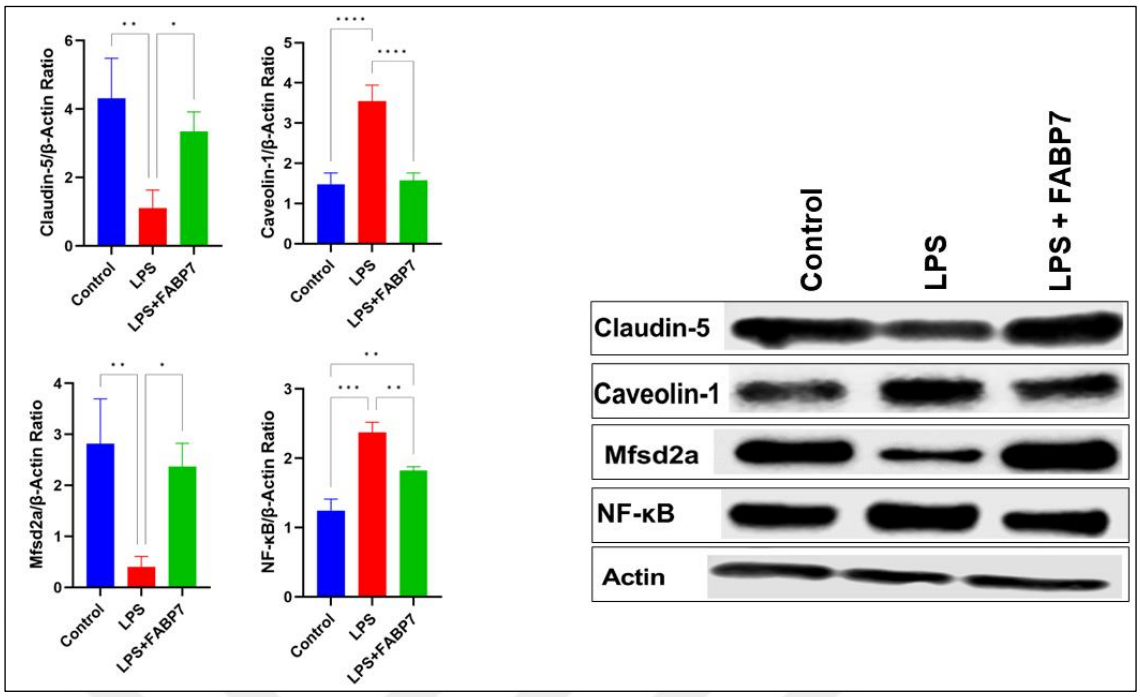

Figure 5.15 Effects of FABP7 on the expression levels of claudin-5, caveolin-1, mfsd2a, and NF-κB in LPS-treated bEnd.3 cells. The data were presented as mean±SD. *p< 0.05, **p < 0.01, ***p< 0.001 and ****p< 0.0001.

5.6 Effects of FABP7 in C57Bl/6 mice under LPS-induced Inflammatory Condition

5.6.1 Effects of FABP7 on Body Temperature

Figure 5.16 shows the body temperature of animals in experimental groups at three time points; 1, 6, and 24 hours following LPS and/or FABP7 administrations. The recorded body temperatures of control animals and those treated with 40 and 80 µg/kg doses of FABP7 animals were within the normal ranges. In LPS-treated animals, the body temperature steadily increased and reached 42°C at 24 hours. FABP7 administration to these animals at 40 µg/kg caused a decrease in body temperature after 6 hours, however, the recorded degrees were found to be over 38°C until 24 hours. When FABP7 was administered 80 µg/kg to LPS-treated animals, a more pronounced decrease in body temperature was observed compared to the lower FABP7 dose, and recorded values were found to be comparable to those of the control animals.

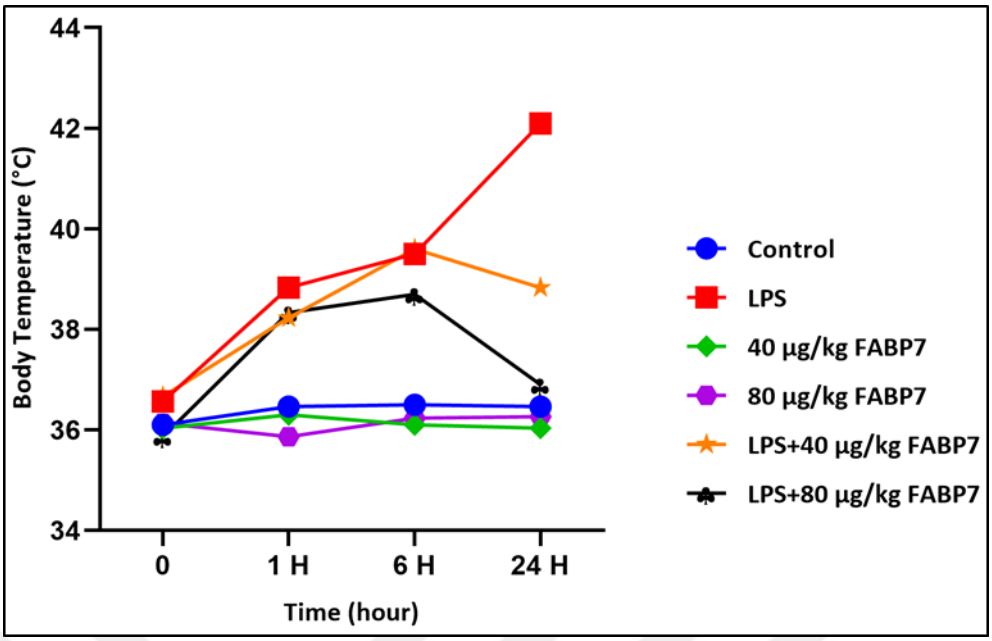

Figure 5.16 Effects of LPS and/or FABP7 on body temperature in mice.

5.6.2 Effects of FABP7 on Inflammatory Biomarkers

Figure 5.17 shows serum levels of CRP of the animals in experimental groups. A significant increase in CRP level was observed by LPS treatment ($p < 0.001$). FABP7 administration to these animals at the dose of 80 µg/kg significantly reduced the serum CRP levels ($p < 0.01$), while the lower dose of FABP7 did not yield a marked alteration.

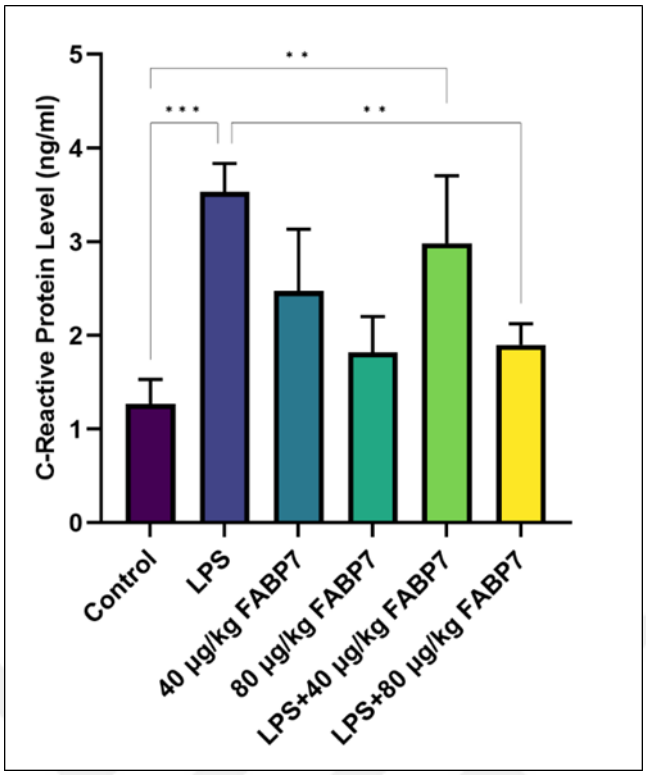

Figure 5.17 Effects of FABP7 on serum levels of CRP in the experimental groups. The data were presented as mean±SD. **p< 0.01 and ***p< 0.001.

Serum levels of PCT of the animals in experimental groups are shown in Figure 5.18. LPS treatment caused a significant increase in PCT level (p< 0.0001). FABP7 administration to these animals at the dose of 80 µg/kg yielded a significant decrease in the increased serum PCT levels (p< 0.0001), while the lower dose of FABP7 did not cause a marked alteration.

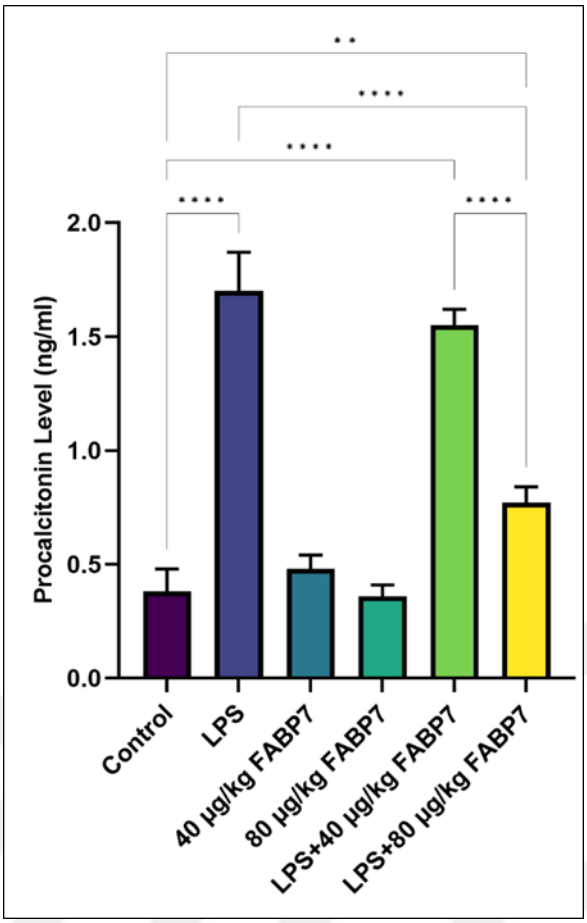

Figure 5.18 Effects of FABP7 on serum levels of PCT in experimental groups. The data were presented as mean±SD. **$p < 0.01$ and ****$p < 0.0001$.

Figure 5.19 shows serum levels of ROS of the animals in experimental groups. A significant increase in ROS level was observed by LPS treatment ($p < 0.001$). FABP7 administrations to these animals at the doses of 40 and 80 µg/kg FABP7 significantly decreased the increased serum ROS levels ($p < 0.01$, $p < 0.001$).

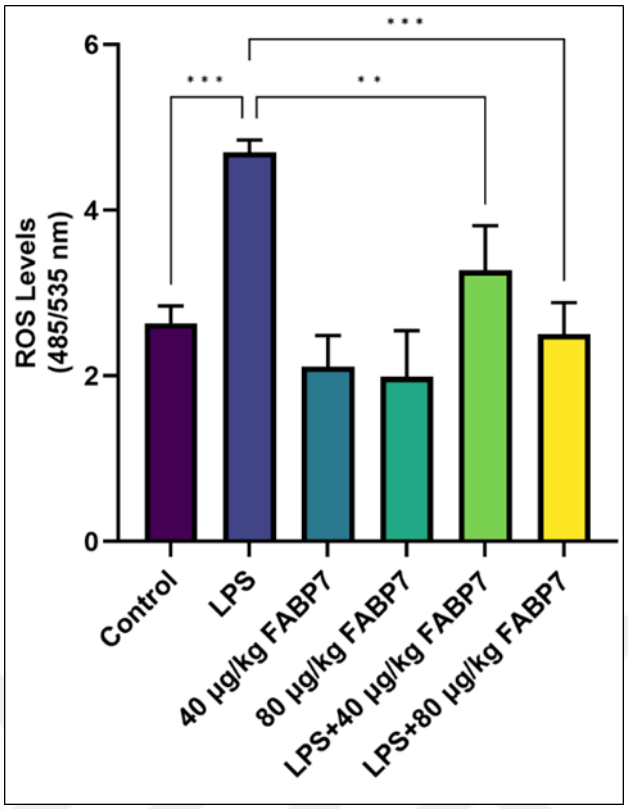

Figure 5.19 Effects of FABP7 on serum levels of ROS in experimental groups. The data were presented as mean±SD. **$p < 0.01$ and ***$p < 0.001$.

5.6.3 Effects of FABP7 on Anxiety-like Behavior

Figure 5.20 shows the anxiety levels of the animals in experimental groups. The treatment with LPS significantly increased immobility time and the tendency to stay in the closed arm compared with the control group ($p < 0.05$). When FABP7 was administered to LPS-treated animals at the dose of 80 µg/kg, a significant increase in the decreased mobility time and the tendency to stay in the open arm was observed ($p < 0.01$). However, the lower dose of FABP7 did not decrease the level of anxiety in LPS-injected mice.

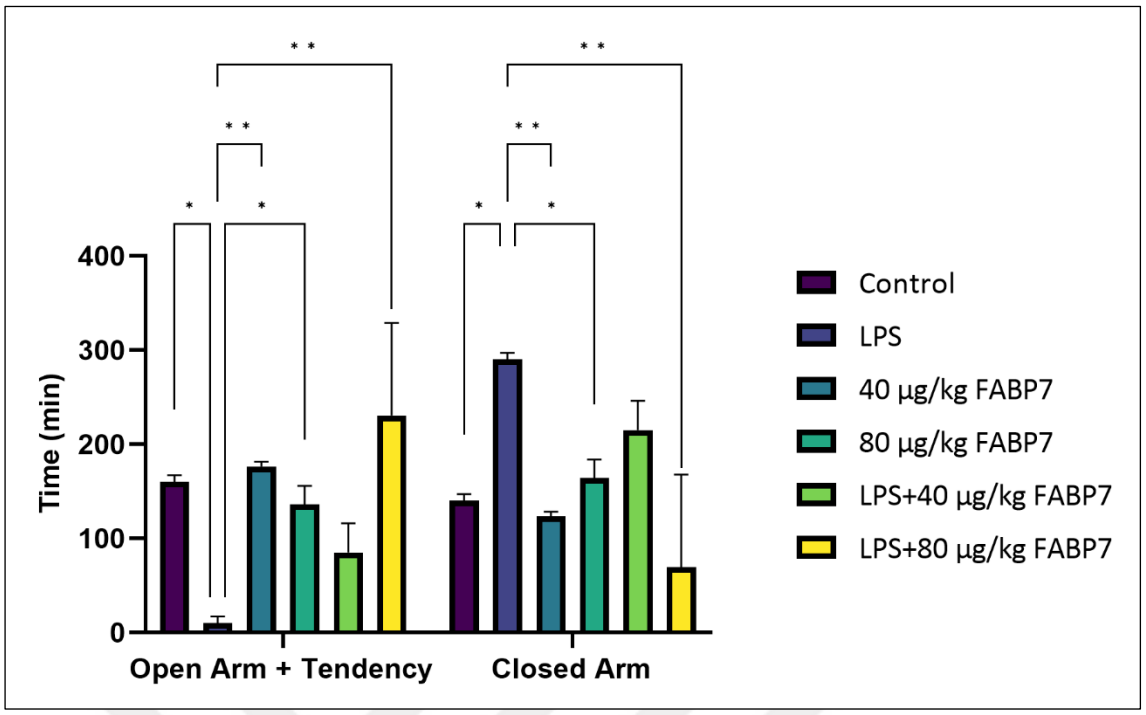

Figure 5.20 Effects of FABP7 on anxiety-like behavior in experimental groups. The data were presented as mean±SD. *$p < 0.05$ and **$p < 0.01$.

5.6.4 Effects of FABP7 on Blood-Brain Barrier Permeability

Figure 5.21 shows the effect of FABP7 on the *in vivo* BBB leakage caused by exposure to LPS as detected by IVIS imaging. A strong fluorescent signal was observed in the brains of animals following treatment with LPS. When these animals were administered with 80 µg/kg FABP7, the fluorescent signal in the brain was found to be diminished. When the radiant efficiency of albumin Alexa fluor 594 was quantified, it was found that LPS treatment caused a significant increase in the fluorescence intensity of the tracer in the brain compared to the control animals ($p < 0.01$) and the administration of FABP7 at the dose of 80 µg/kg markedly decreased the increased fluorescence intensity of tracer in the brain ($p < 0.05$). In addition, no significant differences were detected in the brains of LPS-treated animals administered the lower dose of FABP7 compared to the LPS group.

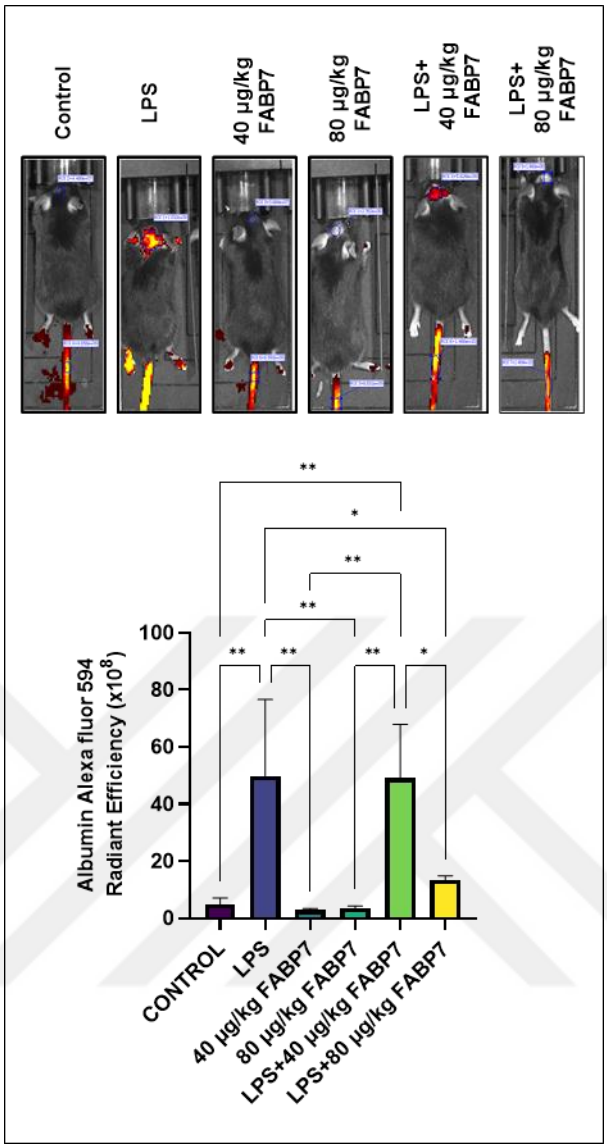

Figure 5.21 The *in vivo* effects of FABP7 on BBB leakage following LPS treatment. The data were presented as mean±SD. *p< 0.05 and **p< 0.01

Figure 5.22 shows the effect of FABP7 on the severity of *ex vivo* BBB leakage caused by LPS as detected by IVIS imaging. The treatment of LPS caused a severe enhancement of fluorescent signals in the brains of animals, while the fluorescent signal in the brain was found to be reduced in these animals following the administration of 80 µg/kg FABP7. When the radiant efficiency of albumin Alexa fluor 594 was quantified, LPS treatment caused a significant increase in the fluorescence intensity of the tracer in the brain compared to the control animals (p< 0.0001). However, the high dose of FABP7 administration significantly decreased the increased fluorescence intensity of the tracer in the *ex vivo* brain (p< 0.0001). In addition, no marked alteration was observed in the

fluorescent intensity of tracer in the brains of LPS-treated animals following 40 µg/kg FABP7 administration.

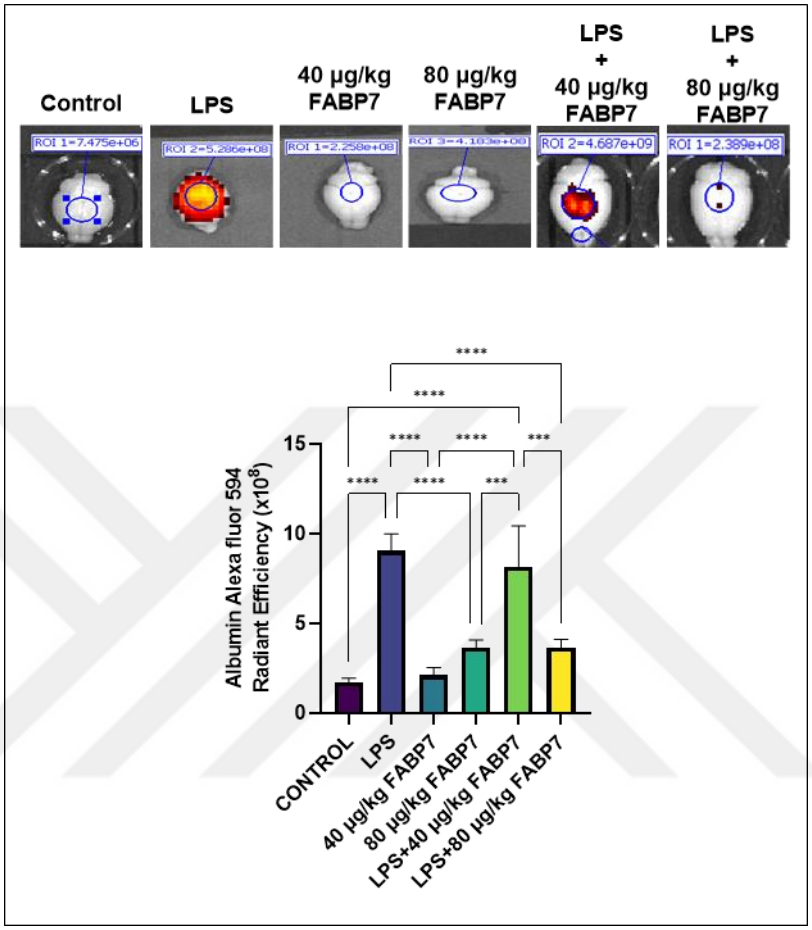

Figure 5.22 The *ex vivo* effects of FABP7 on BBB leakage following LPS treatment. The data were presented as mean±SD. ***p< 0.001 and ****p< 0.0001.

5.6.5 Effects of FABP7 on Blood-Brain Barrier Permeability

Figures 5.23, 24, and 25 show the effect of FABP7 on the BBB extravasation of albumin Alexa fluor 594 tracer caused by exposure to LPS in the cerebral cortex, hippocampus, and midbrain, respectively, as detected by confocal microscopy.

The animals treated with LPS showed a significantly higher extravasation of albumin Alexa fluor 594 in the cerebral cortex compared to control animals (Figure 5.23; p< 0.0001). When these animals were administered FABP7 at the dose of 80 µg/kg, a significant decrease of the increased fluorescence intensity of the tracer was noted (p< 0.0001). Meanwhile, the administration of the lower dose of FABP7 to LPS-treated

animals caused a significant increase in the leakage of the tracer ($p< 0.0001$). In addition, the fluorescence intensity of albumin Alexa fluor 594 was found to be significantly higher in LPS-untreated mice administered 40 and 80 µg/kg FABP7 with respect to control animals, however, the increases were observed to be to a lesser extent than that noted by LPS.

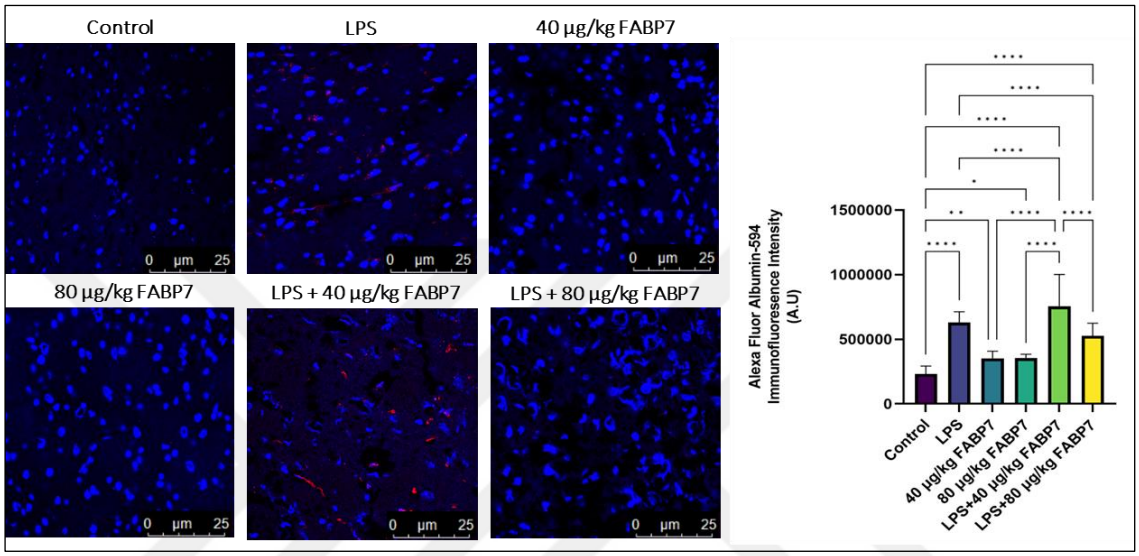

Figure 5.23 The effects of FABP7 on the increased BBB permeability by LPS in cerebral cortex. In the micrographs, red color represents the fluorescence of albumin Alexa fluor 594 tracer, and the nuclei are stained with Hoechst (blue). The data were presented as mean±SD. *$p< 0.05$, **$p< 0.01$ and ****$p< 0.0001$.

The extravasation of albumin Alexa fluor 594 was significantly increased by LPS treatment in the hippocampus of mice compared to control animals (Figure 5.24; $p< 0.0001$). However, a significant decrease of the increased fluorescence intensity of the tracer was noted in these animals by administration of FABP7 at the dose of 80 µg/kg ($p< 0.0001$). Moreover, the fluorescence intensity of albumin Alexa fluor 594 was found to be significantly increased in LPS-untreated mice administered 80 µg/kg FABP7 compared to control animals, however, the increases were observed to be to a lesser extent than that noted by LPS.

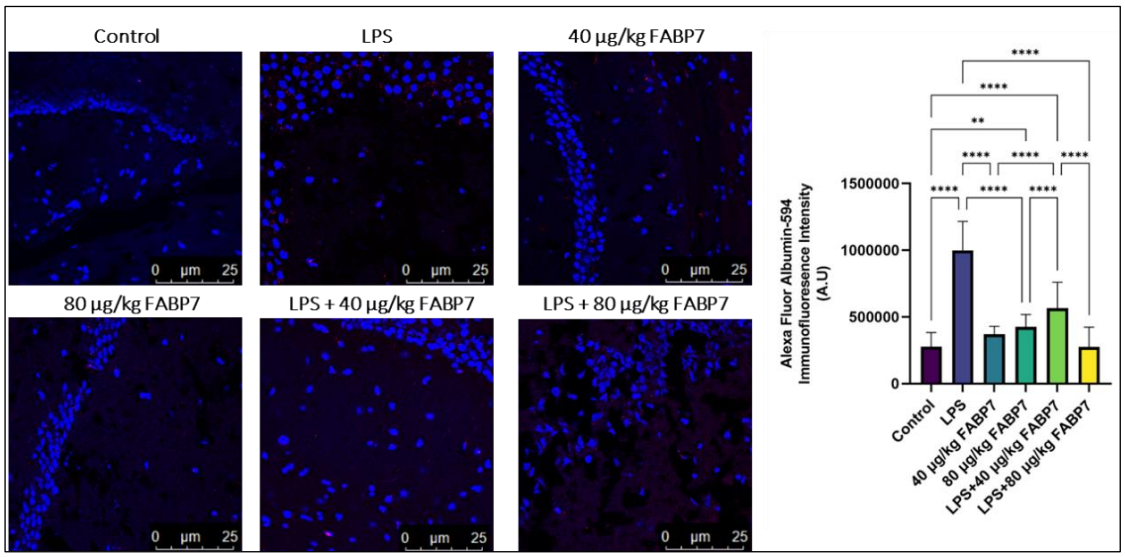

Figure 5.24 The effects of FABP7 on the increased BBB permeability by LPS in the hippocampus. In the micrographs, red color represents the fluorescence of albumin Alexa fluor 594 tracer, and the nuclei are stained with Hoechst (blue). The data were presented as mean±SD. **p< 0.01 and ****p< 0.0001.

The treatment of LPS caused a significantly increased extravasation of albumin Alexa fluor 594 in the midbrain compared to control mice (Figure 5.25; p< 0.0001). In contrast to other regions of the brain, the fluorescence intensity of the tracer was found to be significantly decreased in LPS-treated mice administered 40 and 80 µg/kg FABP7 compared to the LPS group (p< 0.0001).

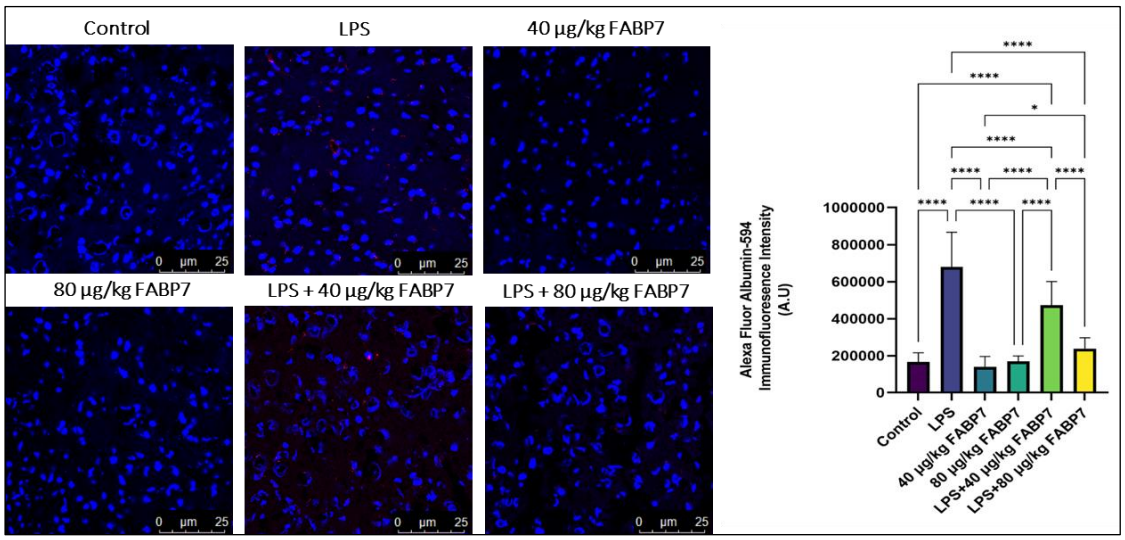

Figure 5.25 The effects of FABP7 on the increased BBB permeability by LPS in midbrain. In the micrographs, red color represents the fluorescence of albumin Alexa fluor 594 tracers, and the nuclei are stained with Hoechst (blue). The data were presented as mean±SD. *p< 0.05 and ****p< 0.0001.

5.6.6 Effects of FABP7 on the Claudin-5 Immunoreactivity in Cerebral Cortex and Hippocampus

The brain microvessels of the cerebral cortex in control mice were observed to display a strong immunostaining for claudin-5 along the capillary wall, while LPS treatment to these animals yielded a considerably weaker staining. 80 µg/kg FABP7 administration led to a stronger claudin-5 staining in LPS-treated animals. When the claudin-5 immunoreactivity was quantified by image analysis, it was found that LPS treatment significantly decreased the immunofluorescence intensity of claudin-5 in the cerebral cortex ($p < 0.0001$), while a significant increase of the decreased claudin-5 immunoreactivity was noted by high dose of FABP7 administration to LPS-injected mice ($p < 0.05$). Moreover, in LPS-treated and -untreated animals, the administration of FABP7 at the dose of 40 µg/kg decreased claudin-5 immunoreactivity being statistically significant in the latter experimental group.

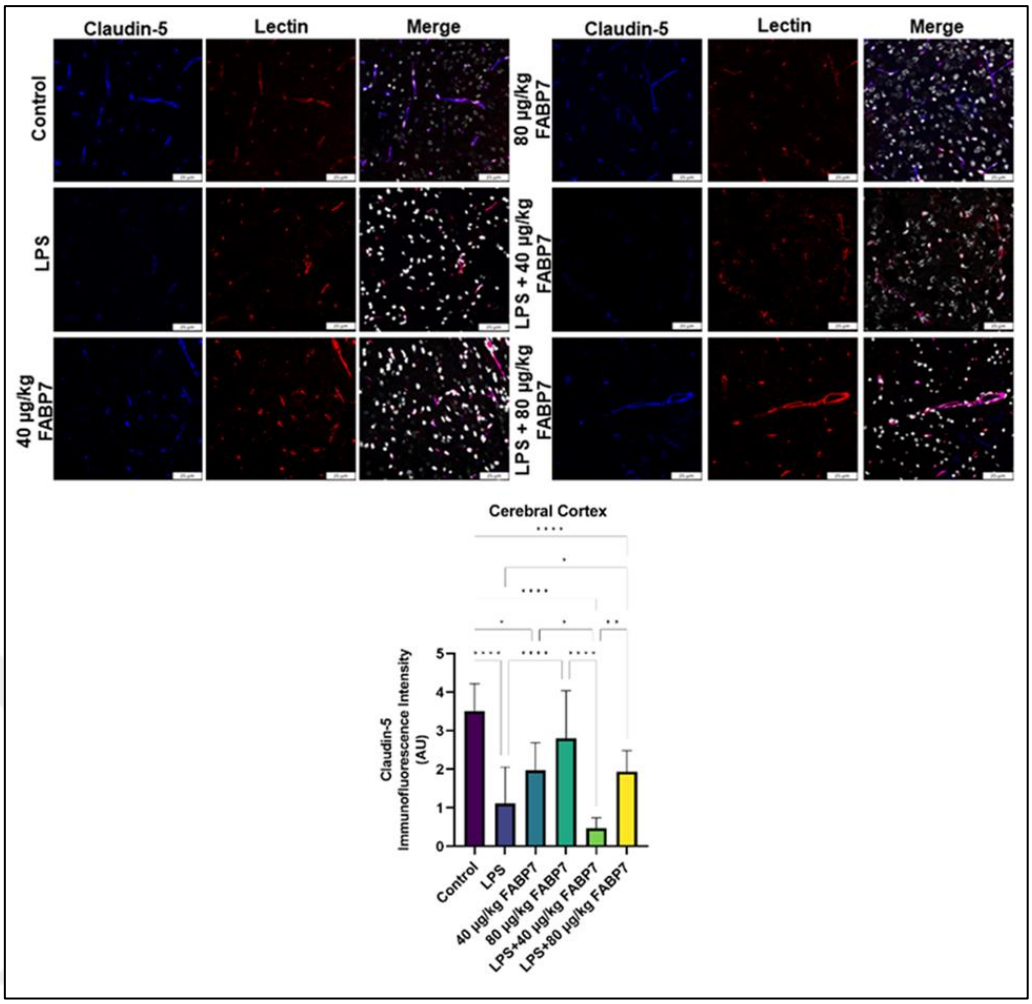

Figure 5.26 Effects of FABP7 on the immunofluorescence intensity of claudin-5 in the cerebral cortex following LPS treatment. In the micrographs, blue and red colors represent immunoreactivity for claudin-5 and lectin, respectively, while the nuclei are stained with Hoechst (gray). The data were presented as mean±SD. *p< 0.05, **p< 0.01 and ****p< 0.0001.

The LPS-treated mice demonstrated poor immunostaining for claudin-5 in the hippocampus. In these animals, a stronger staining of claudin-5 was observed when 80 µg/kg FABP7 was administered in contrast to the animals administered 40 µg/kg FABP7. Moreover, the quantification of claudin-5 immunoreactivity by image analysis showed that LPS treatment markedly decreased the immunofluorescence intensity of claudin-5 in the hippocampus (Figure 5.27; $p < 0.0001$), while a significant increase of the decreased claudin-5 immunoreactivity was found in mice administered a high dose of FABP7 following LPS treatment ($p < 0.05$). In addition, no significant alteration in the immunofluorescence intensity of claudin-5 was detected in the mice administered low and high doses of FABP7 compared to the control group.

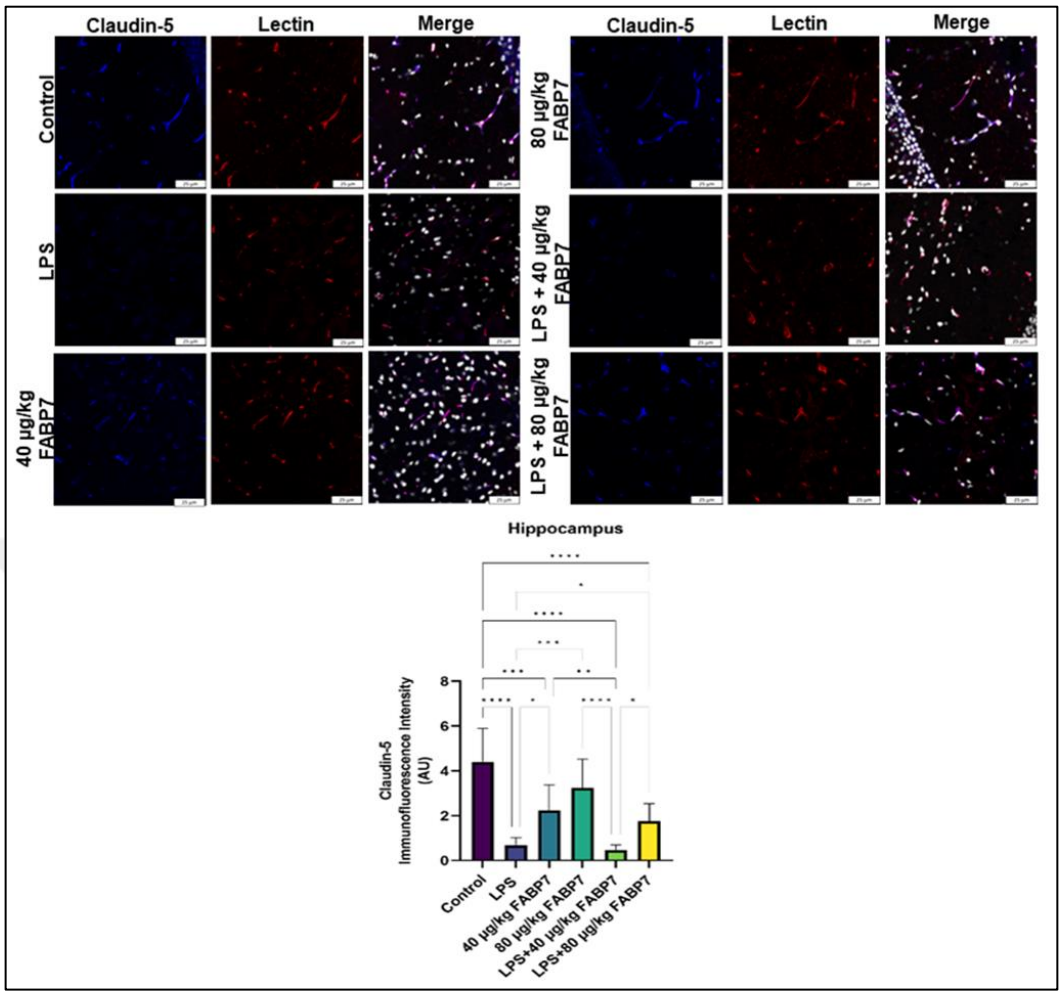

Figure 5.27 Effects of FABP7 on the immunofluorescence intensity of claudin-5 in the hippocampus following LPS treatment. In the micrographs, blue and red colors represent immunoreactivity for claudin-5 and lectin, respectively, while the nuclei are stained with Hoechst (gray). The data were presented as mean±SD. *p< 0.05, **p< 0.01, ***p< 0.001 and ****p< 0.0001.

5.6.7 Effects of FABP7 on the Expression Levels of BBB Proteins and NF-κB *in the Brain*

The treatment of LPS significantly decreased claudin-5 expression in the cerebral cortex compared to control animals (Figure 5.28; p< 0.001). In these animals, high dose FABP7 administration significantly increased the decreased claudin-5 expression (p< 0.01). In addition, the administration of FABP7 to LPS-untreated animals at both doses yielded significantly higher claudin-5 expression levels compared to controls.

Caveolin-1 expression was found to be significantly increased in the cerebral cortex of LPS-treated mice compared to control animals (Figure 5.28; p< 0.0001). 80

μg/kg FABP7 administration to these animals significantly reduced the increased caveolin-1 expression ($p < 0.01$), while low dose FABP7 administration did not cause any significant alteration. On the other hand, the administration of FABP7 to LPS-untreated animals at both doses yielded higher caveolin-1 expression levels compared to controls, with the differences being significant only by 80 μg/kg FABP7.

The treatment of LPS significantly decreased the expression level of mfsd2a in the cerebral cortex (5.28; $p < 0.001$), while a significant increase in the decreased mfsd2a expression was observed when a high dose of FABP7 was administered to these animals ($p < 0.01$).

A significant increase in the expression level of NF-κB was observed by LPS in the cerebral cortex of mice compared to controls (Figure 5.28; $p < 0.0001$), while in these animals, FABP7 administration at the dose of 80 μg/kg significantly decreased the increased NF-κB expression ($p < 0.001$). No significant alteration in NF-κB expression was detected by the administration of low and high doses of FABP7 to LPS-untreated animals.

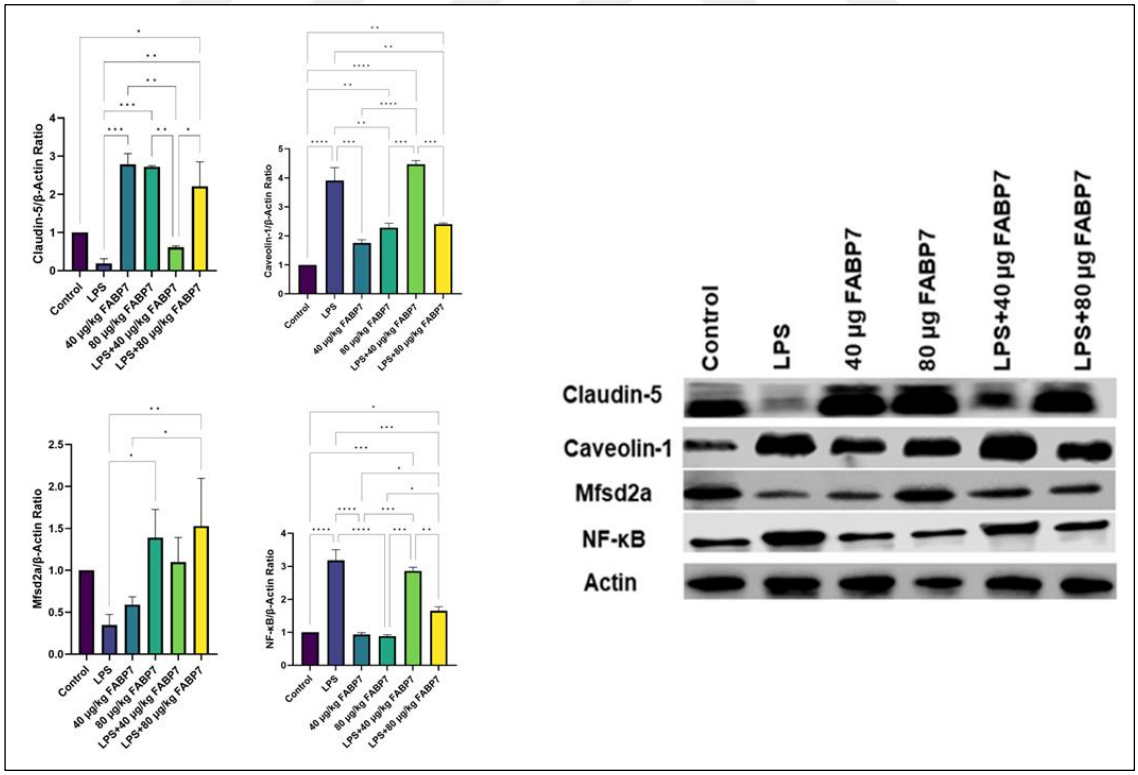

Figure 5.28 Effects of FABP7 on the expression levels of claudin-5, caveolin-1, mfsd2a, and NF-κB in cerebral cortex of mice following LPS treatment. The data were presented as means±SD. *$p < 0.05$, **$p < 0.01$, ***$p < 0.001$ and ****$p < 0.0001$.

No significant changes in the claudin-5 expression was found in the hippocampus between the experimental groups (Figure 5.29).

LPS treatment significantly increased the expression level of caveolin-1 compared to control animals (Figure 5.29; $p< 0.0001$). In these animals, the administrations of 40 and 80 µg/kg FABP7 significantly reduced the increased caveolin-1 expression in the hippocampus ($p< 0.01$ and $p< 0.001$). In addition, both low and high doses of FABP7 did not change the caveolin-1 expression in the hippocampus compared to the control group.

The treatment of LPS decreased the expression level of mfsd2a (Figure 5.29; $p< 0.5$) while no significant increase in the mfsd2a expression was noted by the administrations of 40 and 80 µg/kg FABP7 in the hippocampus of mice. In addition, the administration of both doses of FABP7 to LPS-untreated mice significantly enhanced the expression level of mfsd2a ($p< 0.01$).

When the mice were treated with LPS, a significant increase in the expression level of NF-κB was observed in the hippocampus of mice compared to that of the control group (Figure 5.29; $p< 0.01$). Although the low and high doses of FABP7 administration decreased NF-κB expression in LPS-treated animals, the difference failed to reach statistical significance in the mice administered 40 µg/kg FABP7. Moreover, 80 µg/kg FABP7 markedly decreased the increased NF-κB expression under LPS conditions ($p< 0.05$).

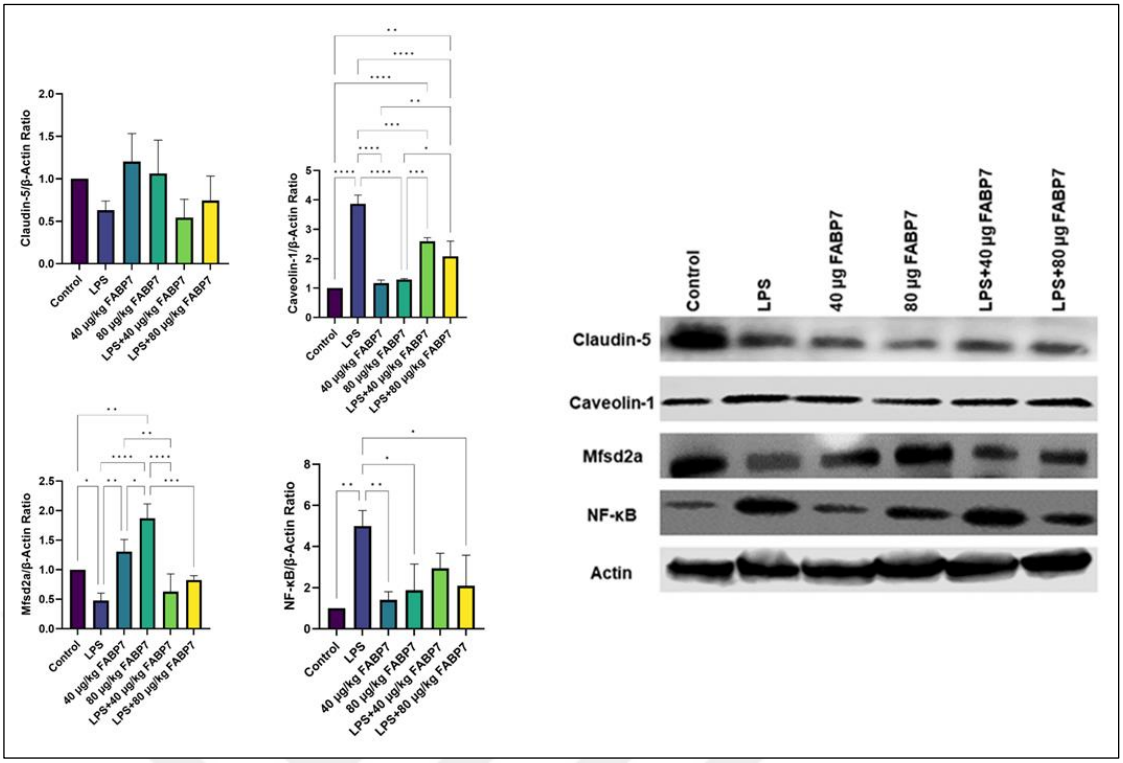

Figure 5.29 Effects of FABP7 on the expression levels of claudin-5, caveolin-1, mfsd2a, and NF-κB in hippocampus of mice following LPS treatment. The data were presented as means±SD. *p< 0.05, **p< 0.01, ***p< 0.001 and ****p< 0.0001.

CHAPTER 6:

DISCUSSION

Sepsis is one of the most common health problems in the intensive care unit and leads to various pathophysiological alterations in the body, including SAE. It has long been known that inflammation or SAE caused by LPS administration damage the BBB integrity (Xaio et al., 2001; Descamps et al.,2003; Banks et al., 2015), however, certain aspects of BBB disruption in this setting are still undiscovered. In the past few years, FABP7, an essential trophic factor in astrocytes expressed under both physiological and pathological conditions, has been reported to upregulate caveolar transport in endothelial cell in TBI (Rui et al., 2019b). In this study, we investigated the *in vitro* and *in vivo* effects of FABP7 on the structural and functional properties of BBB in LPS-induced inflammatory conditions. In this context, the changes in BBB permeability were evaluated using various methodological approaches and tracers, while the alterations in the expression of BBB proteins that are functional in paracellular and transcellular pathways and inflammatory mediators were explored by immunofluorescence and western blotting. Our data showed for the first time that the exogenous administration of FABP7 ameliorates the LPS-induced BBB impairment in *in vitro* and *in vivo* conditions by acting on both transcellular and paracellular pathways.

Neuroinflammation plays a central role in the progression of neurodegenerative diseases including PD, MS, AD, and Huntington's disease resulting in cognitive impairment (Mohamed et al., 2023; Rauf et al., 2022; Stephenson et al., 2018). Owing to the complexity of the pathogenesis of these neurodegenerative diseases, current therapeutic modalities are insufficient for effective treatment. At that point, establishing proper *in vitro* and *in vivo* experimental models are essential to explore the underlying mechanisms of neurodegenerative diseases and develop novel treatment strategies. LPS, the main component of the cell wall of gram negative bacteria, has been commonly used

to mimic septic conditions in *in vitro* and *in vivo* settings. Recent studies have demonstrated that LPS administration gives rise to the development of neuroinflammatory processes which damages the BBB integrity (C. Gao et al., 2020; Gonçalves et al., 2018; T. Li et al., 2020). Accumulated data from *in vitro* and *in vivo* studies showed that LPS causes BBB disruption through its effects on the expression of proteins involved in paracellular and transcellular pathways of transport across BBB causing the penetration of unwanted substances from the circulation into the brain (Li et al., 2018; Peng et al., 2021; Yang et al., 2023). Therefore, in light of the above-mentioned literature data, in order to explore the impact of FABP7 on BBB integrity under septic conditions, we used LPS administration in both *in vitro* and *in vivo* settings to evoke sepsis related inflammation.

In clinical studies, CRP and PCT values have been used as reliable markers for the detection of the presence and severity of inflammation (Kooistra et al., 2021). Another indicator of inflammation is an increased concentration of ROS in serum. ROS is involved in oxygen metabolism and cell signaling to maintain redox homeostasis under physiological conditions (Baek et al., 2020). In our study, we investigated the impact of FABP7 on these biomarkers in the serum of LPS-treated mice. We observed that LPS injection increased the levels of CRP, PCT, and ROS in serum, and we detected significant decreases in the increased levels of these biomarkers by the administration of FABP7, more pronouncedly with the high dose of the agent. In the meantime, LPS is one of the main inducers of fever under septic conditions. It mediates the fever response through its effects on IL-1 and IL-6 and causes increases in the levels of other pro-inflammatory mediators (Nilsberth et al., 2009; Ogawa & Kanoh, 1984). In our study, LPS treatment to mice significantly increased the body temperature of the animals, while a significant decrease in the increased body temperature was observed by high dose FABP7 administration. In a previous study, it is reported that LPS administration increases the levels of CRP and PCT and activates PRRs which results in BBB disruption (Tavares et al., 2005). In the meantime, increased level of ROS in serum stimulates the production of proinflammatory cytokines via the activation of MAPK signaling pathway (Wu et al., 2018), and leads to the oxidization of proteins and nucleic acids, resulting in toxic effects on brain tissue (Massaad, C. A., & Klann, E., 2011). Furthermore, LPS is reported to trigger the generation of proinflammatory mediators and ROS leading to BBB impairment (Bargi et al., 2021). In parallel, the overexpression of ROS has been shown

to promote the activation of the NF-κB signaling pathway via the release of TNF-α, IL-1β, IL-6, and MMPs leading to dislocation of TJ proteins in BBB (Erikson et al., 2020; Lehner et al., 2011). According to a recent study, FABP7 exerted protective effects on astrocytes exposed to high levels of ROS through the regulation of lipid droplet formation (Islam et al., 2019b). In light of the afore-mentioned literature data, the decreases in LPS-induced increased serum levels of CRP, PCT, and ROS achieved in our study by exogenous FABP7 administration can be suggested to contribute to its observed protective effect on BBB.

Neuroinflammation caused by LPS induces the development of anxiety in rodents (Lee et al., 2018). It is reported that LPS increases the production of IL-6 and TNF-α, and decreases IL-10 in cortical brain tissue which results in increases in the level of anxiety in mice (Beheshti et al., 2020). A recent study showed that selenium administration enhanced the performance of rats in the EPM platform by reducing neuroinflammation (Mansouri et al., 2021). On the other hand, it has been suggested that increased oxidative stress is directly associated with behavioral disturbances (Patki et al., 2013). The enhancement of iNOS activity and the resultant increased levels of nitric oxide induced by LPS has been shown to cause learning impairment and memory decline (Abdel-Zaher et al., 2017; Hosseini et al., 2010). In accordance with these literature data, in our study, LPS treatment triggered anxiety-like behavior in mice, while high-dose FABP7 administration caused a significant decrease in the time spent by these animals on the closed-arm, which was also associated with significant decreases in ROS levels.

The NF-κB and IL-1β are the key players in the inflammatory processes and therefore, are the hallmarks in the pathogenesis of sepsis. It is reported that LPS treatment activates the NF-κB via TLR-4 signaling pathway, which increases the expression level of IL-1β (Badshah et al., 2016). In our study, we investigated the effects of LPS exposure on the expression of NF-κB and IL-1β and evaluated whether FABP7 administration modulates these inflammatory mediators under septic conditions. In accordance with the above-mentioned literature data, we observed that LPS treatment significantly increased the expression level of NF-κB in bEnd.3 cells and septic mice while FABP7 administrations significantly decreased the increased NF-κB protein expression both *in vitro* and *in vivo*. In addition, the immunofluorescence intensity of IL-1β was markedly increased in LPS-treated bEnd.3 cells and FABP7 treatment drastically decreased the increased IL-1β immunoreactivity. In the meantime, the inhibition of the NF-κB signaling

pathway is considered to be favorable for astrocytes by decreasing glial damage in spinal cord injury (Lukacova et al., 2021; G. L. Yu et al., 2021). A recent study showed that the activated NF-κB pathway caused by IL-1β is downregulated by the fatty acid administration via decreasing the level of ROS in astrocytes (Zgórzyńska et al., 2021). It is also reported that 2-deoxyglucose, an inhibitor of glycolytic capacity in astrocytes, suppresses the NF-κB signaling pathway and decreases the level of cytokines (Puschel et al., 2020; Uehara et al., 2022). These literature data provide evidence on the roles of inflammatory mediators in the mechanisms of cellular damage in the neurovascular unit under septic conditions and suggest that the protective effect of exogenous FABP7 administration on BBB observed in our study correlated strongly with the alterations in NF-κB and IL-1β. In contrast to our results, a recent study showed that overexpression of FABP7 induces the generation of NF-κB related pro-inflammatory mediators in ALS mice (Killoy et al., 2020). Moreover, the increased level of IL-1β following LPS treatment was reported to be significantly decreased by M6 treatment via the downregulation of FABP5 and FABP7 in astrocytes (Cheng et al., 2021). Interestingly, previous studies have also suggested that the proliferation of glioblastoma cells is promoted by FABP7, and the survival rate in patients with glioblastoma is negatively correlated with FABP7 expression level (de Rosa et al., 2012; Liang et al., 2005; Mita et al., 2010).

In the *in vitro* part of our study, we assessed the alterations in the electrical resistance of bEnd.3 cell monolayers following different doses of LPS and/or FABP7 treatments. The integrity of the barriers constituted by endothelial/epithelial cells has been commonly evaluated by the measurements of TEER. A decrease in TEER values in *in vitro* BBB models is interpreted as disrupted barrier integrity and increased permeability. In a previous study, LPS was shown to decrease TEER values and increase barrier permeability in capillary endothelial cells (Boitsova et al., 2018). Furthermore, the BBB integrity has been shown to be impaired dose- and time-dependently by LPS as assessed by TEER measurements in *in vitro* experimental models (Hoyles et al., 2021; Pu et al., 2022; Skrzypczak-Wiercioch & Sałat, 2022; W. Zhang et al., 2017; Fujimoto et al., 2021). In line with these observations, in our study, we have found dose-dependent marked decreases in TEER values in bEnd.3 cell monolayers exposed to LPS treatment, while FABP7 administration led to increased electrical resistance of bEnd.3 cells which further implies the protective effect of exogenous FABP7 administration on the integrity of BBB.

Previous studies exploring the impact of septic conditions on brain microvessels have shown increased BBB permeability along with disruption of BBB integrity associated with substantially elevated inflammatory factors, including TNF-α, IL-1, and IL-6, in brain tissue and serum (Takata et al., 2021; J. Yang et al., 2022; Avtan et al., 2011). In addition, accumulated data have shown significantly increased BBB permeability by LPS treatment in *in vitro* endothelial cell culture and *in vivo* experimental models (Banks et al., 2015; Jangula & Murphy, 2013; Kikuchi et al., 2019; Takata et al., 2021). Our data on the effects of LPS-induced inflammatory conditions on BBB permeability are in line with the findings from the above-mentioned studies. In our study, we evaluated the *in vitro* effects of LPS on the permeability of BBB by measuring the permeability of barrier type endothelial cells using NaFl tracer. Upon exposure to LPS, we observed marked enhancement of the transport of NaFl across the bEnd.3 cell monolayers seeded on top of the transwell inserts resulting in significant increases in the fluorescence intensity of the tracer in the abluminal compartment of transwells. Moreover, to detect the extent of BBB leakage *in vivo* and *ex vivo* following LPS injections, the extravasation of albumin Alexa fluor 594 was measured using IVIS imaging and confocal microscopy. We observed significant increases of fluorescent signals in the brains of animals by IVIS imaging following treatment with LPS. Moreover, we assessed significant increases in the fluorescence intensity of albumin Alexa fluor 594 in the cerebral cortex, hippocampus, and mid-brain regions of LPS-injected animals by confocal microscopy. When we evaluated the impact of FABP7 administration on the LPS-induced BBB leakage, we found significant decreases in the increased fluorescence intensity of NaFl tracer permeated across the bEnd.3 cell monolayer *in vitro*. Moreover, we noted significant decreases in the increased fluorescent signals in the brains of LPS-treated animals by administration of high dose of FABP7 using IVIS imaging. Accordingly, we also observed significant decreases in the increased fluorescence intensity of albumin Alexa fluor 594 in all the brain regions of LPS-treated mice following high dose of FABP7 administration using confocal microscopy. However, when we administered FABP7 at the dose of 40 µg/kg to LPS-treated animals, we found no significant alterations in the increased fluorescent signals of the tracer in the brain regions except the midbrain. While these findings clearly underline the beneficial effects of FABP7 administration at the dose of 80 µg/kg on LPS-induced BBB disruption, the

effects of the lower dose of FABP7 in the same settings appear to be more complex and controversial.

It is well-known that the transport of substances across the paracellular pathway in barrier type endothelial cells is highly limited due to the presence of TJs comprised by proteins, including claudin-5 and ZO-1. It is reported that the overexpression of claudin-5 enhances the barrier integrity in brain microvessel endothelial cells, as assessed by TEER measurements (Jia et al., 2014). Previous studies showed that, in brain capillary endothelial cells, *in vitro* exposure to LPS decreased the expression levels of occludin and claudin-5, and resulted in reduced electrical resistance and increased permeability (Nitta et al., 2003; Peng et al., 2021). Accumulated data have indicated that LPS challenge caused decreased expression of claudin-5 and VE-cadherin associated with activation of NF-κB signaling pathway and resultant increased production of IL-1β in *in vitro* and *in vivo* conditions (Namyen et al., 2020; Park et al., 2021; Srivastava et al., 2020; H. Li et al., 2018). In line with these literature data, in our study, treatment with LPS caused marked reduction of electrical resistance along with significant decreases in claudin-5 expression *in vitro* in bEnd.3 cells and *in vivo* in the cerebral cortex and hippocampus of C57BL/6 mice, associated with increased expression levels of NF-κB and IL-1β, as assessed *in vitro* by immunofluorescence staining and *in vivo* by western blotting. When we investigated the effect of FABP7 administration on these alterations, we noted marked enhancement of the reduced TEER values along with significant increases in the decreased claudin-5 expression *in vitro* and *in vivo* by the high dose of FABP7. Importantly, we also observed that these beneficial effects of FABP7 were associated with decreases in the increased expression level of NF-κB and IL-1β, as assessed both in *in vitro* and *in vivo* settings which suggest that these inflammatory mediators play a central role in the alterations of TJ protein expression and hence BBB permeability. In the meantime, our data on the impact of FABP7 on the expression of TJ proteins under inflammatory conditions are further supported by a recent study in which exogenous FABP7 administration was reported to increase the decreased claudin-5 expression in a rat model of TBI (Rui et al., 2019a).

ZO-1 is an intracellular scaffolding protein that interacts with cytosolic actin and supports the integrity of BBB. In recent studies, it is reported that LPS challenge downregulates ZO-1 expression via activation of PI3K/Akt signaling pathway and causes a reduction in TEER values in bEnd.3 cells (Zou et al., 2022; R. Yang et al., 2023). In

addition, it has been shown that protein levels of claudin-5 and ZO-1 are negatively associated with the IL-1β mRNA level in bacteria-infected mice (Dong et al., 2019). Moreover, TNF-α-induced BBB disruption is related to reduced ZO-1 expression level via activation of the NF-κB signaling pathway in the primary culture of bovine endothelial cells (Aveleira et al., 2010). In accordance with these observations, in our study, we noted significant decreases in ZO-1 immunoreactivity in bEnd.3 cells associated with a reduction in TEER values and increases in NF-κB and IL-1β expressions following LPS treatment. However, although we have observed beneficial effects of FABP7 administration on BBB integrity and inflammatory mediators under septic conditions, we found no significant alteration in ZO-1 expression in bEnd.3 cells which suggests that the ZO-1 protein may not be a key player in our experimental settings.

It is widely recognized that caveolin-1 protein, a key component of caveolae, is involved in the transcellular trafficking of substances across the BBB (Y. L. Zhao et al., 2014). A previous study showed that exposure to LPS increases the expression of caveolin-1 protein and reduces the expression of claudin-5 leading to an enhancement of BBB permeability (W. Y. Liu et al., 2015). Moreover, LPS-induced activation of the NF-κB/TLR4 signaling pathway and the resultant increased expression of IL-1β which are strongly linked with the enhanced paracellular pathway as mentioned above, are also shown to be effective on the transcellular pathway by increasing the expression of caveolin-1 (Oakley et al., 2009). In this regard, our observations that both *in vitro* and *in vivo* exposure to LPS increased caveolin-1 expression along with NF-κB and IL-1β production conform well with the above-mentioned studies. Furthermore, when our data on the effect of FABP7 administration on LPS-induced BBB alterations are considered, the marked reduction in the increased BBB permeability to tracers along with the significant decreases in the increased caveolin-1 expression *in vitro* and *in vivo* provide further evidence on the beneficial effect of FABP7 in our experimental setting. In addition, our results also point out that inflammatory mediators including NF-κB and IL-1β play an important role in the alterations of not only the paracellular pathway but also of the transcellular pathway under septic conditions.

A growing body of evidence suggest that mfsd2a serves as a potent inhibitor of transcytosis across the BBB. An increase in mfsd2a expression has been shown to reduce the severity of neurologic damage in surgical brain injury, while the downregulation of mfsd2a has been linked to the increased production of caveolar vesicles leading to BBB

disruption in the same pathologic condition (Eser Ocak et al., 2020). Moreover, the mfsd2a knockout mice exhibited increased BBB permeability and neurological impairment in an experimental model of intracerebral hemorrhage (Y. R. Yang et al., 2017). In the meantime, LPS-induced inflammatory condition has been shown to cause increased permeability of BBB by decreasing the expression of mfsd2a (He et al., 2018; Tiwary et al., 2018; C. Zhao et al., 2020). Furthermore, the reduction in the mfsd2a expression in LPS-induced BBB disruption has been suggested to occur via activation of the caveolin-1/Nrf-2/HO-1 signaling pathway (Qu et al., 2020; B. Huang & Li, 2021). In our study, we have observed significant decreases in the expression level of mfsd2a following *in vitro* and *in vivo* exposure to LPS in bEnd.3 cells and C57BL/6 mice associated with increase in the caveolin-1 expression and enhancement of BBB leakage, which are in accordance with the above-mentioned previous research. Moreover, our data regarding the increase of the decreased mfsd2a expression by *in vitro* and *in vivo* FABP7 administration provide further evidence on the beneficial effects of FABP7 on caveolin-1 expression and BBB permeability that we have observed in our study in LPS-induced BBB disruption. Meanwhile, it is also reported that mfsd2a acts as a lipid transporter of DHA across the BBB into the brain, thereby providing structural support and protective effects to the neurons and modulating cognitive function (Wood et al., 2021). In a previous study, the suppression of mfsd2a protein significantly decreased the level of DHA in the brain, which resulted in severe anxiety and cognitive deficits (Nguyen et al., 2014b). In this regard, our data on the significant alleviation of anxiety-like behavior by FABP7 administration to LPS-treated mice associated with increase of mfsd2a expression suggest that the beneficial effects of FABP7 may have occurred via an increase of DHA level in the brain, although we have not targeted this omega-3 fatty acid in our study.

CHAPTER 7:

CONCLUSION

Our study shows for the first time that exogenous FABP7 administration restores the LPS-induced BBB disruption by enhancing the transendothelial resistance, increasing the expressions of claudin-5 and mfsd2a and decreasing caveolin-1 expression, thereby decreasing the increased paracellular and transcellular BBB permeability and alleviates anxiety-like behavior. In addition, we found that high-dose FABP7 administration decreased the elevated body temperature and reduced the increased CRP, PCT, and ROS levels in LPS-induced septic mice. Furthermore, we demonstrated that the expressions of IL-1β and NF-κB decreased in a significant manner by FABP7 in our experimental setup.

In conclusion, our study demonstrates that exogenously administered FABP7 improves BBB integrity through its effects on antioxidant and anti-inflammatory signaling pathways *in vitro* in bEnd.3 cells and *in vivo* in mice exposed to LPS.

BIBLIOGRAPHY

Abbott, N. J., Rönnbäck, L., & Hansson, E. (2006). Astrocyte-endothelial interactions at the blood-brain barrier. In *Nature Reviews Neuroscience* (Vol. 7, Issue 1). https://doi.org/10.1038/nrn1824

Abdel-Zaher, A. O., Farghaly, H. S. M., Farrag, M. M. Y., Abdel-Rahman, M. S., & Abdel-Wahab, B. A. (2017). A potential mechanism for the ameliorative effect of thymoquinone on pentylenetetrazole-induced kindling and cognitive impairments in mice. *Biomedicine and Pharmacotherapy*, *88*. https://doi.org/10.1016/j.biopha.2017.01.009

Abuznait, A. H., & Kaddoumi, A. (2012). Role of ABC transporters in the pathogenesis of Alzheimers disease. In *ACS Chemical Neuroscience* (Vol. 3, Issue 11, pp. 820–831). https://doi.org/10.1021/cn300077c

Ando, Y., Okada, H., Takemura, G., Suzuki, K., Takada, C., Tomita, H., Zaikokuji, R., Hotta, Y., Miyazaki, N., Yano, H., Muraki, I., Kuroda, A., Fukuda, H., Kawasaki, Y., Okamoto, H., Kawaguchi, T., Watanabe, T., Doi, T., Yoshida, T., … Ogura, S. (2018). Brain-Specific Ultrastructure of Capillary Endothelial Glycocalyx and Its Possible Contribution for Blood Brain Barrier. *Scientific Reports*, *8*(1). https://doi.org/10.1038/s41598-018-35976-2

Ando-Akatsuka, Y., Saitou, M., Hirase, T., Kishi, M., Sakakibara, A., Itoh, M., Yonemura, S., Furuse, M., & Tsukita, S. (1996). Interspecies diversity of the occludin sequence: CDNA cloning of human, mouse, dog, and rat-kangaroo homologues. *Journal of Cell Biology*, *133*(1). https://doi.org/10.1083/jcb.133.1.43

Andreone, B. J., Chow, B. W., Tata, A., Lacoste, B., Ben-Zvi, A., Bullock, K., Deik, A. A., Ginty, D. D., Clish, C. B., & Gu, C. (2017a). Blood-Brain Barrier Permeability Is Regulated by Lipid Transport-Dependent

Suppression of Caveolae-Mediated Transcytosis. *Neuron*, *94*(3). https://doi.org/10.1016/j.neuron.2017.03.043

Andreone, B. J., Chow, B. W., Tata, A., Lacoste, B., Ben-Zvi, A., Bullock, K., Deik, A. A., Ginty, D. D., Clish, C. B., & Gu, C. (2017b). Blood-Brain Barrier Permeability Is Regulated by Lipid Transport-Dependent Suppression of Caveolae-Mediated Transcytosis. *Neuron*, *94*(3), 581-594.e5. https://doi.org/10.1016/j.neuron.2017.03.043

Aragón-González, A., Shaw, P. J., & Ferraiuolo, L. (2022). Blood–Brain Barrier Disruption and Its Involvement in Neurodevelopmental and Neurodegenerative Disorders. In *International Journal of Molecular Sciences* (Vol. 23, Issue 23). MDPI. https://doi.org/10.3390/ijms232315271

Arima, M., Nakao, S., Yamaguchi, M., Feng, H., Fujii, Y., Shibata, K., Wada, I., Kaizu, Y., Ahmadieh, H., Ishibashi, T., Stitt, A. W., & Sonoda, K. H. (2020). Claudin-5 redistribution induced by inflammation leads to anti-VEGF–resistant diabetic macular edema. *Diabetes*, *69*(5). https://doi.org/10.2337/db19-1121

Artym, J., & Zimecki, M. (2023). Colostrum and Lactoferrin Protect against Side Effects of Therapy with Antibiotics, Anti-inflammatory Drugs and Steroids, and Psychophysical Stress: A Comprehensive Review. In *Biomedicines* (Vol. 11, Issue 4). MDPI. https://doi.org/10.3390/biomedicines11041015

Aurrand-Lions, M., Johnson-Leger, C., Wong, C., Du Pasquier, L., & Imhof, B. A. (2001). Heterogeneity of endothelial junctions is reflected by differential expression and specific subcellular localization of the three JAM family members. *Blood*, *98*(13). https://doi.org/10.1182/blood.V98.13.3699

Aveleira, C. A., Lin, C. M., Abcouwer, S. F., Ambrósio, A. F., & Antonetti, D. A. (2010). TNF-α signals through PKCζ/NF-κB to alter the tight junction complex and increase retinal endothelial cell permeability. *Diabetes*, *59*(11), 2872–2882. https://doi.org/10.2337/db09-1606

Avtan, S. M., Kaya, M., Orhan, N., Arslan, A., Arican, N., Toklu, A. S., Gürses, C., Elmas, I., Kucuk, M., & Ahishali, B. (2011). The effects of

hyperbaric oxygen therapy on blood-brain barrier permeability in septic rats. *Brain Research*, *1412*. https://doi.org/10.1016/j.brainres.2011.07.020

Badshah, H., Ali, T., & Kim, M. O. (2016). Osmotin attenuates LPS-induced neuroinflammation and memory impairments via the TLR4/NFκB signaling pathway. *Scientific Reports*, *6*. https://doi.org/10.1038/srep24493

Baek, S. H., Park, T., Kang, M. G., & Park, D. (2020). Anti-inflammatory activity and ROS regulation effect of sinapaldehyde in LPS-stimulated RAW 264.7 macrophages. *Molecules*, *25*(18). https://doi.org/10.3390/molecules25184089

Balcom, E., Liu, R.-Z., Poon, S., & Godbout, R. (2017). FABP5 (fatty acid binding protein 5 (psoriasis-associated)). *Atlas of Genetics and Cytogenetics in Oncology and Haematology*, *7*. https://doi.org/10.4267/2042/62185

Balda, M. S., González-Mariscal, L., Contreras, R. G., Macias-Silva, M., Torres-Marquez, M. E., Sáinz, J. A. G., & Cereijido, M. (1991). Assembly and sealing of tight junctions: Possible participation of G-proteins, phospholipase C, protein kinase C and calmodulin. *The Journal of Membrane Biology*, *122*(3). https://doi.org/10.1007/BF01871420

Ballabh, P., Braun, A., & Nedergaard, M. (2004). The blood-brain barrier: An overview: Structure, regulation, and clinical implications. In *Neurobiology of Disease* (Vol. 16, Issue 1). https://doi.org/10.1016/j.nbd.2003.12.016

Banks, W. A., Gray, A. M., Erickson, M. A., Salameh, T. S., Damodarasamy, M., Sheibani, N., Meabon, J. S., Wing, E. E., Morofuji, Y., Cook, D. G., & Reed, M. J. (2015). Lipopolysaccharide-induced blood-brain barrier disruption: Roles of cyclooxygenase, oxidative stress, neuroinflammation, and elements of the neurovascular unit. *Journal of Neuroinflammation*, *12*(1). https://doi.org/10.1186/s12974-015-0434-1

Banks, W. A., & Robinson, S. M. (2010). Minimal penetration of lipopolysaccharide across the murine blood-brain barrier. *Brain, Behavior, and Immunity*, *24*(1). https://doi.org/10.1016/j.bbi.2009.09.001

Bargi, R., Hosseini, M., Asgharzadeh, F., Khazaei, M., Shafei, M. N., & Beheshti, F. (2021). Protection against blood-brain barrier permeability as a possible mechanism for protective effects of thymoquinone against sickness behaviors induced by lipopolysaccharide in rats. *Jundishapur Journal of Natural Pharmaceutical Products*, *16*(2). https://doi.org/10.5812/JJNPP.67765

Barichello, T., Generoso, J. S., Collodel, A., Petronilho, F., & Dal-Pizzol, F. (2021). The blood-brain barrier dysfunction in sepsis. In *Tissue Barriers* (Vol. 9, Issue 1). Bellwether Publishing, Ltd. https://doi.org/10.1080/21688370.2020.1840912

Barrett, K. E. (2020). Claudin-2 pore causes leak that breaches the dam in intestinal inflammation. In *Journal of Clinical Investigation* (Vol. 130, Issue 10). https://doi.org/10.1172/JCI140528

Batista, C. R. A., Gomes, G. F., Candelario-Jalil, E., Fiebich, B. L., & de Oliveira, A. C. P. (2019). Lipopolysaccharide-induced neuroinflammation as a bridge to understand neurodegeneration. In *International Journal of Molecular Sciences* (Vol. 20, Issue 9). https://doi.org/10.3390/ijms20092293

Bauer, H., Zweimueller-Mayer, J., Steinbacher, P., Lametschwandtner, A., & Bauer, H. C. (2010). The dual role of zonula occludens (ZO) proteins. In *Journal of Biomedicine and Biotechnology* (Vol. 2010). https://doi.org/10.1155/2010/402593

Begley, D. J. (2004). Efflux Mechanisms in the Central Nervous System: A Powerful Influence on Drug Distribution within the Brain. In *Blood-Spinal Cord and Brain Barriers in Health and Disease*. https://doi.org/10.1016/B978-012639011-7/50013-9

Beheshti, F., Hashemzehi, M., Hosseini, M., Marefati, N., & Memarpour, S. (2020). Inducible nitric oxide synthase plays a role in depression- and anxiety-like behaviors chronically induced by lipopolysaccharide in rats: Evidence from inflammation and oxidative stress. *Behavioural Brain Research*, *392*. https://doi.org/10.1016/j.bbr.2020.112720

Bentivoglio, M., Kristensson, K., & Rottenberg, M. E. (2018). Circumventricular organs and parasite neurotropism: Neglected gates to the brain? In *Frontiers in Immunology* (Vol. 9). https://doi.org/10.3389/fimmu.2018.02877

Ben-Zvi, A., Lacoste, B., Kur, E., Andreone, B. J., Mayshar, Y., Yan, H., & Gu, C. (2014). Mfsd2a is critical for the formation and function of the blood-brain barrier. *Nature*, *509*(7501). https://doi.org/10.1038/nature13324

Bilici, D., Nur Banoğlu, Z., Kiziltunç, A., Avci, B., Çiftçioğlu, A., & Bilici, S. (2002). Antioxidant effect of T-type calcium channel blockers in gastric injury. *Digestive Diseases and Sciences*, *47*(4). https://doi.org/10.1023/A:1014712621794

Boitsova, E. B., Morgun, A. V., Osipova, E. D., Pozhilenkova, E. A., Martinova, G. P., Frolova, O. V., Olovannikova, R. Y., Tohidpour, A., Gorina, Y. V., Panina, Y. A., & Salmina, A. B. (2018). The inhibitory effect of LPS on the expression of GPR81 lactate receptor in blood-brain barrier model in vitro. *Journal of Neuroinflammation*, *15*(1). https://doi.org/10.1186/s12974-018-1233-2

Bothwell, S. W., Janigro, D., & Patabendige, A. (2019). Cerebrospinal fluid dynamics and intracranial pressure elevation in neurological diseases. In *Fluids and Barriers of the CNS* (Vol. 16, Issue 1). https://doi.org/10.1186/s12987-019-0129-6

Boullerne, A. I., & Feinstein, D. L. (2020). History of Neuroscience I. Pío del Río-Hortega (1882–1945): The Discoverer of Microglia and Oligodendroglia. In *ASN Neuro* (Vol. 12). https://doi.org/10.1177/1759091420953259

Bovijn, C., Desmet, A. S., Uyttendaele, I., Van Acker, T., Tavernier, J., & Peelman, F. (2013). Identification of binding sites for myeloid differentiation primary response gene 88 (MyD88) and Toll-like receptor 4 in MyD88 adapter-like (Mal). *Journal of Biological Chemistry*, *288*(17). https://doi.org/10.1074/jbc.M112.415810

Breuza, L., Corby, S., Arsanto, J. P., Delgrossi, M. H., Scheiffele, P., & Le Bivic, A. (2002). The scaffolding domain of caveolin 2 is responsible for its Golgi localization in Caco-2 cells. In *Journal of Cell Science* (Vol. 115, Issue 23). https://doi.org/10.1242/jcs.00130

Brindle, N. P. J., Saharinen, P., & Alitalo, K. (2006). Signaling and functions of angiopoietin-1 in vascular protection. In *Circulation Research* (Vol. 98, Issue 8). https://doi.org/10.1161/01.RES.0000218275.54089.12

Cabezas, R., Ávila, M., Gonzalez, J., El-Bachá, R. S., Báez, E., García-Segura, L. M., Coronel, J. C. J., Capani, F., Cardona-Gomez, G. P., & Barreto, G. E. (2014). Astrocytic modulation of blood brain barrier: Perspectives on Parkinson's disease. In *Frontiers in Cellular Neuroscience* (Vol. 8, Issue AUG). https://doi.org/10.3389/fncel.2014.00211

Cabral-Pacheco, G. A., Garza-Veloz, I., Castruita-De la Rosa, C., Ramirez-Acuña, J. M., Perez-Romero, B. A., Guerrero-Rodriguez, J. F., Martinez-Avila, N., & Martinez-Fierro, M. L. (2020). The Roles of Matrix Metalloproteinases and Their Inhibitors in Human Diseases. *International Journal of Molecular Sciences*, *21*(24), 9739. https://doi.org/10.3390/ijms21249739

Camire, R. B., Beaulac, H. J., & Willis, C. L. (2015). Transitory loss of glia and the subsequent modulation in inflammatory cytokines/chemokines regulate paracellular claudin-5 expression in endothelial cells. *Journal of Neuroimmunology*, *284*. https://doi.org/10.1016/j.jneuroim.2015.05.008

Carbonetti, G., Wilpshaar, T., Kroonen, J., Studholme, K., Converso, C., d'Oelsnitz, S., & Kaczocha, M. (2019). FABP5 coordinates lipid signaling that promotes prostate cancer metastasis. *Scientific Reports*, *9*(1). https://doi.org/10.1038/s41598-019-55418-x

Chen, L., Deng, H., Cui, H., Fang, J., Zuo, Z., Deng, J., Li, Y., Wang, X., & Zhao, L. (2018). Inflammatory responses and inflammation-associated diseases in organs. In *Oncotarget* (Vol. 9, Issue 6). https://doi.org/10.18632/oncotarget.23208

Cheng, A., Jia, W., Kawahata, I., & Fukunaga, K. (2021). A novel fatty acid-binding protein 5 and 7 inhibitor ameliorates oligodendrocyte injury in multiple sclerosis mouse models. *EBioMedicine*, *72*. https://doi.org/10.1016/j.ebiom.2021.103582

Choi, W. S., Xu, X., Goruk, S., Wang, Y., Patel, S., Chow, M., Field, C. J., & Godbout, R. (2021). Fabp7 facilitates uptake of docosahexaenoic acid in glioblastoma neural stem-like cells. *Nutrients*, *13*(8). https://doi.org/10.3390/nu13082664

Clarke, D. C., Miskovic, D., Han, X. X., Calles-Escandon, J., Glatz, J. F. C., Luiken, J. J. F. P., Heikkila, J. J., & Bonen, A. (2004). Overexpression of membrane-associated fatty acid binding protein (FABPpm) in vivo increases fatty acid sarcolemmal transport and metabolism. *Physiological Genomics*, *17*. https://doi.org/10.1152/physiolgenomics.00190.2003

Cockerill, I., Oliver, J. A., Xu, H., Fu, B. M., & Zhu, D. (2018). Blood-brain barrier integrity and clearance of amyloid-β from the BBB. In *Advances in Experimental Medicine and Biology* (Vol. 1097). https://doi.org/10.1007/978-3-319-96445-4_14

Cocucci, E., Kim, J. Y., Bai, Y., & Pabla, N. (2017). Role of Passive Diffusion, Transporters, and Membrane Trafficking-Mediated Processes in Cellular Drug Transport. In *Clinical Pharmacology and Therapeutics* (Vol. 101, Issue 1). https://doi.org/10.1002/cpt.545

Cohen, A. W., Hnasko, R., Schubert, W., & Lisanti, M. P. (2004). Role of caveolae and caveolins in health and disease. In *Physiological Reviews* (Vol. 84, Issue 4). https://doi.org/10.1152/physrev.00046.2003

Conrad, A., Bull, D. F., King, M. G., & Husband, A. J. (1997). The effects of lipopolysaccharide (LPS) on the fever response in rats at different ambient temperatures. *Physiology and Behavior*, *62*(6). https://doi.org/10.1016/S0031-9384(97)00166-2

Correale, J., & Villa, A. (2004). The neuroprotective role of inflammation in nervous system Injuries. In *Journal of Neurology* (Vol. 251, Issue 11). https://doi.org/10.1007/s00415-004-0649-z

Costea, L., Mészáros, Bauer, H., Bauer, H. C., Traweger, A., Wilhelm, I., Farkas, A. E., & Krizbai, I. A. (2019). The blood–brain barrier and its intercellular junctions in age-related brain disorders. In *International Journal of Molecular Sciences* (Vol. 20, Issue 21). https://doi.org/10.3390/ijms20215472

Cubelos, B., González-González, I. M., Giménez, C., & Zafra, F. (2005). Amino acid transporter SNAT5 localizes to glial cells in the rat brain. *GLIA*, *49*(2). https://doi.org/10.1002/glia.20106

Cummins, P. M. (2012). Occludin: One Protein, Many Forms. *Molecular and Cellular Biology*, *32*(2). https://doi.org/10.1128/mcb.06029-11

Dal-Pizzol, F., Rojas, H. A., Dos Santos, E. M., Vuolo, F., Constantino, L., Feier, G., Pasquali, M., Comim, C. M., Petronilho, F., Gelain, D. P., Quevedo, J., Moreira, J. C. F., & Ritter, C. (2013). Matrix metalloproteinase-2 and metalloproteinase-9 activities are associated with blood-brain barrier dysfunction in an animal model of severe sepsis. In *Molecular Neurobiology* (Vol. 48, Issue 1). https://doi.org/10.1007/s12035-013-8433-7

Danielski, L. G., Giustina, A. Della, Badawy, M., Barichello, T., Quevedo, J., Dal-Pizzol, F., & Petronilho, F. (2018). Brain Barrier Breakdown as a Cause and Consequence of Neuroinflammation in Sepsis. In *Molecular Neurobiology* (Vol. 55, Issue 2). https://doi.org/10.1007/s12035-016-0356-7

Davson, H. (1989). History of the Blood-Brain Barrier Concept. In *Implications of the Blood-Brain Barrier and Its Manipulation*. https://doi.org/10.1007/978-1-4613-0701-3_2

de Rosa, A., Pellegatta, S., Rossi, M., Tunici, P., Magnoni, L., Speranza, M. C., Malusa, F., Miragliotta, V., Mori, E., Finocchiaro, G., & Bakker, A. (2012). A Radial Glia Gene Marker, Fatty Acid Binding Protein 7 (FABP7), Is Involved in Proliferation and Invasion of Glioblastoma Cells. *PLoS ONE*, *7*(12). https://doi.org/10.1371/journal.pone.0052113

De Rose, D. U., Gallini, F., Battaglia, D. I., Tiberi, E., Gaudino, S., Contaldo, I., Veredice, C., Romeo, D. M., Massimi, L., Asaro, A., Cereda, C., Vento, G., & Mercuri, E. M. (2021). A novel homozygous variant in JAM3

gene causing hemorrhagic destruction of the brain, subependymal calcification, and congenital cataracts (HDBSCC) with neonatal onset. *Neurological Sciences*, *42*(11). https://doi.org/10.1007/s10072-021-05480-z

Descamps, L., Coisne, C., Dehouck, B., Cecchelli, R., & Torpier, G. (2003). Protective effect of glial cells against lipopolysaccharide-mediated blood-brain barrier injury. *Glia*, *42*(1), 46-58.

Destefano, J. G., Jamieson, J. J., Linville, R. M., & Searson, P. C. (2018). Benchmarking in vitro tissue-engineered blood-brain barrier models. *Fluids and Barriers of the CNS*, *15*(1). https://doi.org/10.1186/s12987-018-0117-2

DHA and AA: Neuroprotective Nutrient. (n.d.).

Dieriks, B. V., Dean, J. M., Aronica, E., Waldvogel, H. J., Faull, R. L. M., & Curtis, M. A. (2018). Differential fatty acid-binding protein expression in persistent radial glia in the human and sheep subventricular zone. *Developmental Neuroscience*, *40*(2). https://doi.org/10.1159/000487633

Ding, B., Lin, C., Liu, Q., He, Y., Ruganzu, J. B., Jin, H., Peng, X., Ji, S., Ma, Y., & Yang, W. (2020). Tanshinone IIA attenuates neuroinflammation via inhibiting RAGE/NF-κB signaling pathway in vivo and in vitro. *Journal of Neuroinflammation*, *17*(1). https://doi.org/10.1186/s12974-020-01981-4

DiSabato, D. J., Quan, N., & Godbout, J. P. (2016). Neuroinflammation: the devil is in the details. *Journal of Neurochemistry*, *139*. https://doi.org/10.1111/jnc.13607

Doege, H., & Stah, A. (2006). Protein-mediated fatty acid uptake: Novel insights from in vivo models. In *Physiology* (Vol. 21, Issue 4). https://doi.org/10.1152/physiol.00014.2006

Donahue, J. E., Flaherty, S. L., Johanson, C. E., Duncan, J. A., Silverberg, G. D., Miller, M. C., Tavares, R., Yang, W., Wu, Q., Sabo, E., Hovanesian, V., & Stopa, E. G. (2006). RAGE, LRP-1, and amyloid-beta protein in Alzheimer's disease. *Acta Neuropathologica*, *112*(4). https://doi.org/10.1007/s00401-006-0115-3

Dong, N., Xu, X., Xue, C., Wang, C., Li, X., Shan, A., Xu, L., & Li, D. (2019). Ethyl pyruvate protects against Salmonella intestinal infection in mice through down-regulation of pro-inflammatory factors and inhibition of TLR4/MAPK pathway. *International Immunopharmacology*, *71*. https://doi.org/10.1016/j.intimp.2019.03.019

Dore-Duffy, P. (2008). Pericytes: Pluripotent Cells of the Blood Brain Barrier. *Current Pharmaceutical Design*, *14*(16). https://doi.org/10.2174/138161208784705469

Du, H., & Wang, S. (2020). Omarigliptin Mitigates Lipopolysaccharide-Induced Neuroinflammation and Dysfunction of the Integrity of the Blood-Brain Barrier. *ACS Chemical Neuroscience*, *11*(24), 4262–4269. https://doi.org/10.1021/acschemneuro.0c00537

Dulewicz, M., Kulczyńska-Przybik, A., Słowik, A., Borawska, R., & Mroczko, B. (2021). Fatty acid binding protein 3 (Fabp3) and apolipoprotein e4 (apoe4) as lipid metabolism-related biomarkers of alzheimer's disease. *Journal of Clinical Medicine*, *10*(14). https://doi.org/10.3390/jcm10143009

Edwards, D. N., & Bix, G. J. (2019). Roles of blood-brain barrier integrins and extracellular matrix in stroke. *American Journal of Physiology - Cell Physiology*, *316*(2). https://doi.org/10.1152/ajpcell.00151.2018

Ericsson, A., Liu, C., Hart, R. P., & Sawchenko, P. E. (1995). Type 1 interleukin-1 receptor in the rat brain: Distribution, regulation, and relationship to sites of IL-1–induced cellular activation. *Journal of Comparative Neurology*, *361*(4). https://doi.org/10.1002/cne.903610410

Erikson, K., Tuominen, H., Vakkala, M., Liisanantti, J. H., Karttunen, T., Syrjälä, H., & Ala-Kokko, T. I. (2020). Brain tight junction protein expression in sepsis in an autopsy series. *Critical Care*, *24*(1). https://doi.org/10.1186/s13054-020-03101-3

Eser Ocak, P., Ocak, U., Sherchan, P., Gamdzyk, M., Tang, J., & Zhang, J. H. (2020). Overexpression of Mfsd2a attenuates blood brain barrier dysfunction via Cav-1/Keap-1/Nrf-2/HO-1 pathway in a rat model of surgical

brain injury. *Experimental Neurology*, *326*. https://doi.org/10.1016/j.expneurol.2020.113203

Evans, T. (2018). Diagnosis and management of sepsis. In *Clinical Medicine, Journal of the Royal College of Physicians of London* (Vol. 18, Issue 2). https://doi.org/10.7861/clinmedicine.18-2-146

Falomir-Lockhart, L. J., Cavazzutti, G. F., Giménez, E., & Toscani, A. M. (2019). Fatty acid signaling mechanisms in neural cells: Fatty acid receptors. In *Frontiers in Cellular Neuroscience* (Vol. 13). https://doi.org/10.3389/fncel.2019.00162

Farooqui, A. A., Horrocks, L. A., & Farooqui, T. (2007). Modulation of inflammation in brain: A matter of fat. In *Journal of Neurochemistry* (Vol. 101, Issue 3). https://doi.org/10.1111/j.1471-4159.2006.04371.x

Feingold, K. R. (2021). Introduction to Lipids and Lipoproteins. In *Endotext*.

Fiedler, U., Krissl, T., Koidl, S., Weiss, C., Koblizek, T., Deutsch, U., Martiny-Baron, G., Marmé, D., & Augustin, H. G. (2003). Angiopoietin-1 and angiopoietin-2 share the same binding domains in the Tie-2 receptor involving the first Ig-like loop and the epidermal growth factor-like repeats. *Journal of Biological Chemistry*, *278*(3). https://doi.org/10.1074/jbc.M208550200

Fontana, I. C., Souza, D. G., Souza, D. O., Gee, A., Zimmer, E. R., & Bongarzone, S. (2022). A Medicinal Chemistry Perspective on Excitatory Amino Acid Transporter 2 Dysfunction in Neurodegenerative Diseases. In *Journal of Medicinal Chemistry*. American Chemical Society. https://doi.org/10.1021/acs.jmedchem.2c01572

Förster, C. (2008). Tight junctions and the modulation of barrier function in disease. In *Histochemistry and Cell Biology* (Vol. 130, Issue 1). https://doi.org/10.1007/s00418-008-0424-9

Fujimoto, T., Morofuji, Y., Kovac, A., Erickson, M. A., Deli, M. A., Niwa, M., & Banks, W. A. (2021). Pitavastatin ameliorates lipopolysaccharide-induced blood-brain barrier dysfunction. *Biomedicines*, *9*(7). https://doi.org/10.3390/biomedicines9070837

Furuse, M. (2010). Molecular basis of the core structure of tight junctions. In *Cold Spring Harbor perspectives in biology* (Vol. 2, Issue 1). https://doi.org/10.1101/cshperspect.a002907

Furuse, M., Hirase, T., Itoh, M., Nagafuchi, A., Yonemura, S., Tsukita, S., & Tsukita, S. (1993). Occludin: A novel integral membrane protein localizing at tight junctions. *Journal of Cell Biology*, *123*(6 II). https://doi.org/10.1083/jcb.123.6.1777

Furuse, M., Sasaki, H., & Tsukita, S. (1999). Manner of interaction of heterogeneous claudin species within and between tight junction strands. *Journal of Cell Biology*, *147*(4). https://doi.org/10.1083/jcb.147.4.891

Galea, I. (2021). The blood–brain barrier in systemic infection and inflammation. In *Cellular and Molecular Immunology* (Vol. 18, Issue 11). https://doi.org/10.1038/s41423-021-00757-x

Galea, I., Bechmann, I., & Perry, V. H. (2007). What is immune privilege (not)? *Trends in Immunology*, *28*(1). https://doi.org/10.1016/j.it.2006.11.004

Gao, C., Wang, H., Wang, T., Luo, C., Wang, Z., Zhang, M., Chen, X., & Tao, L. (2020). Platelet regulates neuroinflammation and restores blood–brain barrier integrity in a mouse model of traumatic brain injury. *Journal of Neurochemistry*, *154*(2), 190–204. https://doi.org/10.1111/jnc.14983

Gao, Q., & Hernandes, M. S. (2021). Sepsis-Associated Encephalopathy and Blood-Brain Barrier Dysfunction. In *Inflammation* (Vol. 44, Issue 6). https://doi.org/10.1007/s10753-021-01501-3

Garcia Corrales, A. V., Haidar, M., Bogie, J. F. J., & Hendriks, J. J. A. (2021). Fatty acid synthesis in glial cells of the cns. In *International Journal of Molecular Sciences* (Vol. 22, Issue 15). https://doi.org/10.3390/ijms22158159

Gautier-Stein, A., Chilloux, J., Soty, M., Thorens, B., Place, C., Zitoun, C., Duchampt, A., Da Costa, L., Rajas, F., Lamaze, C., & Mithieux, G. (2023). A caveolin-1 dependent glucose-6-phosphatase trafficking contributes to hepatic glucose production. *Molecular Metabolism*, *70*, 101700. https://doi.org/10.1016/j.molmet.2023.101700

Gee, J. R., & Keller, J. N. (2005). Astrocytes: Regulation of brain homeostasis via apolipoprotein E. In *International Journal of Biochemistry and Cell Biology* (Vol. 37, Issue 6). https://doi.org/10.1016/j.biocel.2004.10.004

Georgieva, J. V., Hoekstra, D., & Zuhorn, I. S. (2014a). Smuggling drugs into the brain: An overview of ligands targeting transcytosis for drug delivery across the blood–brain barrier. In *Pharmaceutics* (Vol. 6, Issue 4). https://doi.org/10.3390/pharmaceutics6040557

Georgieva, J. V., Hoekstra, D., & Zuhorn, I. S. (2014b). Smuggling drugs into the brain: An overview of ligands targeting transcytosis for drug delivery across the blood–brain barrier. In *Pharmaceutics* (Vol. 6, Issue 4, pp. 557–583). MDPI AG. https://doi.org/10.3390/pharmaceutics6040557

Glass, C. K., Saijo, K., Winner, B., Marchetto, M. C., & Gage, F. H. (2010). Mechanisms Underlying Inflammation in Neurodegeneration. In *Cell* (Vol. 140, Issue 6). https://doi.org/10.1016/j.cell.2010.02.016

Gofton, T. E., & Bryan Young, G. (2012). Sepsis-associated encephalopathy. In *Nature Reviews Neurology* (Vol. 8, Issue 10, pp. 557–566). https://doi.org/10.1038/nrneurol.2012.183

Gomes-Leal, W. (2012). Microglial physiopathology: How to explain the dual role of microglia after acute neural disorders? *Brain and Behavior*, *2*(3). https://doi.org/10.1002/brb3.51

Gonçalves, C. L., dos Santos, D. B., Portilho, S. S., Lopes, M. W., Ghizoni, H., de Souza, V., Mack, J. M., Naime, A. A., Dafre, A. L., de Souza Brocardo, P., Prediger, R. D., & Farina, M. (2018). Lipopolysaccharide-Induced Striatal Nitrosative Stress and Impaired Social Recognition Memory Are Not Magnified by Paraquat Coexposure. *Neurochemical Research*, *43*(3), 745–759. https://doi.org/10.1007/s11064-018-2477-z

Grant, R., & Guest, J. (2016). Role of Omega-3 PUFAs in neurobiological health. In *Advances in Neurobiology* (Vol. 12). https://doi.org/10.1007/978-3-319-28383-8_13

Greene, C., & Campbell, M. (2016). Tight junction modulation of the blood brain barrier: CNS delivery of small molecules. In *Tissue Barriers* (Vol. 4, Issue 1). https://doi.org/10.1080/21688370.2015.1138017

Gumbiner, B. M. (2005). Regulation of cadherin-mediated adhesion in morphogenesis. In *Nature Reviews Molecular Cell Biology* (Vol. 6, Issue 8). https://doi.org/10.1038/nrm1699

Guo, S., Wang, H., & Yin, Y. (2022). Microglia Polarization From M1 to M2 in Neurodegenerative Diseases. In *Frontiers in Aging Neuroscience* (Vol. 14). https://doi.org/10.3389/fnagi.2022.815347

Gutierrez, E. G., Banks, W. A., & Kastin, A. J. (1993). Murine tumor necrosis factor alpha is transported from blood to brain in the mouse. *Journal of Neuroimmunology*, *47*(2). https://doi.org/10.1016/0165-5728(93)90027-V

Gyimesi, G., Pujol-Giménez, J., Kanai, Y., & Hediger, M. A. (2020). Sodium-coupled glucose transport, the SLC5 family, and therapeutically relevant inhibitors: from molecular discovery to clinical application. In *Pflugers Archiv European Journal of Physiology* (Vol. 472, Issue 9). https://doi.org/10.1007/s00424-020-02433-x

Halbleib, J. M., & Nelson, W. J. (2006). Cadherins in development: Cell adhesion, sorting, and tissue morphogenesis. In *Genes and Development* (Vol. 20, Issue 23). https://doi.org/10.1101/gad.1486806

Handa, O., Stephen, J., & Cepinskas, G. (2008). Role of endothelial nitric oxide synthase-derived nitric oxide in activation and dysfunction of cerebrovascular endothelial cells during early onsets of sepsis. *American Journal of Physiology - Heart and Circulatory Physiology*, *295*(4). https://doi.org/10.1152/ajpheart.00476.2008

Hariharan, A., Robertson, C. D., Garcia, D. C. G., & Longden, T. A. (2022). Brain capillary pericytes are metabolic sentinels that control blood flow through a KATP channel-dependent energy switch. *Cell Reports*, *41*(13). https://doi.org/10.1016/j.celrep.2022.111872

Harris, T. J. C., & Tepass, U. (2010). Adherens junctions: From molecules to morphogenesis. In *Nature Reviews Molecular Cell Biology* (Vol. 11, Issue 7). https://doi.org/10.1038/nrm2927

Hashimoto, Y., Campbell, M., Tachibana, K., Okada, Y., & Kondoh, M. (2021). Claudin-5: A Pharmacological Target to Modify the Permeability of the Blood–Brain Barrier. In *Biological and Pharmaceutical Bulletin* (Vol. 44, Issue 10). https://doi.org/10.1248/bpb.b21-00408

Hashimoto, Y., Michiba, K., Maeda, K., & Kusuhara, H. (2022). Quantitative prediction of pharmacokinetic properties of drugs in humans: Recent advance in in vitro models to predict the impact of efflux transporters in the small intestine and blood–brain barrier. In *Journal of Pharmacological Sciences* (Vol. 148, Issue 1). https://doi.org/10.1016/j.jphs.2021.10.010

Haskins, J., Gu, L., Wittchen, E. S., Hibbard, J., & Stevenson, B. R. (1998). ZO-3, a novel member of the MAGUK protein family found at the tight junction, interacts with ZO-1 and occludin. *Journal of Cell Biology*, *141*(1). https://doi.org/10.1083/jcb.141.1.199

Hattori, Y. (2022). The Multiple Roles of Pericytes in Vascular Formation and Microglial Functions in the Brain. In *Life* (Vol. 12, Issue 11). https://doi.org/10.3390/life12111835

Hawkins, R. A., O'Kane, R. L., Simpson, I. A., & Viña, J. R. (2006). Structure of the blood-brain barrier and its role in the transport of amino acids. *Journal of Nutrition*, *136*(1). https://doi.org/10.1093/jn/136.1.218s

He, Y. J., Xu, H., Fu, Y. J., Lin, J. Y., & Zhang, M. W. (2018). Intraperitoneal hypertension, a novel risk factor for sepsis-associated encephalopathy in sepsis mice. *Scientific Reports*, *8*(1). https://doi.org/10.1038/s41598-018-26500-7

Heine, H., & Zamyatina, A. (2022). Therapeutic Targeting of TLR4 for Inflammation, Infection, and Cancer: A Perspective for Disaccharide Lipid A Mimetics. *Pharmaceuticals*, *16*(1), 23. https://doi.org/10.3390/ph16010023

Heithoff, B. P., George, K. K., Phares, A. N., Zuidhoek, I. A., Munoz-Ballester, C., & Robel, S. (2021). Astrocytes are necessary for blood–brain

barrier maintenance in the adult mouse brain. *GLIA*, *69*(2). https://doi.org/10.1002/glia.23908

Hervé, F., Ghinea, N., & Scherrmann, J. M. (2008). CNS delivery via adsorptive transcytosis. In *AAPS Journal* (Vol. 10, Issue 3). https://doi.org/10.1208/s12248-008-9055-2

Hiyama, T. Y., Watanabe, E., Okado, H., & Noda, M. (2004). The subfornical organ is the primary locus of sodium-level sensing by Nax sodium channels for the control of salt-intake behavior. *Journal of Neuroscience*, *24*(42), 9276–9281. https://doi.org/10.1523/JNEUROSCI.2795-04.2004

Hori, S., Ohtsuki, S., Hosoya, K. I., Nakashima, E., & Terasaki, T. (2004). A pericyte-derived angiopoietin-1 multimeric complex induces occludin gene expression in brain capillary endothelial cells through Tie-2 activation in vitro. *Journal of Neurochemistry*, *89*(2). https://doi.org/10.1111/j.1471-4159.2004.02343.x

Horsburgh, A., & Massoud, T. F. (2013). The circumventricular organs of the brain: Conspicuity on clinical 3T MRI and a review of functional anatomy. In *Surgical and Radiologic Anatomy* (Vol. 35, Issue 4). https://doi.org/10.1007/s00276-012-1048-2

Hosseini, M., Dastghaib, S. S., Rafatpanah, H., Hadjzadeh, M. A. R., Nahrevanian, H., & Farrokhi, I. (2010). Nitric oxide contributes to learning and memory deficits observed in hypothyroid rats during neonatal and juvenile growth. *Clinics*, *65*(11). https://doi.org/10.1590/S1807-59322010001100021

Hoyles, L., Pontifex, M. G., Rodriguez-Ramiro, I., Anis-Alavi, M. A., Jelane, K. S., Snelling, T., Solito, E., Fonseca, S., Carvalho, A. L., Carding, S. R., Müller, M., Glen, R. C., Vauzour, D., & McArthur, S. (2021). Regulation of blood–brain barrier integrity by microbiome-associated methylamines and cognition by trimethylamine N-oxide. *Microbiome*, *9*(1). https://doi.org/10.1186/s40168-021-01181-z

Huang, B., & Li, X. (2021). The Role of Mfsd2a in Nervous System Diseases. In *Frontiers in Neuroscience* (Vol. 15). https://doi.org/10.3389/fnins.2021.730534

Huang, Q., Zhong, W., Hu, Z., & Tang, X. (2018a). A review of the role of cav-1 in neuropathology and neural recovery after ischemic stroke. In *Journal of Neuroinflammation* (Vol. 15, Issue 1). https://doi.org/10.1186/s12974-018-1387-y

Huang, Q., Zhong, W., Hu, Z., & Tang, X. (2018b). A review of the role of cav-1 in neuropathology and neural recovery after ischemic stroke. In *Journal of Neuroinflammation* (Vol. 15, Issue 1). BioMed Central Ltd. https://doi.org/10.1186/s12974-018-1387-y

Huang, Y., Kang, B. N., Tian, J., Liu, Y., Luo, H. R., Hester, L., & Snyder, S. H. (2007). The cationic amino acid transporters CAT1 and CAT3 mediate NMDA receptor activation-dependent changes in elaboration of neuronal processes via the mammalian target of rapamycin mTOR pathway. *Journal of Neuroscience*, *27*(3). https://doi.org/10.1523/JNEUROSCI.4489-06.2007

Huttunen, K. M., Terasaki, T., Urtti, A., Montaser, A. B., & Uchida, Y. (2022). Pharmacoproteomics of Brain Barrier Transporters and Substrate Design for the Brain Targeted Drug Delivery. In *Pharmaceutical Research* (Vol. 39, Issue 7). https://doi.org/10.1007/s11095-022-03193-2

Iadecola, C. (2004). Neurovascular regulation in the normal brain and in Alzheimer's disease. In *Nature Reviews Neuroscience* (Vol. 5, Issue 5). https://doi.org/10.1038/nrn1387

Islam, A., Kagawa, Y., Miyazaki, H., Shil, S. K., Umaru, B. A., Yasumoto, Y., Yamamoto, Y., & Owada, Y. (2019a). FABP7 Protects Astrocytes Against ROS Toxicity via Lipid Droplet Formation. *Molecular Neurobiology*, *56*(8), 5763–5779. https://doi.org/10.1007/s12035-019-1489-2

Islam, A., Kagawa, Y., Miyazaki, H., Shil, S. K., Umaru, B. A., Yasumoto, Y., Yamamoto, Y., & Owada, Y. (2019b). FABP7 Protects Astrocytes Against ROS Toxicity via Lipid Droplet Formation. *Molecular Neurobiology*, *56*(8), 5763–5779. https://doi.org/10.1007/s12035-019-1489-2

Itoh, M., Furuse, M., Morita, K., Kubota, K., Saitou, M., & Tsukita, S. (1999). Direct binding of three tight junction-associated MAGUKs, ZO-1, ZO-

2, and ZO-3, with the COOH termini of claudins. *Journal of Cell Biology*, *147*(6). https://doi.org/10.1083/jcb.147.6.1351

Iwashyna, T. J., Ely, E. W., Smith, D. M., & Langa, K. M. (2010). Long-term cognitive impairment and functional disability among survivors of severe sepsis. *JAMA*, *304*(16). https://doi.org/10.1001/jama.2010.1553

Jangula, A., & Murphy, E. J. (2013). Lipopolysaccharide-induced blood brain barrier permeability is enhanced by alpha-synuclein expression. *Neuroscience Letters*, *551*, 23–27. https://doi.org/10.1016/j.neulet.2013.06.058

Jeong, J. K., Dow, S. A., & Young, C. N. (2021). Sensory circumventricular organs, neuroendocrine control, and metabolic regulation. In *Metabolites* (Vol. 11, Issue 8). https://doi.org/10.3390/metabo11080494

Jia, W., Lu, R., Martin, T. A., & Jiang, W. G. (2014). The role of claudin-5 in blood-brain barrier (BBB) and brain metastases (Review). *Molecular Medicine Reports*, *9*(3). https://doi.org/10.3892/mmr.2013.1875

Jungnickel, K. E. J., Parker, J. L., & Newstead, S. (2018). Structural basis for amino acid transport by the CAT family of SLC7 transporters. *Nature Communications*, *9*(1). https://doi.org/10.1038/s41467-018-03066-6

Kadoi, Y., & Goto, F. (2004). Selective inducible nitric oxide inhibition can restore hemodynamics, but does not improve neurological dysfunction in experimentally-induced septic shock in rats. *Anesthesia and Analgesia*, *99*(1). https://doi.org/10.1213/01.ANE.0000118111.94913.22

Kadry, H., Noorani, B., & Cucullo, L. (2020a). A blood–brain barrier overview on structure, function, impairment, and biomarkers of integrity. In *Fluids and Barriers of the CNS* (Vol. 17, Issue 1). https://doi.org/10.1186/s12987-020-00230-3

Kadry, H., Noorani, B., & Cucullo, L. (2020b). A blood–brain barrier overview on structure, function, impairment, and biomarkers of integrity. In *Fluids and Barriers of the CNS* (Vol. 17, Issue 1). https://doi.org/10.1186/s12987-020-00230-3

Kaduce, T. L., Chen, Y., Hell, J. W., & Spector, A. A. (2008). Docosahexaenoic acid synthesis from n-3 fatty acid precursors in rat hippocampal neurons. *Journal of Neurochemistry*, *105*(4). https://doi.org/10.1111/j.1471-4159.2008.05274.x

Kagan, T., Stoyanova, G., Lockshin, R. A., & Zakeri, Z. (2022). Ceramide from sphingomyelin hydrolysis induces neuronal differentiation, whereas de novo ceramide synthesis and sphingomyelin hydrolysis initiate apoptosis after NGF withdrawal in PC12 Cells. *Cell Communication and Signaling*, *20*(1). https://doi.org/10.1186/s12964-021-00767-2

Kamizato, K., Sato, S., Shil, S. K., Umaru, B. A., Kagawa, Y., Yamamoto, Y., Ogata, M., Yasumoto, Y., Okuyama, Y., Ishii, N., Owada, Y., & Miyazaki, H. (2019). The role of fatty acid binding protein 7 in spinal cord astrocytes in a mouse model of experimental autoimmune encephalomyelitis. *Neuroscience*, *409*, 120–129. https://doi.org/10.1016/j.neuroscience.2019.03.050

Kang, J.-B., Park, D.-J., Shah, M.-A., Kim, M.-O., & Koh, P.-O. (2019). Lipopolysaccharide induces neuroglia activation and NF-κB activation in cerebral cortex of adult mice. *Laboratory Animal Research*, *35*(1). https://doi.org/10.1186/s42826-019-0018-9

Kaplan, L., Chow, B. W., & Gu, C. (2020). Neuronal regulation of the blood–brain barrier and neurovascular coupling. In *Nature Reviews Neuroscience* (Vol. 21, Issue 8). https://doi.org/10.1038/s41583-020-0322-2

Kawai, T., & Akira, S. (2010). The role of pattern-recognition receptors in innate immunity: Update on toll-like receptors. In *Nature Immunology* (Vol. 11, Issue 5). https://doi.org/10.1038/ni.1863

Kaya, M., & Ahishali, B. (2021). Basic physiology of the blood-brain barrier in health and disease: a brief overview. In *Tissue Barriers* (Vol. 9, Issue 1). https://doi.org/10.1080/21688370.2020.1840913

Kazantzis, M., & Stahl, A. (2012). Fatty acid transport proteins, implications in physiology and disease. In *Biochimica et Biophysica Acta* -

Molecular and Cell Biology of Lipids (Vol. 1821, Issue 5). https://doi.org/10.1016/j.bbalip.2011.09.010

Keaney, J., & Campbell, M. (2015). The dynamic blood-brain barrier. *FEBS Journal*, *282*(21), 4067–4079. https://doi.org/10.1111/febs.13412

Khalilzadeh, M., Abdollahi, A., Abdolahi, F., Abdolghaffari, A. H., Dehpour, A. R., & Jazaeri, F. (2018). Protective effects of magnesium sulfate against doxorubicin induced cardiotoxicity in rats. *Life Sciences*, *207*. https://doi.org/10.1016/j.lfs.2018.06.022

Khan, N. U., Miao, T., Ju, X., Guo, Q., & Han, L. (2018). Carrier-mediated transportation through BBB. In *Brain Targeted Drug Delivery Systems: A Focus on Nanotechnology and Nanoparticulates*. https://doi.org/10.1016/B978-0-12-814001-7.00006-8

Kikuchi, D. S., Campos, A. C. P., Qu, H., Forrester, S. J., Pagano, R. L., Lassègue, B., Sadikot, R. T., Griendling, K. K., & Hernandes, M. S. (2019). Poldip2 mediates blood-brain barrier disruption in a model of sepsis-associated encephalopathy. *Journal of Neuroinflammation*, *16*(1). https://doi.org/10.1186/s12974-019-1575-4

Killoy, K. M., Harlan, B. A., Pehar, M., & Vargas, M. R. (2020). FABP7 upregulation induces a neurotoxic phenotype in astrocytes. *GLIA*, *68*(12). https://doi.org/10.1002/glia.23879

Kim, D. E., & Priefer, R. (2020). Therapeutic potential of direct clearance of the amyloid-β in alzheimer's disease. *Brain Sciences*, *10*(2). https://doi.org/10.3390/brainsci10020093

Kimelberg, H. K. (2004). Water homeostasis in the brain: Basic concepts. *Neuroscience*, *129*(4). https://doi.org/10.1016/j.neuroscience.2004.07.033

Kirkley, K. S., Popichak, K. A., Afzali, M. F., Legare, M. E., & Tjalkens, R. B. (2017). Microglia amplify inflammatory activation of astrocytes in manganese neurotoxicity. *Journal of Neuroinflammation*, *14*(1). https://doi.org/10.1186/s12974-017-0871-0

Klein, R. S., Garber, C., Funk, K. E., Salimi, H., Soung, A., Kanmogne, M., Manivasagam, S., Agner, S., & Cain, M. (2019). Neuroinflammation During RNA Viral Infections. In *Annual Review of Immunology* (Vol. 37). https://doi.org/10.1146/annurev-immunol-042718-041417

Knox, E. G., Aburto, M. R., Clarke, G., Cryan, J. F., & O'Driscoll, C. M. (2022). The blood-brain barrier in aging and neurodegeneration. In *Molecular Psychiatry* (Vol. 27, Issue 6, pp. 2659–2673). Springer Nature. https://doi.org/10.1038/s41380-022-01511-z

Koepsell, H. (2020). Glucose transporters in brain in health and disease. In *Pflugers Archiv European Journal of Physiology* (Vol. 472, Issue 9). https://doi.org/10.1007/s00424-020-02441-x

Kokaia, M. (2009). Neurotrophic Factors: GDNF: A Neurotrophic Factor Against Epilepsy. In *Encyclopedia of Basic Epilepsy Research*. https://doi.org/10.1016/B978-012373961-2.00110-7

Komarova, Y., & Malik, A. B. (2009). Regulation of endothelial permeability via paracellular and transcellular transport pathways. In *Annual Review of Physiology* (Vol. 72). https://doi.org/10.1146/annurev-physiol-021909-135833

Kooistra, E. J., van Berkel, M., van Kempen, N. F., van Latum, C. R. M., Bruse, N., Frenzel, T., van den Berg, M. J. W., Schouten, J. A., Kox, M., & Pickkers, P. (2021). Dexamethasone and tocilizumab treatment considerably reduces the value of C-reactive protein and procalcitonin to detect secondary bacterial infections in COVID-19 patients. *Critical Care*, *25*(1). https://doi.org/10.1186/s13054-021-03717-z

Kopitar-Jeraia, N. (2015). Innate immune response in brain, nf-kappa b signaling and cystatins. In *Frontiers in Molecular Neuroscience* (Vol. 8, Issue DEC). https://doi.org/10.3389/fnmol.2015.00073

Kubotera, H., Ikeshima-Kataoka, H., Hatashita, Y., Allegra Mascaro, A. L., Pavone, F. S., & Inoue, T. (2019). Astrocytic endfeet re-cover blood vessels after removal by laser ablation. *Scientific Reports*, *9*(1). https://doi.org/10.1038/s41598-018-37419-4

Kummer, D., & Ebnet, K. (2018). Junctional adhesion molecules (JAMs): The JAM-integrin connection. In *Cells* (Vol. 7, Issue 4). https://doi.org/10.3390/cells7040025

Langen, U. H., Ayloo, S., & Gu, C. (2019). Development and cell biology of the blood-brain barrier. In *Annual Review of Cell and Developmental Biology* (Vol. 35). https://doi.org/10.1146/annurev-cellbio-100617-062608

Lee, B., Shim, I., Lee, H., & Hahm, D. H. (2018). Gypenosides attenuate lipopolysaccharide-induced neuroinflammation and anxiety-like behaviors in rats. *Animal cells and systems*, *22*(5), 305–316. https://doi.org/10.1080/19768354.2018.1517825

Lee, J. A., Hall, B., Allsop, J., Alqarni, R., & Allen, S. P. (2021a). Lipid metabolism in astrocytic structure and function. In *Seminars in Cell and Developmental Biology* (Vol. 112, pp. 123–136). Elsevier Ltd. https://doi.org/10.1016/j.semcdb.2020.07.017

Lehner, C., Gehwolf, R., Tempfer, H., Krizbai, I., Hennig, B., Bauer, H. C., & Bauer, H. (2011). Oxidative stress and blood-brain barrier dysfunction under particular consideration of matrix metalloproteinases. In *Antioxidants and Redox Signaling* (Vol. 15, Issue 5, pp. 1305–1323). https://doi.org/10.1089/ars.2011.3923

Lei, M. G., & Morrison, D. C. (2000). Differential expression of caveolin-1 in lipopolysaccharide-activated murine macrophages. *Infection and Immunity*, *68*(9). https://doi.org/10.1128/IAI.68.9.5084-5089.2000

Lei, S., Li, J., Yu, J., Li, F., Pan, Y., Chen, X., Ma, C., Zhao, W., & Tang, X. (2023). Porphyromonas gingivalis bacteremia increases the permeability of the blood-brain barrier via the Mfsd2a/Caveolin-1 mediated transcytosis pathway. *International Journal of Oral Science*, *15*(1). https://doi.org/10.1038/s41368-022-00215-y

Leligdowicz, A., & Matthay, M. A. (2019). Heterogeneity in sepsis: New biological evidence with clinical applications. In *Critical Care* (Vol. 23, Issue 1). https://doi.org/10.1186/s13054-019-2372-2

Leng, F., & Edison, P. (2021). Neuroinflammation and microglial activation in Alzheimer disease: where do we go from here? In *Nature Reviews Neurology* (Vol. 17, Issue 3). https://doi.org/10.1038/s41582-020-00435-y

Li, D., & Wu, M. (2021). Pattern recognition receptors in health and diseases. In *Signal Transduction and Targeted Therapy* (Vol. 6, Issue 1). https://doi.org/10.1038/s41392-021-00687-0

Li, H., Wang, P., Huang, F., Jin, J., Wu, H., Zhang, B., Wang, Z., Shi, H., & Wu, X. (2018). Astragaloside IV protects blood-brain barrier integrity from LPS-induced disruption via activating Nrf2 antioxidant signaling pathway in mice. *Toxicology and Applied Pharmacology*, *340*. https://doi.org/10.1016/j.taap.2017.12.019

Li, T., Zheng, L. N., & Han, X. H. (2020). Fenretinide attenuates lipopolysaccharide (LPS)-induced blood-brain barrier (BBB) and depressive-like behavior in mice by targeting Nrf-2 signaling. *Biomedicine and Pharmacotherapy*, *125*. https://doi.org/10.1016/j.biopha.2019.109680

Li, W., Chen, Z., Chin, I., Chen, Z., & Dai, H. (2018). The Role of VE-cadherin in Blood-brain Barrier Integrity Under Central Nervous System Pathological Conditions. *Current Neuropharmacology*, *16*(9). https://doi.org/10.2174/1570159x16666180222164809

Liang, Y., Diehn, M., Watson, N., Bollen, A. W., Aldape, K. D., Nicholas, M. K., Lamborn, K. R., Berger, M. S., Botstein, D., Brown, P. O., & Israel, M. A. (2005). Gene expression profiling reveals molecularly and clinically distinct subtypes of glioblastoma multiforme. *Proceedings of the National Academy of Sciences of the United States of America*, *102*(16). https://doi.org/10.1073/pnas.0402870102

Lippmann, E. S., Azarin, S. M., Kay, J. E., Nessler, R. A., Wilson, H. K., Al-Ahmad, A., Palecek, S. P., & Shusta, E. V. (2012). Human Blood-Brain Barrier Endothelial Cells Derived from Pluripotent Stem Cells. *Nature Biotechnology*, *30*(6).

Liu, W. Y., Wang, Z. Bin, Wang, Y., Tong, L. C., Li, Y., Wei, X., Luan, P., & Li, L. (2015). Increasing the Permeability of the Blood-brain Barrier in

Three Different Models in vivo. *CNS Neuroscience and Therapeutics*, *21*(7). https://doi.org/10.1111/cns.12405

Liu, W. Y., Wang, Z. Bin, Zhang, L. C., Wei, X., & Li, L. (2012). Tight junction in blood-brain barrier: An overview of structure, regulation, and regulator substances. In *CNS Neuroscience and Therapeutics* (Vol. 18, Issue 8). https://doi.org/10.1111/j.1755-5949.2012.00340.x

Liu, X., Nemeth, D. P., McKim, D. B., Zhu, L., DiSabato, D. J., Berdysz, O., Gorantla, G., Oliver, B., Witcher, K. G., Wang, Y., Negray, C. E., Vegesna, R. S., Sheridan, J. F., Godbout, J. P., Robson, M. J., Blakely, R. D., Popovich, P. G., Bilbo, S. D., & Quan, N. (2019). Cell-Type-Specific Interleukin 1 Receptor 1 Signaling in the Brain Regulates Distinct Neuroimmune Activities. *Immunity*, *50*(2). https://doi.org/10.1016/j.immuni.2018.12.012

Lochhead, J. J., Yang, J., Ronaldson, P. T., & Davis, T. P. (2020). Structure, Function, and Regulation of the Blood-Brain Barrier Tight Junction in Central Nervous System Disorders. In *Frontiers in Physiology* (Vol. 11). https://doi.org/10.3389/fphys.2020.00914

Luissint, A. C., Artus, C., Glacial, F., Ganeshamoorthy, K., & Couraud, P. O. (2012). Tight junctions at the blood brain barrier: Physiological architecture and disease-associated dysregulation. In *Fluids and Barriers of the CNS* (Vol. 9, Issue 1). https://doi.org/10.1186/2045-8118-9-23

Lukacova, N., Kisucka, A., Bimbova, K. K., Bacova, M., Ileninova, M., Kuruc, T., & Galik, J. (2021). Glial-neuronal interactions in pathogenesis and treatment of spinal cord injury. In *International Journal of Molecular Sciences* (Vol. 22, Issue 24). https://doi.org/10.3390/ijms222413577

Lyck, R., & Engelhardt, B. (2012). Going against the tide - How encephalitogenic T cells breach the blood-brain barrier. In *Journal of Vascular Research* (Vol. 49, Issue 6). https://doi.org/10.1159/000341232

Lyman, M., Lloyd, D. G., Ji, X., Vizcaychipi, M. P., & Ma, D. (2014). Neuroinflammation: The role and consequences. In *Neuroscience Research* (Vol. 79, Issue 1). https://doi.org/10.1016/j.neures.2013.10.004

Macvicar, B. A., & Newman, E. A. (2015). Astrocyte regulation of blood flow in the brain. *Cold Spring Harbor Perspectives in Biology*, *7*(5). https://doi.org/10.1101/cshperspect.a020388

Maher, F., Davies-Hill, T. M., Lysko, P. G., Henneberry, R. C., & Simpson, I. A. (1991). Expression of two glucose transporters, GLUT1 and GLUT3, in cultured cerebellar neurons: Evidence for neuron-specific expression of GLUT3. *Molecular and Cellular Neuroscience*, *2*(4). https://doi.org/10.1016/1044-7431(91)90066-W

Manabe, T., & Heneka, M. T. (2022). Cerebral dysfunctions caused by sepsis during ageing. In *Nature Reviews Immunology* (Vol. 22, Issue 7). https://doi.org/10.1038/s41577-021-00643-7

Mansouri, M., Sotoudeh, M. M., Shamshirian, A., Beheshti, F., Hosseini, M., & Sadeghnia, H. R. (2021). Beneficial effects of selenium against the behavioral consequences of lipopolysaccharide administration in rats. *Learning and Motivation*, *74*. https://doi.org/10.1016/j.lmot.2021.101713

Massaad, C. A., & Klann, E. (2011). Reactive oxygen species in the regulation of synaptic plasticity and memory. *Antioxidants & redox signaling*, *14*(10), 2013–2054. https://doi.org/10.1089/ars.2010.3208

Matsumata, M., Sakayori, N., Maekawa, M., Owada, Y., Yoshikawa, T., & Osumi, N. (2012). The effects of Fabp7 and Fabp5 on postnatal hippocampal neurogenesis in the mouse. *Stem Cells*, *30*(7), 1532–1543. https://doi.org/10.1002/stem.1124

Matter, K., & Balda, M. S. (2003). Signalling to and from tight junctions. In *Nature Reviews Molecular Cell Biology* (Vol. 4, Issue 3). https://doi.org/10.1038/nrm1055

Matthaeus, C., & Taraska, J. W. (2021). Energy and Dynamics of Caveolae Trafficking. In *Frontiers in Cell and Developmental Biology* (Vol. 8). https://doi.org/10.3389/fcell.2020.614472

Mayes, C., Burdge, G. C., Bingham, A., Murphy, J. L., Tubman, R., & Wootton, S. A. (2006). Variation in [U-13C] α linolenic acid absorption, β-oxidation and conversion to docosahexaenoic acid in the pre-term infant fed a

DHA-enriched formula. *Pediatric Research*, *59*(2). https://doi.org/10.1203/01.pdr.0000196372.29648.7a

McCaffrey, G., Willis, C. L., Staatz, W. D., Nametz, N., Quigley, C. A., Hom, S., Lochhead, J. J., & Davis, T. P. (2009). Occludin oligomeric assemblies at tight junctions of the blood-brain barrier are altered by hypoxia and reoxygenation stress. *Journal of Neurochemistry*, *110*(1). https://doi.org/10.1111/j.1471-4159.2009.06113.x

McCarthy, K. M., Skare, I. B., Stankewich, M. C., Furuse, M., Tsukita, S., Rogers, R. A., Lynch, R. D., & Schneeberger, E. E. (1996). Occludin is a functional component of the tight junction. *Journal of Cell Science*, *109*(9). https://doi.org/10.1242/jcs.109.9.2287

Micheau, O., & Tschopp, J. (2003). Induction of TNF receptor I-mediated apoptosis via two sequential signaling complexes. *Cell*, *114*(2). https://doi.org/10.1016/S0092-8674(03)00521-X

Mishra, A., Kim, H. J., Shin, A. H., & Thayer, S. A. (2012). Synapse loss induced by interleukin-1β requires pre-and post-synaptic mechanisms. *Journal of Neuroimmune Pharmacology*, *7*(3). https://doi.org/10.1007/s11481-012-9342-7

Mita, R., Beaulieu, M. J., Field, C., & Godbout, R. (2010). Brain fatty acid-binding protein and ω-3/ω-6 fatty acids: Mechanistic insight into malignant glioma cell migration. *Journal of Biological Chemistry*, *285*(47), 37005–37015. https://doi.org/10.1074/jbc.M110.170076

Mitchell, R. W., On, N. H., Del Bigio, M. R., Miller, D. W., & Hatch, G. M. (2011). Fatty acid transport protein expression in human brain and potential role in fatty acid transport across human brain microvessel endothelial cells. *Journal of Neurochemistry*, *117*(4). https://doi.org/10.1111/j.1471-4159.2011.07245.x

Mitic, L. L., Van Itallie, C. M., & Anderson, J. M. (2000). Molecular physiology and pathophysiology of tight junctions I. Tight junction structure and function: Lessons from mutant animals and proteins. In *American Journal*

of Physiology - Gastrointestinal and Liver Physiology (Vol. 279, Issues 2 42-2). https://doi.org/10.1152/ajpgi.2000.279.2.g250

Möckl, L. (2020). The Emerging Role of the Mammalian Glycocalyx in Functional Membrane Organization and Immune System Regulation. In *Frontiers in Cell and Developmental Biology* (Vol. 8). https://doi.org/10.3389/fcell.2020.00253

Mohamed, W., Kumar, J., Alghamdi, B. S., Soliman, A. H., & Toshihide, Y. (2023). Neurodegeneration and inflammation crosstalk: Therapeutic targets and perspectives. *IBRO Neuroscience Reports*, *14*. https://doi.org/10.1016/j.ibneur.2022.12.003

Moolayil, J. (2019). Learn Keras for Deep Neural Networks: A Fast-Track Approach to Modern Deep Learning with Python. In *Learn Keras for Deep Neural Networks*.

Morris, M. E., Rodriguez-Cruz, V., & Felmlee, M. A. (2017). SLC and ABC Transporters: Expression, Localization, and Species Differences at the Blood-Brain and the Blood-Cerebrospinal Fluid Barriers. *AAPS Journal*, *19*(5). https://doi.org/10.1208/s12248-017-0110-8

Mosser, D. M., & Edwards, J. P. (2008). Exploring the full spectrum of macrophage activation. In *Nature Reviews Immunology* (Vol. 8, Issue 12). https://doi.org/10.1038/nri2448

Murakami, T., Felinski, E. A., & Antonetti, D. A. (2009). Occludin phosphorylation and ubiquitination regulate tight junction trafficking and vascular endothelial growth factor-induced permeability. *Journal of Biological Chemistry*, *284*(31). https://doi.org/10.1074/jbc.M109.016766

Nadeau, S., & Rivest, S. (1999). Regulation of the gene encoding tumor necrosis factor alpha (TNF-α) in the rat brain and pituitary in response to different models of systemic immune challenge. *Journal of Neuropathology and Experimental Neurology*, *58*(1). https://doi.org/10.1097/00005072-199901000-00008

Namyen, J., Permpoonputtana, K., Nopparat, C., Tocharus, J., Tocharus, C., & Govitrapong, P. (2020). Protective Effects of Melatonin on

Methamphetamine-Induced Blood–Brain Barrier Dysfunction in Rat Model. *Neurotoxicity Research*, *37*(3). https://doi.org/10.1007/s12640-019-00156-1

Nedeva, C., Menassa, J., & Puthalakath, H. (2019). Sepsis: Inflammation is a necessary evil. In *Frontiers in Cell and Developmental Biology* (Vol. 7, Issue JUN). Frontiers Media S.A. https://doi.org/10.3389/fcell.2019.00108

Needham, H., Torpey, G., Flores, C. C., Davis, C. J., Vanderheyden, W. M., & Gerstner, J. R. (2022). A Dichotomous Role for FABP7 in Sleep and Alzheimer's Disease Pathogenesis: A Hypothesis. *Frontiers in Neuroscience*, *16*. https://doi.org/10.3389/fnins.2022.798994

Nguyen, L. N., Ma, D., Shui, G., Wong, P., Cazenave-Gassiot, A., Zhang, X., Wenk, M. R., Goh, E. L. K., & Silver, D. L. (2014a). Mfsd2a is a transporter for the essential omega-3 fatty acid docosahexaenoic acid. *Nature*, *509*(7501). https://doi.org/10.1038/nature13241

Nguyen, L. N., Ma, D., Shui, G., Wong, P., Cazenave-Gassiot, A., Zhang, X., Wenk, M. R., Goh, E. L. K., & Silver, D. L. (2014b). Mfsd2a is a transporter for the essential omega-3 fatty acid docosahexaenoic acid. *Nature*, *509*(7501), 503–506. https://doi.org/10.1038/nature13241

Nilsberth, C., Elander, L., Hamzic, N., Norell, M., Lönn, J., Engström, L., & Blomqvist, A. (2009). The role of interleukin-6 in lipopolysaccharide-induced fever by mechanisms independent of prostaglandin e2. *Endocrinology*, *150*(4). https://doi.org/10.1210/en.2008-0806

Nitta, T., Hata, M., Gotoh, S., Seo, Y., Sasaki, H., Hashimoto, N., Furuse, M., & Tsukita, S. (2003). Size-selective loosening of the blood-brain barrier in claudin-5-deficient mice. *Journal of Cell Biology*, *161*(3). https://doi.org/10.1083/jcb.200302070

Nordgreen, J., Munsterhjelm, C., Aae, F., Popova, A., Boysen, P., Ranheim, B., Heinonen, M., Raszplewicz, J., Piepponen, P., Lervik, A., Valros, A., & Janczak, A. M. (2018). The effect of lipopolysaccharide (LPS) on inflammatory markers in blood and brain and on behavior in individually-housed pigs. *Physiology and Behavior*, *195*. https://doi.org/10.1016/j.physbeh.2018.07.013

Nwafor, D. C., Brichacek, A. L., Mohammad, A. S., Griffith, J., Lucke-Wold, B. P., Benkovic, S. A., Geldenhuys, W. J., Lockman, P. R., & Brown, C. M. (2019). Targeting the Blood-Brain Barrier to Prevent Sepsis-Associated Cognitive Impairment. *Journal of Central Nervous System Disease*, *11*. https://doi.org/10.1177/1179573519840652

Oakley, F. O., Smith, R. L., & Engelhardt, J. F. (2009). Lipid rafts and caveolin-1 coordinate interleukin-1β (IL-1β)-dependent activation of NFκB by controlling endocytosis of Nox2 and IL-1β receptor 1 from the plasma membrane. *Journal of Biological Chemistry*, *284*(48), 33255–33264. https://doi.org/10.1074/jbc.M109.042127

Ogawa, Y., & Kanoh, S. (1984). Involvement of Central Action of Lipopolysaccharide in Pyrogen Fever. *The Japanese Journal of Pharmacology*, *36*(3). https://doi.org/10.1254/jjp.36.389

O'Kane, R. L., Martínez-López, I., DeJoseph, M. R., Viña, J. R., & Hawkins, R. A. (1999). Na+-dependent glutamate transporters (EAAT1, EAAT2, and EAAT3) of the blood-brain barrier. A mechanism for glutamate removal. *Journal of Biological Chemistry*, *274*(45), 31891–31895. https://doi.org/10.1074/jbc.274.45.31891

Oldfield, B. J., & McKinley, M. J. (2015). Chapter 15 – Circumventricular Organs. In *The Rat Nervous System*.

Oliva, C., Escobedo, P., Astorga, C., Molina, C., & Sierralta, J. (2012). Role of the maguk protein family in synapse formation and function. In *Developmental Neurobiology* (Vol. 72, Issue 1). https://doi.org/10.1002/dneu.20949

O'Loughlin, E., Madore, C., Lassmann, H., & Butovsky, O. (2018). Microglial phenotypes and functions in multiple sclerosis. *Cold Spring Harbor Perspectives in Medicine*, *8*(2). https://doi.org/10.1101/cshperspect.a028993

Orhun, G., Bebek, N., Ergin Özcan, P., Ali, A., & Esen, F. (2020). Clinical and Electroencephalographic Findings in Patients with Sepsis-associated Encephalopathy and the Evaluation of Their Effects on Survival.

European Archives of Medical Research, *36*(1). https://doi.org/10.4274/eamr.galenos.2020.93585

Orihuela, R., McPherson, C. A., & Harry, G. J. (2016). Microglial M1/M2 polarization and metabolic states. In *British Journal of Pharmacology* (Vol. 173, Issue 4). https://doi.org/10.1111/bph.13139

Örnek Ergüzeloğlu, C., Kara, B., Karacan, İ., Özdemir, Ö., Kesim, Y., Bebek, N., Özbek, U., & Uğur İşeri, S. A. (2020). Screenıng Slc2a1 Gene for Sequence and Copy Number Variations Associated with Glut-1 Deficiency Syndrome. *İstanbul Tıp Fakültesi Dergisi*, *83*(3). Https://Doi.Org/10.26650/İuitfd.2019.0064

Overgaard, C. E., Daugherty, B. L., Mitchell, L. A., & Koval, M. (2011). Claudins: Control of barrier function and regulation in response to oxidant stress. In *Antioxidants and Redox Signaling* (Vol. 15, Issue 5). https://doi.org/10.1089/ars.2011.3893

Owada, Y. (2008). Fatty acid binding protein: Localization and functional significance in the brain. In *Tohoku Journal of Experimental Medicine* (Vol. 214, Issue 3). https://doi.org/10.1620/tjem.214.213

Pachter, J. S., De Vries, H. E., & Fabry, Z. (2003). The blood-brain barrier and its role in immune privilege in the central nervous system. In *Journal of Neuropathology and Experimental Neurology* (Vol. 62, Issue 6). https://doi.org/10.1093/jnen/62.6.593

Page, M. J., Kell, D. B., & Pretorius, E. (2022). The Role of Lipopolysaccharide-Induced Cell Signalling in Chronic Inflammation. In *Chronic Stress* (Vol. 6). https://doi.org/10.1177/24705470221076390

Pajouhesh, H., & Lenz, G. R. (2005). Medicinal chemical properties of successful central nervous system drugs. *NeuroRx*, *2*(4). https://doi.org/10.1602/neurorx.2.4.541

Pardridge, W. M. (1995). Transport of small molecules through the blood-brain barrier: biology and methodology. In *Advanced Drug Delivery Reviews* (Vol. 15, Issues 1–3). https://doi.org/10.1016/0169-409X(95)00003-P

Pardridge, W. M. (2005a). The blood-brain barrier and neurotherapeutics. In *NeuroRx* (Vol. 2, Issue 1). https://doi.org/10.1602/neurorx.2.1.1

Pardridge, W. M. (2005b). The blood-brain barrier: Bottleneck in brain drug development. *NeuroRx*, *2*(1). https://doi.org/10.1602/neurorx.2.1.3

Park, J. H., Choi, J. Y., Lee, H. K., Jo, C., & Koh, Y. H. (2021). Notch1-mediated inflammation is associated with endothelial dysfunction in human brain microvascular endothelial cells upon particulate matter exposure. *Archives of Toxicology*, *95*(2). https://doi.org/10.1007/s00204-020-02942-9

Patki, G., Solanki, N., Atrooz, F., Allam, F., & Salim, S. (2013). Depression, anxiety-like behavior and memory impairment are associated with increased oxidative stress and inflammation in a rat model of social stress. *Brain Research*, *1539*. https://doi.org/10.1016/j.brainres.2013.09.033

Peng, X., Luo, Z., He, S., Zhang, L., & Li, Y. (2021). Blood-Brain Barrier Disruption by Lipopolysaccharide and Sepsis-Associated Encephalopathy. In *Frontiers in Cellular and Infection Microbiology* (Vol. 11). Frontiers Media S.A. https://doi.org/10.3389/fcimb.2021.768108

Perrot, C. Y., Herrera, J. L., Fournier-Goss, A. E., & Komatsu, M. (2020). Prostaglandin E2 breaks down pericyte–endothelial cell interaction via EP1 and EP4-dependent downregulation of pericyte N-cadherin, connexin-43, and R-Ras. *Scientific Reports*, *10*(1). https://doi.org/10.1038/s41598-020-68019-w

Peruzzu, D., Boussadia, Z., Fratini, F., Spadaro, F., Bertuccini, L., Sanchez, M., Carollo, M., Matarrese, P., Falchi, M., Iosi, F., Raggi, C., Parolini, I., Carè, A., Sargiacomo, M., Gagliardi, M. C., & Fecchi, K. (2022). Inhibition of cholesterol transport impairs Cav-1 trafficking and small extracellular vesicles secretion, promoting amphisome formation in melanoma cells. *Traffic*. https://doi.org/10.1111/tra.12878

Prinz, M., Jung, S., & Priller, J. (2019). Microglia Biology: One Century of Evolving Concepts. In *Cell* (Vol. 179, Issue 2). https://doi.org/10.1016/j.cell.2019.08.053

Pu, Y., Zhao, L., Xi, Y., Xia, Y., & Qian, Y. (2022). The protective effects of Mirtazapine against lipopolysaccharide (LPS)-induced brain vascular hyperpermeability. *Bioengineered*, *13*(2). https://doi.org/10.1080/21655979.2021.2024962

Puris, E., Fricker, G., & Gynther, M. (2022). Targeting Transporters for Drug Delivery to the Brain: Can We Do Better? In *Pharmaceutical Research* (Vol. 39, Issue 7, pp. 1415–1455). Springer. https://doi.org/10.1007/s11095-022-03241-x

Puschel, F., Favaro, F., Redondo-Pedraza, J., Lucendo, E., Iurlaro, R., Marchetti, S., Majem, B., Eldering, E., Nadal, E., Ricci, J. E., Chevet, E., & Muñoz-Pinedo, C. (2020). Starvation and antimetabolic therapy promote cytokine release and recruitment of immune cells. *Proceedings of the National Academy of Sciences of the United States of America*, *117*(18). https://doi.org/10.1073/pnas.1913707117

Qu, C., Song, H., Shen, J., Xu, L., Li, Y., Qu, C., Li, T., & Zhang, J. (2020). Mfsd2a Reverses Spatial Learning and Memory Impairment Caused by Chronic Cerebral Hypoperfusion via Protection of the Blood–Brain Barrier. *Frontiers in Neuroscience*, *14*. https://doi.org/10.3389/fnins.2020.00461

Räpple, D., & Schilling, T. (2020). Sepsis and septic shock. In *Tagliche Praxis* (Vol. 61, Issue 4). https://doi.org/10.5005/jp/books/12233_16

Rauf, A., Badoni, H., Abu-Izneid, T., Olatunde, A., Rahman, M. M., Painuli, S., Semwal, P., Wilairatana, P., & Mubarak, M. S. (2022). Neuroinflammatory Markers: Key Indicators in the Pathology of Neurodegenerative Diseases. In *Molecules* (Vol. 27, Issue 10). https://doi.org/10.3390/molecules27103194

Rempe, R. G., Hartz, A. M. S., & Bauer, B. (2016a). Matrix metalloproteinases in the brain and blood-brain barrier: Versatile breakers and makers. In *Journal of Cerebral Blood Flow and Metabolism* (Vol. 36, Issue 9). https://doi.org/10.1177/0271678X16655551

Rempe, R. G., Hartz, A. M. S., & Bauer, B. (2016b). Matrix metalloproteinases in the brain and blood-brain barrier: Versatile breakers and

makers. In *Journal of Cerebral Blood Flow and Metabolism* (Vol. 36, Issue 9, pp. 1481–1507). Nature Publishing Group. https://doi.org/10.1177/0271678X16655551

Roepstorff, C., Wulff Helge, J., Vistisen, B., & Kiens, B. (2004). Studies of plasma membrane fatty acid-binding protein and other lipid-binding proteins in human skeletal muscle. *Proceedings of the Nutrition Society*, *63*(2). https://doi.org/10.1079/pns2004332

Roy, A., & Patra, S. K. (2023). Lipid Raft Facilitated Receptor Organization and Signaling: A Functional Rheostat in Embryonic Development, Stem Cell Biology and Cancer. In *Stem Cell Reviews and Reports* (Vol. 19, Issue 1, pp. 2–25). Springer. https://doi.org/10.1007/s12015-022-10448-3

Rui, Q., Ni, H., Lin, X., Zhu, X., Li, D., Liu, H., & Chen, G. (2019a). Astrocyte-derived fatty acid-binding protein 7 protects blood-brain barrier integrity through a caveolin-1/MMP signaling pathway following traumatic brain injury. *Experimental Neurology*, *322*. https://doi.org/10.1016/j.expneurol.2019.113044

Rui, Q., Ni, H., Lin, X., Zhu, X., Li, D., Liu, H., & Chen, G. (2019b). Astrocyte-derived fatty acid-binding protein 7 protects blood-brain barrier integrity through a caveolin-1/MMP signaling pathway following traumatic brain injury. *Experimental Neurology*, *322*. https://doi.org/10.1016/j.expneurol.2019.113044

Saitou, M., Furuse, M., Sasaki, H., Schulzke, J. D., Fromm, M., Takano, H., Noda, T., & Tsukita, S. (2000). Complex phenotype of mice lacking occludin, a component of tight junction strands. *Molecular Biology of the Cell*, *11*(12). https://doi.org/10.1091/mbc.11.12.4131

Sakai, J., Cammarota, E., Wright, J. A., Cicuta, P., Gottschalk, R. A., Li, N., Fraser, I. D. C., & Bryant, C. E. (2017). Lipopolysaccharide-induced NF-κB nuclear translocation is primarily dependent on MyD88, but TNFα expression requires TRIF and MyD88. *Scientific Reports*, *7*(1). https://doi.org/10.1038/s41598-017-01600-y

Saunders, N. R., Ek, C. J., Habgood, M. D., & Dziegielewska, K. M. (2008). Barriers in the brain: a renaissance? In *Trends in Neurosciences* (Vol. 31, Issue 6). https://doi.org/10.1016/j.tins.2008.03.003

Semmler, A., Frisch, C., Debeir, T., Ramanathan, M., Okulla, T., Klockgether, T., & Heneka, M. T. (2007). Long-term cognitive impairment, neuronal loss and reduced cortical cholinergic innervation after recovery from sepsis in a rodent model. *Experimental Neurology*, *204*(2). https://doi.org/10.1016/j.expneurol.2007.01.003

Shi, D. Y., Bierhaus, A., Nawroth, P. P., & Stern, D. M. (2009). RAGE and Alzheimer's disease: A progression factor for amyloid-β- induced cellular perturbation? In *Journal of Alzheimer's Disease* (Vol. 16, Issue 4). https://doi.org/10.3233/JAD-2009-1030

Shimizu, F., Nishihara, H., & Kanda, T. (2018). Blood–brain barrier dysfunction in immuno-mediated neurological diseases. In *Immunological Medicine* (Vol. 41, Issue 3). https://doi.org/10.1080/25785826.2018.1531190

Shioda, N., Yabuki, Y., Kobayashi, Y., Onozato, M., Owada, Y., & Fukunaga, K. (2014). FABP3 protein promotes α-synuclein oligomerization associated with 1-Methyl-1,2,3,6-tetrahydropiridine-induced neurotoxicity. *Journal of Biological Chemistry*, *289*(27). https://doi.org/10.1074/jbc.M113.527341

Simon, D. W., McGeachy, M. J., Baylr, H., Clark, R. S. B., Loane, D. J., & Kochanek, P. M. (2017). The far-reaching scope of neuroinflammation after traumatic brain injury. In *Nature Reviews Neurology* (Vol. 13, Issue 3). https://doi.org/10.1038/nrneurol.2017.13

Singh, A., & Vellapandian, C. (2022). Structure of the Blood Brain Barrier and the Role of Transporters in the movement of substrates across the barriers. *Qeios*. https://doi.org/10.32388/5giw6a

Sisó, S., Jeffrey, M., & González, L. (2010). Sensory circumventricular organs in health and disease. In *Acta Neuropathologica* (Vol. 120, Issue 6). https://doi.org/10.1007/s00401-010-0743-5

Skelly, D. T., Hennessy, E., Dansereau, M. A., & Cunningham, C. (2013). A Systematic Analysis of the Peripheral and CNS Effects of Systemic LPS, IL-1B, TNF-α and IL-6 Challenges in C57BL/6 Mice. *PLoS ONE*, *8*(7). https://doi.org/10.1371/journal.pone.0069123

Skrzypczak-Wiercioch, A., & Sałat, K. (2022). Lipopolysaccharide-Induced Model of Neuroinflammation: Mechanisms of Action, Research Application and Future Directions for Its Use. In *Molecules* (Vol. 27, Issue 17). https://doi.org/10.3390/molecules27175481

Sonneville, R., Verdonk, F., Rauturier, C., Klein, I. F., Wolff, M., Annane, D., Chretien, F., & Sharshar, T. (2013). Understanding brain dysfunction in sepsis. *Annals of Intensive Care*, *3*(1). https://doi.org/10.1186/2110-5820-3-15

Sörensson, J., Matejka, G. L., Ohlson, M., & Haraldsson, B. (1999). Human endothelial cells produce orosomucoid, an important component of the capillary barrier. *American Journal of Physiology - Heart and Circulatory Physiology*, *276*(2 45-2). https://doi.org/10.1152/ajpheart.1999.276.2.h530

Srivastava, P., Cronin, C. G., Scranton, V. L., Jacobson, K. A., Liang, B. T., & Verma, R. (2020). Neuroprotective and neuro-rehabilitative effects of acute purinergic receptor P2X4 (P2X4R) blockade after ischemic stroke. *Experimental Neurology*, *329*. https://doi.org/10.1016/j.expneurol.2020.113308

Steed, E., Balda, M. S., & Matter, K. (2010). Dynamics and functions of tight junctions. In *Trends in Cell Biology* (Vol. 20, Issue 3). https://doi.org/10.1016/j.tcb.2009.12.002

Stephenson, J., Nutma, E., van der Valk, P., & Amor, S. (2018). Inflammation in CNS neurodegenerative diseases. In *Immunology* (Vol. 154, Issue 2). https://doi.org/10.1111/imm.12922

Storck, S. E., Hartz, A. M. S., Bernard, J., Wolf, A., Kachlmeier, A., Mahringer, A., Weggen, S., Pahnke, J., & Pietrzik, C. U. (2018). The concerted amyloid-beta clearance of LRP1 and ABCB1/P-gp across the blood-brain

barrier is linked by PICALM. *Brain, Behavior, and Immunity*, *73*. https://doi.org/10.1016/j.bbi.2018.07.017

Strazielle, N., & Ghersi-Egea, J. F. (2015). Efflux transporters in blood-brain interfaces of the developing brain. In *Frontiers in Neuroscience* (Vol. 9, Issue FEB). https://doi.org/10.3389/fnins.2015.00021

Streit, W. J., Mrak, R. E., & Griffin, W. S. T. (2004). Microglia and neuroinflammation: A pathological perspective. *Journal of Neuroinflammation*, *1*. https://doi.org/10.1186/1742-2094-1-14

Subhramanyam, C. S., Wang, C., Hu, Q., & Dheen, S. T. (2019). Microglia-mediated neuroinflammation in neurodegenerative diseases. In *Seminars in Cell and Developmental Biology* (Vol. 94). https://doi.org/10.1016/j.semcdb.2019.05.004

Sun, Y., Koyama, Y., & Shimada, S. (2022). Inflammation From Peripheral Organs to the Brain: How Does Systemic Inflammation Cause Neuroinflammation? In *Frontiers in Aging Neuroscience* (Vol. 14). Frontiers Media S.A. https://doi.org/10.3389/fnagi.2022.903455

Sun, Z., Gao, C., Gao, D., Sun, R., Li, W., Wang, F., Wang, Y., Cao, H., Zhou, G., Zhang, J., & Shang, J. (2021). Reduction in pericyte coverage leads to blood–brain barrier dysfunction via endothelial transcytosis following chronic cerebral hypoperfusion. *Fluids and Barriers of the CNS*, *18*(1). https://doi.org/10.1186/s12987-021-00255-2

Svec, A. (2008). Rafting in the membrane. A lesson learnt from lymphoproliferative disorders. In *Ceskoslovenská patologie* (Vol. 44, Issue 4).

Sweeney, M. D., Ayyadurai, S., & Zlokovic, B. V. (2016). Pericytes of the neurovascular unit: Key functions and signaling pathways. In *Nature Neuroscience* (Vol. 19, Issue 6). https://doi.org/10.1038/nn.4288

T. Ronaldson, P., & P. Davis, T. (2012). Blood-Brain Barrier Integrity and Glial Support: Mechanisms that can be Targeted for Novel Therapeutic Approaches in Stroke. *Current Pharmaceutical Design*, *18*(25). https://doi.org/10.2174/138161212802002625

Tachibana, K., Iwashita, Y., Wakayama, E., Nishino, I., Nishikaji, T., & Kondoh, M. (2020). Tight junction modulating bioprobes for drug delivery system to the brain: A review. In *Pharmaceutics* (Vol. 12, Issue 12). https://doi.org/10.3390/pharmaceutics12121236

Tajes, M., Ramos-Fernández, E., Weng-Jiang, X., Bosch-Morató, M., Guivernau, B., Eraso-Pichot, A., Salvador, B., Fernàndez-Busquets, X., Roquer, J., & Muñoz, F. J. (2014). The blood-brain barrier: Structure, function and therapeutic approaches to cross it. In *Molecular Membrane Biology* (Vol. 31, Issue 5, pp. 152–167). Informa Healthcare. https://doi.org/10.3109/09687688.2014.937468

Takata, F., Nakagawa, S., Matsumoto, J., & Dohgu, S. (2021). Blood-Brain Barrier Dysfunction Amplifies the Development of Neuroinflammation: Understanding of Cellular Events in Brain Microvascular Endothelial Cells for Prevention and Treatment of BBB Dysfunction. In *Frontiers in Cellular Neuroscience* (Vol. 15). https://doi.org/10.3389/fncel.2021.661838

Tan, N. S., Vázquez-Carrera, M., Montagner, A., Sng, M. K., Guillou, H., & Wahli, W. (2016). Transcriptional control of physiological and pathological processes by the nuclear receptor PPARβ/δ. In *Progress in Lipid Research* (Vol. 64). https://doi.org/10.1016/j.plipres.2016.09.001

Taraboletti, G., D'Ascenzo, S., Borsotti, P., Giavazzi, R., Pavan, A., & Dolo, V. (2002). Shedding of the matrix metalloproteinases MMP-2, MMP-9, and MT1-MMP as membrane vesicle-associated components by endothelial cells. *American Journal of Pathology*, *160*(2). https://doi.org/10.1016/S0002-9440(10)64887-0

Tarran, R., Grubb, B. R., Gatzy, J. T., Davis, C. W., & Boucher, R. C. (2001). The relative roles of passive surface forces and active ion transport in the modulation of airway surface liquid volume and composition. *Journal of General Physiology*, *118*(2). https://doi.org/10.1085/jgp.118.2.223

Taslimifar, M., Buoso, S., Verrey, F., & Kurtcuoglu, V. (2018). Functional polarity of microvascular brain endothelial cells supported by neurovascular unit computational model of large neutral amino acid

homeostasis. *Frontiers in Physiology*, *9*(MAR). https://doi.org/10.3389/fphys.2018.00171

Tavares, E., Maldonado, R., Ojeda, M. L., & Minano, F. J. (2005). Circulating inflammatory mediators during start of fever in differential diagnosis of gram-negative and gram-positive infections in leukopenic rats. *Clinical and Diagnostic Laboratory Immunology*, *12*(9), 1085–1093. https://doi.org/10.1128/CDLI.12.9.1085-1093.2005

Te Velthuis, A. J. W., Admiraal, J. F., & Bagowski, C. P. (2007). Molecular evolution of the MAGUK family in metazoan genomes. *BMC Evolutionary Biology*, *7*. https://doi.org/10.1186/1471-2148-7-129

Thomas, C. M., & Smart, E. J. (2008). Caveolae structure and function. *Journal of Cellular and Molecular Medicine*, *12*(3). https://doi.org/10.1111/j.1582-4934.2008.00295.x

Tiwary, S., Morales, J. E., Kwiatkowski, S. C., Lang, F. F., Rao, G., & McCarty, J. H. (2018). Metastatic brain tumors disrupt the blood-brain barrier and alter lipid metabolism by inhibiting expression of the endothelial cell fatty acid transporter Mfsd2a. *Scientific Reports*, *8*(1). https://doi.org/10.1038/s41598-018-26636-6

Torres-Garcia, L., Joana, J. M., Brandi, E., Haikal, C., Mudannayake, J. M., Brás, I. C., Gerhardt, E., Li, W., Svanbergsson, A., Outeiro, T. F., Gouras, G. K., & Li, J. Y. (2022). Monitoring the interactions between alpha-synuclein and Tau in vitro and in vivo using bimolecular fluorescence complementation. *Scientific Reports*, *12*(1). https://doi.org/10.1038/s41598-022-06846-9

Tracey, T. J., Steyn, F. J., Wolvetang, E. J., & Ngo, S. T. (2018). Neuronal lipid metabolism: Multiple pathways driving functional outcomes in health and disease. In *Frontiers in Molecular Neuroscience* (Vol. 11). https://doi.org/10.3389/fnmol.2018.00010

Trask, O. J. (2004). Nuclear Factor Kappa B (NF-κB) Translocation Assay Development and Validation for High Content Screening. In *Assay Guidance Manual*.

Turner, R. J., & Sharp, F. R. (2016). Implications of MMP9 for blood brain barrier disruption and hemorrhagic transformation following ischemic stroke. In *Frontiers in Cellular Neuroscience* (Vol. 10, Issue MAR2016). https://doi.org/10.3389/fncel.2016.00056

Uc, P. Y., Miranda, J., Sandino, A. R., Alarcón, L., Roldán, M. L., Delgado, R. O., Malagón, E. M. C., Munguía, B. C., Ramírez, G., Asomoza, R., Shoshani, L., Gariglio, P., & Mariscal, L. G. (2020). E7 oncoprotein from human papillomavirus 16 alters claudins expression and the sealing of epithelial tight junctions. *International Journal of Oncology*, *57*(4). https://doi.org/10.3892/ijo.2020.5105

Uehara, I., Kajita, M., Tanimura, A., Hida, S., Onda, M., Naito, Z., Taki, S., & Tanaka, N. (2022). 2-Deoxy-d-glucose induces deglycosylation of proinflammatory cytokine receptors and strongly reduces immunological responses in mouse models of inflammation. *Pharmacology Research and Perspectives*, *10*(2). https://doi.org/10.1002/prp2.940

Ueno, M. (2007). Molecular Anatomy of the Brain Endothelial Barrier: An Overview of the Distributional Features. *Current Medicinal Chemistry*, *14*(11). https://doi.org/10.2174/092986707780597943

Van Der Poll, T., Van De Veerdonk, F. L., Scicluna, B. P., & Netea, M. G. (2017). The immunopathology of sepsis and potential therapeutic targets. In *Nature Reviews Immunology* (Vol. 17, Issue 7). https://doi.org/10.1038/nri.2017.36

Vanlandewijck, M., He, L., Mäe, M. A., Andrae, J., Ando, K., Del Gaudio, F., Nahar, K., Lebouvier, T., Laviña, B., Gouveia, L., Sun, Y., Raschperger, E., Räsänen, M., Zarb, Y., Mochizuki, N., Keller, A., Lendahl, U., & Betsholtz, C. (2018). A molecular atlas of cell types and zonation in the brain vasculature. *Nature*, *554*(7693). https://doi.org/10.1038/nature25739

Villabona-Rueda, A., Erice, C., Pardo, C. A., & Stins, M. F. (2019). The Evolving Concept of the Blood Brain Barrier (BBB): From a Single Static Barrier to a Heterogeneous and Dynamic Relay Center. In *Frontiers in Cellular Neuroscience* (Vol. 13). https://doi.org/10.3389/fncel.2019.00405

Wang, J. Z., Xiao, N., Zhang, Y. Z., Zhao, C. X., Guo, X. H., & Lu, L. M. (2016). Mfsd2a-based pharmacological strategies for drug delivery across the blood-brain barrier. *Pharmacological Research*, *104*. https://doi.org/10.1016/j.phrs.2015.12.024

Wang, Q., Liu, Y., & Zhou, J. (2015). Neuroinflammation in Parkinson's disease and its potential as therapeutic target. In *Translational Neurodegeneration* (Vol. 4, Issue 1). https://doi.org/10.1186/s40035-015-0042-0

Wang, X., Yu, J. ying, Sun, Y., Wang, H., Shan, H., & Wang, S. (2021). Baicalin protects LPS-induced blood–brain barrier damage and activates Nrf2-mediated antioxidant stress pathway. *International Immunopharmacology*, *96*. https://doi.org/10.1016/j.intimp.2021.107725

Wardlaw, J. M., Doubal, F., Armitage, P., Chappell, F., Carpenter, T., Muñoz Maniega, S., Farrall, A., Sudlow, C., Dennis, M., & Dhillon, B. (2009). Lacunar stroke is associated with diffuse Blood-Brain barrier dysfunction. *Annals of Neurology*, *65*(2). https://doi.org/10.1002/ana.21549

Waring, M. J. (2009). Defining optimum lipophilicity and molecular weight ranges for drug candidates-Molecular weight dependent lower log D limits based on permeability. *Bioorganic and Medicinal Chemistry Letters*, *19*(10). https://doi.org/10.1016/j.bmcl.2009.03.109

Weberpals, M., Hermes, M., Hermann, S., Kummer, M. P., Terwel, D., Semmler, A., Berger, M., Schäfers, M., & Heneka, M. T. (2009). NOS2 gene deficiency protects from sepsis-induced long-term cognitive deficits. *Journal of Neuroscience*, *29*(45). https://doi.org/10.1523/JNEUROSCI.3238-09.2009

Wolburg, H., & Lippoldt, A. (2002). Tight junctions of the blood-brain barrier: Development, composition and regulation. *Vascular Pharmacology*, *38*(6). https://doi.org/10.1016/S1537-1891(02)00200-8

Wolburg, H., Noell, S., Mack, A., Wolburg-Buchholz, K., & Fallier-Becker, P. (2009). Brain endothelial cells and the glio-vascular complex. In *Cell and Tissue Research* (Vol. 335, Issue 1). https://doi.org/10.1007/s00441-008-0658-9

Wolburg, H., Noell, S., Wolburg-Buchholz, K., MacK, A., & Fallier-Becker, P. (2009). Agrin, aquaporin-4, and astrocyte polarity as an important feature of the blood-brain barrier. *Neuroscientist*, *15*(2). https://doi.org/10.1177/1073858408329509

Wolf, S. A., Boddeke, H. W. G. M., & Kettenmann, H. (2017). Microglia in Physiology and Disease. In *Annual Review of Physiology* (Vol. 79). https://doi.org/10.1146/annurev-physiol-022516-034406

Wong, B. H., Chan, J. P., Cazenave-Gassiot, A., Poh, R. W., Foo, J. C., Galam, D. L. A., Ghosh, S., Nguyen, L. N., Barathi, V. A., Yeo, S. W., Luu, C. D., Wenk, M. R., & Silver, D. L. (2016). Mfsd2a is a transporter for the essential ω-3 fatty acid docosahexaenoic acid (DHA) in eye and is important for photoreceptor cell development. *Journal of Biological Chemistry*, *291*(20). https://doi.org/10.1074/jbc.M116.721340

Wood, C. A. P., Zhang, J., Aydin, D., Xu, Y., Andreone, B. J., Langen, U. H., Dror, R. O., Gu, C., & Feng, L. (2021). Structure and mechanism of blood–brain-barrier lipid transporter MFSD2A. *Nature*, *596*(7872). https://doi.org/10.1038/s41586-021-03782-y

Wu, X., Gao, H., Hou, Y., Yu, J., Sun, W., Wang, Y., Chen, X., Feng, Y., Xu, Q. ming, & Chen, X. (2018). Dihydronortanshinone, a natural product, alleviates LPS-induced inflammatory response through NF-κB, mitochondrial ROS, and MAPK pathways. *Toxicology and Applied Pharmacology*, *355*. https://doi.org/10.1016/j.taap.2018.06.007

Xaio, H., Banks, W. A., Niehoff, M. L., & Morley, J. E. (2001). Effect of LPS on the permeability of the blood–brain barrier to insulin. *Brain research*, *896*(1-2), 36-42

Xu, B., Chen, L., Zhan, Y., Marquez, K. N. S., Zhuo, L., Qi, S., Zhu, J., He, Y., Chen, X., Zhang, H., Shen, Y., Chen, G., Gu, J., Guo, Y., Liu, S., & Xie, T. (2022). The Biological Functions and Regulatory Mechanisms of Fatty Acid Binding Protein 5 in Various Diseases. In *Frontiers in Cell and Developmental Biology* (Vol. 10). https://doi.org/10.3389/fcell.2022.857919

Xu, L., Nirwane, A., & Yao, Y. (2019). Basement membrane and blood-brain barrier. In *Stroke and Vascular Neurology* (Vol. 4, Issue 2). https://doi.org/10.1136/svn-2018-000198

Yang, J., Ran, M., Li, H., Lin, Y., Ma, K., Yang, Y., Fu, X., & Yang, S. (2022). New insight into neurological degeneration: Inflammatory cytokines and blood–brain barrier. In *Frontiers in Molecular Neuroscience* (Vol. 15). https://doi.org/10.3389/fnmol.2022.1013933

Yang, R., Wang, J., Wang, F., Zhang, H., Tan, C., Chen, H., & Wang, X. (2023). Blood–Brain Barrier Integrity Damage in Bacterial Meningitis: The Underlying Link, Mechanisms, and Therapeutic Targets. In *International Journal of Molecular Sciences* (Vol. 24, Issue 3). https://doi.org/10.3390/ijms24032852

Yang, Y. R., Xiong, X. Y., Liu, J., Wu, L. R., Zhong, Q., Zhou, K., Meng, Z. Y., Liu, L., Wang, F. X., Gong, Q. W., Liao, M. F., Duan, C. M., Li, J., Yang, M. H., Zhang, Q., Gong, C. X., & Yang, Q. W. (2017). Mfsd2a (major facilitator superfamily domain containing 2a) attenuates intracerebral hemorrhage-induced blood-brain barrier disruption by inhibiting vesicular transcytosis. *Journal of the American Heart Association*, *6*(7). https://doi.org/10.1161/JAHA.117.005811

Yang, Y., & Rosenberg, G. A. (2011). MMP-Mediated Disruption of Claudin-5 in the Blood–Brain Barrier of Rat Brain After Cerebral Ischemia. In *Methods in Molecular Biology* (Vol. 762, pp. 333–345). Humana Press Inc. https://doi.org/10.1007/978-1-61779-185-7_24

Yoon, J. H., Lee, E. S., & Jeong, Y. (2017). In vivo imaging of the cerebral endothelial glycocalyx in mice. *Journal of Vascular Research*, *54*(2). https://doi.org/10.1159/000457799

Yoon, J. H., Seo, Y., Jo, Y. S., Lee, S., Cho, E., Cazenave-Gassiot, A., Shin, Y. S., Moon, M. H., An, H. J., Wenk, M. R., & Suh, P. G. (2022). Brain lipidomics: From functional landscape to clinical significance. In *Science Advances* (Vol. 8, Issue 37). https://doi.org/10.1126/sciadv.adc9317

Yu, G. L., Zhang, Y., & Ning, B. (2021). Reactive Astrocytes in Central Nervous System Injury: Subgroup and Potential Therapy. In *Frontiers in Cellular Neuroscience* (Vol. 15). https://doi.org/10.3389/fncel.2021.792764

Yu, X., Ji, C., & Shao, A. (2020). Neurovascular Unit Dysfunction and Neurodegenerative Disorders. In *Frontiers in Neuroscience* (Vol. 14). https://doi.org/10.3389/fnins.2020.00334

Zaragozá, R. (2020). Transport of Amino Acids Across the Blood-Brain Barrier. In *Frontiers in Physiology* (Vol. 11). https://doi.org/10.3389/fphys.2020.00973

Zhang, J., Xu, Y., Li, D., Fu, L., Zhang, X., Bao, Y., & Zheng, L. (2020). Review of the Correlation of LAT1 with Diseases: Mechanism and Treatment. *Frontiers in chemistry*, *8*, 564809. https://doi.org/10.3389/fchem.2020.564809

Zeiller, C., Mebarek, S., Jaafar, R., Pirola, L., Lagarde, M., Prigent, A. F., & Némoz, G. (2009). Phospholipase D2 regulates endothelial permeability through cytoskeleton reorganization and occludin downregulation. *Biochimica et Biophysica Acta - Molecular Cell Research*, *1793*(7). https://doi.org/10.1016/j.bbamcr.2009.04.001

Zgórzyńska, E., Stulczewski, D., Dziedzic, B., Su, K. P., & Walczewska, A. (2021). Docosahexaenoic fatty acid reduces the pro-inflammatory response induced by IL-1β in astrocytes through inhibition of NF-κB and AP-1 transcription factor activation. *BMC neuroscience*, *22*(1), 4. https://doi.org/10.1186/s12868-021-00611-w

Zhang, S., Shang, D., Shi, H., Teng, W., & Tian, L. (2021). Function of Astrocytes in Neuroprotection and Repair after Ischemic Stroke. In *European Neurology* (Vol. 84, Issue 6). https://doi.org/10.1159/000517378

Zhang, T., Ma, C., Zhang, Z., Zhang, H., & Hu, H. (2021). NF-κB signaling in inflammation and cancer. In *MedComm* (Vol. 2, Issue 4). https://doi.org/10.1002/mco2.104

Zhang, W., Chen, R., Yang, T., Xu, N., Chen, J., Gao, Y., & Stetler, R. A. (2018). Fatty acid transporting proteins: Roles in brain development, aging,

and stroke. In *Prostaglandins Leukotrienes and Essential Fatty Acids* (Vol. 136). https://doi.org/10.1016/j.plefa.2017.04.004

Zhang, W., Zhang, Y., Guo, X., Zeng, Z., Wu, J., Liu, Y., He, J., Wang, R., Huang, Q., & Chen, Z. (2017). Sirt1 protects endothelial cells against LPS-induced barrier dysfunction. *Oxidative Medicine and Cellular Longevity*, *2017*. https://doi.org/10.1155/2017/4082102

Zhang, Z. Y., Monleon, D., Verhamme, P., & Staessen, J. A. (2018). Branched-chain amino acids as critical switches in health and disease. In *Hypertension* (Vol. 72, Issue 5). https://doi.org/10.1161/HYPERTENSIONAHA.118.10919

Zhao, C., Ma, J., Wang, Z., Li, H., Shen, H., Li, X., & Chen, G. (2020). Mfsd2a Attenuates Blood-Brain Barrier Disruption After Sub-arachnoid Hemorrhage by Inhibiting Caveolae-Mediated Transcellular Transport in Rats. *Translational Stroke Research*, *11*(5). https://doi.org/10.1007/s12975-019-00775-y

Zhao, Y. L., Song, J. N., & Zhang, M. (2014). Role of caveolin-1 in the biology of the blood-brain barrier. *Reviews in the Neurosciences*, *25*(2). https://doi.org/10.1515/revneuro-2013-0039

Zheng, P. P., Romme, E., Van Der Spek, P. J., Dirven, C. M. F., Willemsen, R., & Kros, J. M. (2010). Glut1/SLC2A1 is crucial for the development of the blood-brain barrier in vivo. *Annals of Neurology*, *68*(6). https://doi.org/10.1002/ana.22318

Zhong, W., Huang, Q., Zeng, L., Hu, Z., & Tang, X. (2019). Caveolin-1 and MLRs: A potential target for neuronal growth and neuroplasticity after ischemic stroke. In *International Journal of Medical Sciences* (Vol. 16, Issue 11). https://doi.org/10.7150/ijms.35158

Zhou, Y. Q., Wang, K., Wang, X. Y., Cui, H. Y., Zhao, Y., Zhu, P., & Chen, Z. N. (2022). SARS-CoV-2 pseudovirus enters the host cells through spike protein-CD147 in an Arf6-dependent manner. *Emerging Microbes and Infections*, *11*(1). https://doi.org/10.1080/22221751.2022.2059403

Zhuang, L., Mao, Y., Liu, Z., Li, C., Jin, Q., Lu, L., Tao, R., Yan, X., & Chen, K. (2021). FABP3 Deficiency Exacerbates Metabolic Derangement in Cardiac Hypertrophy and Heart Failure via PPARα Pathway. *Frontiers in Cardiovascular Medicine*, *8*. https://doi.org/10.3389/fcvm.2021.722908

Zidarič, T., Gradišnik, L., & Velnar, T. (2022). Astrocytes and human artificial blood-brain barrier models. In *Bosnian Journal of Basic Medical Sciences* (Vol. 22, Issue 5, pp. 651–672). Association of Basic Medical Sciences of FBIH. https://doi.org/10.17305/bjbms.2021.6943

Zlokovic, B. V. (2009). Blood-Brain Barrier and Neurovascular Mechanisms of Neurodegeneration and Injury. In *Encyclopedia of Neuroscience*. https://doi.org/10.1016/B978-008045046-9.00491-5

Zonta, M., Angulo, M. C., Gobbo, S., Rosengarten, B., Hossmann, K. A., Pozzan, T., & Carmignoto, G. (2003). Neuron-to-astrocyte signaling is central to the dynamic control of brain microcirculation. *Nature Neuroscience*, *6*(1). https://doi.org/10.1038/nn980

Zou, P., Yang, F., Ding, Y., Zhang, D., Liu, Y., Zhang, J., Wu, D., & Wang, Y. (2022). Lipopolysaccharide downregulates the expression of ZO-1 protein through the Akt pathway. *BMC Infectious Diseases*, *22*(1). https://doi.org/10.1186/s12879-022-07752-1